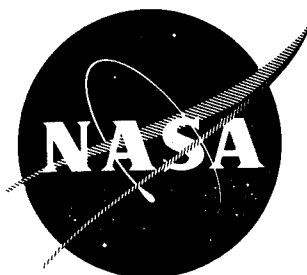## AD NUMBER

ADB211149

NEW LIMITATION CHANGE

TO

Approved for public release, distribution unlimited

FROM

Distribution authorized to U.S. Gov't. agencies and their contractors; Administrative/Operational Use; JAN 1967. Other requests shall be referred to National Aeronautics and Space Administration, Washington, DC.

AUTHORITY

NASA TR Server Website

CR-54870

"DTIC USERS ONLY"

THIOKOL 260-SL NOZZLE DEVELOPMENT PROGRAM

19960607 088

prepared for

NATIONAL AERONAUTICS AND SPACE ADMINISTRATION

CONTRACT NAS 3-6285

THIOKOL CHEMICAL CORPORATION
Space Booster Division
Brunswick, Georgia

DISCLAIMER NOTICE

THIS DOCUMENT IS BEST
QUALITY AVAILABLE. THE
COPY FURNISHED TO DTIC
CONTAINED A SIGNIFICANT
NUMBER OF PAGES WHICH DO
NOT REPRODUCE LEGIBLY.

TABLE OF CONTENTS

TABLE OF CONTENTS (Cont'd)

LIST OF ILLUSTRATIONS

LIST OF ILLUSTRATIONS (Cont'd)

LIST OF TABLES

LIST OF TABLES (Cont'd)

LIST OF TABLES (Cont'd)

LIST OF TABLES (Cont'd)

LIST OF TABLES (Cont'd)

I. SUMMARY AND CONCLUSIONS

Static test of the 156-2C-1 rocket motor provided useful data on the design, ablative materials, and fabrication techniques used in the manufacture of the nozzles for the 156- and 260-inch diameter solid propellant rocket motors. Nozzle erosion rates were higher than predicted, however, demonstration of a tape-wrapped ablative, steel-jacketed nozzle for a three-million pound thrust solid-propellant rocket motor was considered a success. The nozzle test also demonstrated that facilities exist that are suitable for manufacture of tape-wrapped ablative components for use in nozzles of this size. The assembly and shipping of the nozzle proved that a method of handling can be devised for such large ablative structures.

During the fabrication of the ablative components for the 156- and 260-inch diameter motor nozzles, techniques were developed for wrapping ablative tapes at speeds up to 20 fpm without appreciably sacrificing as-wrapped density. It can be concluded that higher speeds could be attained by improved heat application and faster methods of cooling.

Tape wrapping heads with state-of-the-art capabilities were procured and were improved to provide better tracking of the tape, more reliable tape guidance features, and better location for heat application to the tape. The problems associated with bias tape guidance were not solved during this program, but acceptable means of hand guiding and trimming the tape were developed.

Material variation and deficiencies were encountered early in the program. These anomolies encompassed impregnated tape and bare fabric. As a result, fabrication problems caused by lack of resin flow and tack, inadequate splices, and repeated breakage of tape arose. These difficulties were overcome by improving processing techniques and by improved material acceptance tests.

The ablative mandrel design concept was proved adequate for the intended wrapping functions. The mandrel also served as handling and assembling tools for the nozzle components.

The nozzle assembly operation was shortened from a projected 3-month task for assembly of individual components to an 18-day task for a one-step bond and cure operation. Bonding of the 156-2C-1 ablative into the shell was accomplished in less than eight hours.

The problems of distortion, low first-pass properties, and cracking had to be overcome during the steel parts fabrication due to the high energy input of the two-pass submerged-arc weld used in the nozzle and adapter. A solution or a work-around was found for each of these areas so that the resulting processes were adequate for nozzle shell manufacture.

Significant technical advancements verified by the fabrication of the nozzle and nozzle components for the 156- and 260-inch motors included (1) fabrication techniques for large, tape-wrapped ablative components, (2) impregnated tape improvements, (3) wrapping-tool design, and (4) handling techniques.

II. OBJECTIVE

The objective of the nozzle program was to produce a nozzle design that could be used for the fabrication of nozzles for the 156-2C-1, 260-SL-1, and 260-SL-2 rocket motors.

Two adapters using tape-wrapped insulation would also be required to attach the nozzles to the 260-inch diameter cases. In addition, four subscale nozzles were included in the program. The first two subscale nozzles were to be tape-wrapped using the same tape widths and wrapping techniques planned for the 156-2C-1 and 260-SL-1 nozzles. The other two subscale nozzles were to be manufactured with primary emphasis on fabricating the exit cones using a nonhydroclave curing process. Once this technique was successfully demonstrated, the 260-SL-2 nozzle would be fabricated using this same nonhydroclave process for the exit cone.

As the program progressed, changes in the original objectives were necessary. During the initial fabrication of the first subscale nozzle, it was determined that tape widths required for the larger nozzles could not be successfully wrapped on the smaller subscale diameters. The ratio of tape width to mandrel radius was excessive on some of the components. This caused extreme tape wrinkling and neckdown. The original objective of tape wrapping subscale components was modified to allow hand layup of all components that could not be tape wrapped.

Several areas were investigated for possible changes that would result in lower overall program cost. One of the first changes made affected the nozzle adapter for the 260-SL motors. An investigation was made to find a more economical method of insulating the adapter than using a tape-wrapped component. Initially, V-44 Buna-N material appeared to fulfill this objective. To demonstrate the acceptability of the V-44 material, varying thicknesses were applied over the tape-wrapped phenolic impregnated carbon fabric utilized in the entrance cone of the first subscale nozzle. Results of the static test of this nozzle proved this material to be satisfactory.

The Thiokol mastic insulation material TI-H704B that was being developed for use in insulating the 156-2C-1 and 260-SL cases appeared to be even lower in cost than the V-44 Buna-N material. Therefore, the carbon entrance cone was completely deleted in the second subscale nozzle and was replaced by one-half mastic insulation and one-half Buna-N insulation. The results of this test show the mastic insulation to be completely satisfactory.

As a further effort to reduce costs, the third and fourth subscale nozzles were deleted from the program. This resulted in modification of the objective for the 260-SL-2 nozzle. Since the subscale nozzles had now been deleted, the objective of fabricating a 260-SL-2 exit cone by utilizing a nonhydroclave process could not be fulfilled, and was, therefore, also deleted from the program. As a result, the 260-SL-2 nozzle was to be fabricated in basically the same manner as the 156-2C-1 and 260-SL-1 nozzles. Also, in the interest of economy, one of the three nozzle steel shells was also deleted from the program. The plan was to reuse one of the fired shells in one of the 260-SL nozzles.

III. NOZZLE DESIGN

A. DESCRIPTION AND CRITERIA

The basic nozzle design was the same for all three large motors, i.e., 156-2C-1 and 260-SL-1 and -2. This design was a 17.5 degree half angle De Laval nozzle without provisions for thrust vector control. A structural steel shell provided that necessary restraint in the inlet and throat regions and part of the exit region. Plastic structural members were used for the remainder of the exit region. Ablative materials were used to insulate the steel and plastic structural members from the high temperature, erosive, exhaust gases in both the convergent and divergent sections. Thicknesses of the ablative section were based upon erosion and char data from other Thiokol programs and verified by static testing two 65-inch diameter subscale motors.

Table I summarizes the design geometry and weight. Engineering drawing 1S 11004 shows detailed nozzle design. Table II summarizes the materials used in the nozzle final design. The ablative thicknesses and safety factor calculation for the original design were based on the 260-SL-1 motor parameters. The design as shown on 1S 11004 was such that the nozzle could be attached directly to the aft end of the 156-2C-1 motor case or could be used with an adapter and attached to the 260-SL motor cases. This flexibility was built into the nozzle to allow a short burning time test for the 156-2C-1 motor to be conducted without any appreciable difference in the other variables such as motor pressure and temperature. The first nozzle fabricated to this design was static tested on the 156-2C-1 motor. Two additional nozzles of the same configuration were scheduled to be tested on the 260-SL-1 and -2 motors.

B. STRUCTURAL CONCEPT

A literature survey was performed to determine the degree of successful experience associated with the various structural design concepts which could be used for the 260-SL-1 nozzle. The three principal structural concepts studied are listed below:

1. An all-steel shell (steel extends from forward attachment flange aft to the exit plane)

2. A partial-steel structural shell (steel extends from forward attachment flange aft to some point on the forward section of the exit cone with structural plastic aft of the steel termination point)

3. A plastic structural shell (steel used only for attachment)

The partial-steel structural shell and the plastic structural shell concepts exhibited higher reliability than that exhibited by the all-steel concept. Because the number of programs using the plastic structural shell concept were few, even though numbers of tests and successes were high, the partial steel shell, was favored. Facility requirements and processing unknowns associated with

TABLE I

260-INCH NOZZLE GEOMETRY AND WEIGHT
Ref. Drawing 1S 11004

Dimensions	
Length, (in)	217.8
Attach flange outside diameter, (in)	146.8
Exit cone diameter, (in)	163.5
Initial throat diameter, (in)	61.28
Initial expansion ratio	7.12
Average throat area during web time, (in^2)	2974
Average expansion ratio during web time	7.06
Design throat erosion rate, (in/sec on radius)	0.0055
Nozzle Component Weights	
Housing, (lb)	8620
Entrance insulation, (lb)	1280
Throat insulation, (lb)	950
Exit insulation, (lb)	6850
Reinforcements, (lb)	2250
Total (calculated)	19,950
Actual component shipping wt (lb) of 156-2C-1 nozzle	19,850

TABLE II

NOZZLE MATERIALS
260-INCH DESIGN

Component	Material
Steel shell	18 percent nickel maraging steel
Entrance cone ablative, entrance to 1.4 area ratio	U.S. Polymeric Chemicals, Inc. - FM-5063 carbon-phenolic bias tape
Forward, mid, and aft throat ablatives	U.S. Polymeric Chemicals, Inc. - FM-5064 graphite-phenolic bias tape
Exit cone ablative between 1.12 to 3.0 area ratios	Fiberite Corporation - MX-4926 carbon-phenolic wrap tape
Exit cone ablative, aft of 3.0 area ratio	Fiberite Corporation - MX-2600 silica-phenolic wrap tape
Structural laminate	Fiberite Corporation - MX-4600 bidirectional glass-phenolic
Tie laminate	Bidirectional glass fabric and polyester resin
Adhesive	Shell Chemical - Epon 913 epoxy resin
Joint filler	Zinc chromate putty
Roving	20-end "E" glass with ambient curing epoxy resin
Thermal coating	Dyna-Therm Chemical Corporation - X43-24 spray epoxy-asbestos

ADAPTER MATERIALS

Component	Material
Steel shell	18 percent nickel maraging steel
Insulation material	TI-H704B mastic insulation

a plastic structural shell of the type and size required made this approach undesirable.

The structural concept thus selected was that of the partial-steel structural shell. The steel was extended to a point about one-third of the distance from the throat to the exit plane. Beyond this point, structural plastic laminates provided the load-carrying capability needed in the aft exit cone section. Laminates were applied over the external surface of both the exposed exit cone and the steel shell after insertion of the exit cone into the shell. Circumferentially wound rovings were used in the throat area to mechanically lock the overlapping exit cone laminates (called tie laminates) to the steel shell.

The specific configuration of the steel shell was established as being a series of truncated cones welded together. The steel shell contained a convergent 45-degree half-angle, truncated cone entrance section; a throat section formed by two convergent truncated cones with 30- and 10- degree half angles; and a truncated cone exit section. Two cones were selected for the throat area instead of the usual single cone used in nozzles to reduce the cross-sectional thickness of the inner, erosion-resistant liners. This was more economical and created better curing conditions. Thicknesses of the steel conical sections were established on the basis of structural analyses for static pressure and dynamic loading conditions and for strain compatibility with the inner, ablative liners.

C. ABLATIVE CONCEPT

Based upon experiences of Thiokol Chemical Corporation in earlier programs, and verified by literature surveys, ablative materials (phenolic resin base) were the clear choice in entrance and exit regions to resist the erosiveness of the combustion gases and to insulate the steel shell from structurally degrading temperatures. The highly critical throat regions, however, indicated a possible choice of either ablative or refractory graphite materials.

A study of possible methods for providing a refractory graphite throat insert provided four candidates: One monolithic and three segmented. These are illustrated in Figure 1. Two approaches, monolithic and ring segmented were limited by the state-of-the-art size capability in production. Previous testing of longitudinally segmented and ring-arc segmented inserts indicated very low reliability. Because of these factors, an ablative insert was chosen.

Ablative materials having an established record of satisfactory usage in solid rockets all contained a phenolic resin matrix. The reinforcement was found to vary but, typically, was a fiberous material having comparatively low thermal conductivity. Four types of reinforcements were considered, and these are listed below in descending order of erosion resistance capability:

Graphite Fabric

Carbon Fabric

Silica Fabric

Glass Fabric

Section IV describes the selection of material types and specific materials
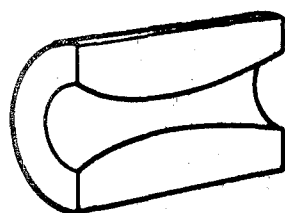
MONOLITHIC GRAPHITE
(SIZE LIMITED)
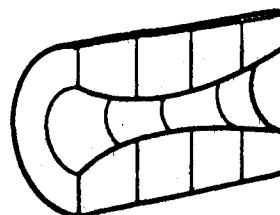
RING-SEGMENTED GRAPHITE
(SIZE LIMITED)
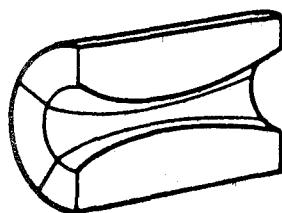
AXIALLY-SEGMENTED
GRAPHITE
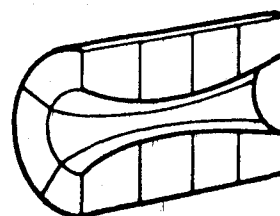
RING-ARC SEGMENTED
GRAPHITE
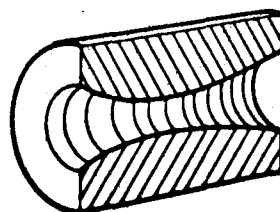
TAPE-WRAPPED ABLATIVE

Figure 1 - Candidate Throat Inserts

for each area of the 260-SL-1 nozzle.

Thicknesses of the ablative sections were established by sizing critical areas using performance data obtained from prior programs. A safety factor of 2.0 was used in the equation shown below:

$$\text{Thickness} = 2.0 \times t_b \times e_r + C$$

$$\text{where } e_r = e_{r_{ss}} \left(\frac{P_{260}}{P_{ss}} \right)^{.8}$$

In the above equations, t_b is web burning time of the 260-SL-1 motor, C is char thickness predicted, e_r is predicted 260-SL-1 erosion rate, $e_{r_{ss}}$ is erosion rate from subscale tests, and P_{260} and P_{ss} are chamber pressures of the 260-SL-1 and subscale motors, respectively.

Thicknesses between critical, calculated points were derived by blending of contours and providing for gradual thickness transitions.

IV. MATERIALS

A. STEEL

The initial design release for the large nozzle required a steel housing of AISI 4340 steel. The two major problems which existed with using this steel for the nozzle and adapter steel shells were:

1. A weld development program would have to be conducted to establish parameters for welding thick sections of AISI 4340.

2. Heat treat and quench facilities were not readily available for the heat treatment of weldments in these diameters.

Since a program was already scheduled for development of welding techniques for thick sections of 18 percent nickel maraging steel, the material for both the 156- and 260-inch nozzle shells and the 260-inch adapter shells was changed to 18 percent nickel maraging steel. Material requirements for composition and mechanical properties are shown in Tables III and IV, respectively.

The strength requirements for the nozzle shell are less than those in the case wall, hence any welding techniques for the thick sections of the case would be directly applicable to the nozzle and adapter shells.

B. ABLATIVES

1. Material Selection

Initially, four different types of ablative materials were selected for use in five areas of the nozzle. The form of the materials selected was, in every case, oriented tape to permit tape wrapping on mandrels. The ablative materials selected consisted of four different fiberous materials woven into homogeneous fabrics, i.e., carbon, graphite, high silica, and glass. Each of these four fabrics was impregnated with a heat-resistant phenolic resin.

In the zone of highest erosion, the throat, graphite fabric was the material selected because it was expected to provide the most resistance to erosion. Carbon fabric ranks next in erosion resistance to graphite and was chosen for use in the convergent and divergent sections adjacent to the throat. High silica and glass fabrics, ranking third and fourth, respectively, in order of erosion resistance in solid motors, were selected for the progressively less severe environment of the mid- and aft-exit cone sections. These material selections were made in the interest of economy.

Products from numerous material suppliers were evaluated to make final specific material selections. Criteria for evaluation included the following:

1. Performance

TABLE III

CHEMICAL COMPOSITION OF MARAGING STEEL

Element	Minimum	Maximum	Check Limits
Nickel	17.0	19.0	± 0.15
Cobalt	7.0	8.5	± 0.05
Molybdenum	4.6	5.1	± 0.10
Titanium	0.35	0.50	± 0.05
Carbon	-	0.03	+ 0.005
Silicon	-	0.10 (aim 0.07)	+ 0.02
Manganese	-	0.10	+ 0.03
Sulfur	-	0.01	+ 0.005
Phosphorus	-	0.01	+ 0.005
Aluminum	0.05	0.15	± 0.01
Boron	-	0.003 1/	-
Zirconium	-	0.02 1/	-
Calcium	-	0.05 1/	-

1 / Add

TABLE IV

PROPERTIES AFTER AGING *

(Plate 1 5/8" thick and under)

Property	Minimum	Maximum
Yield strength, a 2 percent offset, psi	217,000	260,000
Ultimate tensile strength, psi	222,000	-
Elongation in gage required, percent	6	-
Reduction in area, percent	30	-

*Aging cycle, 4 hours at 835°F

2. Processing characteristics

3. Physical and mechanical properties of laminated structures

4. Quality control of raw materials

5. Availability

6. Reliability as measured by performance history

7. Cost

To make maximum use of the nozzle fabricator's previous experience and technology, materials marketed by the Fiberite Corporation were selected for use in the exit cone area of the nozzle. The three materials selected to be used in the exit cone, each of which is impregnated with a phenolic resin or polyamide modification of a phenolic resin, were: MX-4926, MX-2600, and MX-4600. These materials have carbon, high silica, and glass bases, respectively.

Evaluation of manufacturer's capabilities as well as their products resulted in the selection of U. S. Polymeric Corporation as the entrance cone and throat material supplier. Such processing characteristics as flow, tack, compaction, and neckdown, and comparisons of bias tape and warp-cut tape applications were extensively considered. The material ultimately selected for the fabrication of the entrance cone, therefore, was FM-5063, which is U. S Polymeric's carbon fabric material impregnated with USP-39 phenolic resin. The material selected to be used in the throat was FM-5064, which is a graphite fabric impregnated with USP-39 resin.

Phenolic impregnated glass fabric was the selected material for the laminate covering the outside surface of each ablative component. This laminate seals each component against any small gas leaks through circumferential delaminations in the ablative material and provides longitudinal integrity to the structure. Glass fabric was selected because of its low cost and high strength. Phenolic resin was selected because (1) its heat resistance and ablative potential could provide a thermal barrier for some period of time, and (2) it would be resistant to any exposure to hot gases. The specific product selected was MX-4600 which is a bidirectional weave of glass fabric impregnated with a polyamide modified phenolic resin. This product, marketed by the Fiberite Corporation, was the same as that selected for use in the exit cone as an ablative liner.

Tests were conducted on a thermal protective coating selected to prevent structural degradation of the tie laminate caused by radiant heating from the exhaust plume. The surface area involved made a sprayable material highly desirable from a processing standpoint. Such a sprayable system was found which had been used in protection of launch pad facilities exposed to radiant heating and to exhaust gases of rocket motors. The selected material was Dyna-Therm X-43-24, marketed by Dyna-Therm Chemical Corporation. The Dyna-Therm X-43-24 coating is composed of epoxy resins and inert fillers with ketone and aromatic hydrocarbon solvent dispersion. The solvents flash off during curing.

Panels of polyester-glass tie laminate material were coated on one side with different thicknesses of Dyna-Therm X-43-24. Coating thicknesses ranged up to 0.115 inch. The coated specimens were subjected to a 500°F. hot air blast supplied by a hot-air gun. Temperature versus time for the cold surface (back) of the polyester laminates were recorded by thermocouple. Exposure time varied from 30 to 120 seconds. Back side temperature versus coating thickness is shown plotted for various exposure periods in Figure 2.

An ambient curing resin system for wet-dip filament winding was selected for use around the throat area of the assembled nozzle. A system was selected based upon successful experiences by Thiokol in case-on-propellant winding studies. This system was composed of the following materials manufactured by Shell Chemical Corporation:

Epon	100 parts by weight
RTA (room temperature accelerator)	1 1/2 parts by weight
RTH (room temperature hardener)	56 parts by weight

NOL ring tests of the selected resin system and 20-end "E" glass roving with A1100 finish produced hoop tensile strengths of 185,000 psi, average.

Zinc chromate putty was selected to fill the ablative-to-ablative joints in the nozzle. This material satisfied the following selection requirements:

1. Non-curing

2. Resilient

3. Demonstrated good performance in joints

This material was used in thicknesses up to 0.070 inch to seal ablative-to-ablative joints against gas flow.

Figure 3 shows a cross-sectional schematic of material locations.

2. Material Properties

Properties of the ablative materials selected for use in the nozzle were obtained from the respective material suppliers at the start of the program. Testing was performed in accordance with applicable ASTM procedures. Where available, data were obtained for materials subjected to elevated temperature. Those properties and values used in thermal and structural analyses of the full scale nozzle are shown in Tables V thru XI.

Tests of key properties were performed on samples taken from each ablative 156-2C-1 component after processing. A mean value for each tested property of each material was calculated and these are shown in Tables XII thru XV. Presented for comparison are the minimum specification values for in-process acceptance tests. All in-process tests were conducted at room temperature.
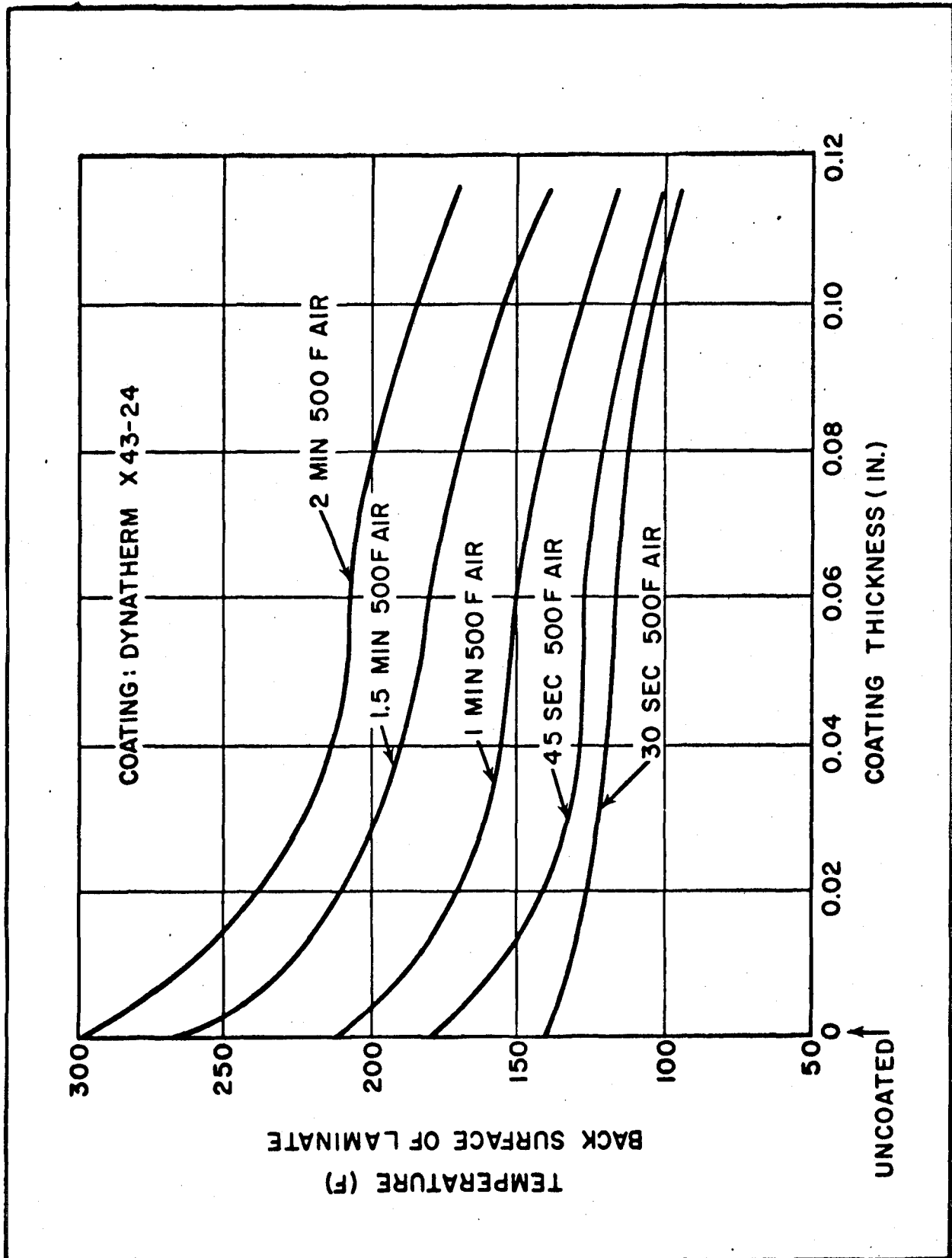
Figure 2 - Laminate Temperature versus Coating Thickness for Selectron 5003 Specimens

NOZZLE ASSEMBLY
MATERIAL

ITEM 1: STEEL, ALLOY, 18 PERCENT NICKEL MARAGING (RESTRICTED STRENGTH)

ITEM 2: CARBON FABRIC TAPE, BIAS CUT, IMPREGNATED WITH PHENOLIC RESIN

ITEM 3: GRAPHITE FABRIC TAPE, BIAS CUT, IMPREGNATED WITH PHENOLIC RESIN

ITEM 4: CARBON FABRIC TAPE, WARP CUT, IMPREGNATED WITH PHENOLIC RESIN

ITEM 5: HIGH-SILICA FABRIC TAPE, WARP CUT, IMPREGNATED WITH PHENOLIC RESIN

ITEM 6: IMPREGNATED GLASS ROVING- EXIT AREA

ITEM 7: BIDIRECTIONAL GLASS FABRIC, IMPREGNATED WITH PHENOLIC RESIN

ITEM 8: STRUCTURAL TIE LAMINATE, BIDIRECTIONAL GLASS FABRIC TAPE, WET DIP-
        COATED WITH POLYESTER RESIN

ITEM 9: GLASS ROVING, WET-DIP COATED WITH EPOXY RESIN – THROAT AND AFT
        STEEL SHELL AREAS

ITEM 10: THERMAL PROTECTIVE COATING, DYNA-THERM X43-24

Figure 3 - Cross-Sectional View of Nozzle Assembly of Motor 156-2C-1
Showing Materials

TABLE V

NOZZLE MATERIALS
PHYSICAL AND THERMAL PROPERTIES OF PLASTICS

Type of Material: Phenolic Resin Impregnated Warp-Cut Carbon Tape per SB-SP-123

Supplier and Designation: Fiberite Corporation, MX-4926

Material Form and Orientation: Warp-Cut Tape, Parallel to Centerline

Raw Material Description:

     (a)   Reinforcement   HITCO CCA-1 Carbon Fabric per SB-SP-130 Type II

     (b)   Resin   SC 1008 Phenolic Resin per SB-SP-117, Type III

     (c)   Resin Content   31 - 37 percent

     (d)   Filler and Percent   Carbonaceous, 3 - 14 percent

Physical and Thermal Properties:

Property	Values at Temperature		
	75°F	500°F	750°F
Hoop Tensile Strength, psi	20,000	14,000	10,000
Hoop Tensile Modulus, psi x 10^6	3.0	1.9	1.7
Hoop Flexural Strength, psi	30,000	24,000	10,000
Hoop Flexural Modulus, psi x 10^6	2.2	1.3	1.0
Edgewise Compressive Strength, psi (longitudinal)	36,000	13,000	10,000
Edgewise Compressive Modulus, psi x 10^6 (longitudinal)	1.75	1.0	0.6
Interlaminar Shear Strength, psi	4,000	2,600	1,800
Shear Strength Across Plies, psi	---	---	---
Poisson's Ratio	.25	---	---
Coefficient of Thermal Expansion (in/in/°F) x 10^{-6} Parallel	8.3	9.8	11.3
Perpendicular	38.3	45.0	52.0
Thermal Conductivity, BTU/in/sec/°F x 10^{-4}	.0979	---	.35
Specific Heat, BTU/lb/°F	.29	---	.25
Char Temperature, °F	N/A	750	N/A
Heat of Ablation, BTU/lb of volatiles	N/A	650	N/A
Density, lb/in^3	.053	---	.044

TABLE VI

NOZZLE MATERIALS
PHYSICAL AND THERMAL PROPERTIES OF PLASTICS

Type of Material: Phenolic Resin Impregnated Bias-Cut Carbon Tape per SB-SP-123

Supplier and Designation: U. S. Polymeric Chemicals, FM-5063

Material Form and Orientation: 45° Bias Tape, 60° Shingle Angle

Raw Material Description:

     (a)   Reinforcement   HITCO CCA-1 Carbon Fabric per SB-SP-130, Type II

     (b)   Resin   U. S. P. 39 Phenolic Resin per SB-SP-117, Type I

     (c)   Resin Content   31 - 37 percent

     (d)   Filler and Percent   Carbonaceous, 5 - 14 percent

Physical and Thermal Properties:

Property	Values at Temperature		
	75°F	500°F	1,000°F
Hoop Tensile Strength, psi	12,000	10,000	7,000
Hoop Tensile Modulus, psi x 10^6	2.5	1.5	1.1
Hoop Flexural Strength, psi	16,000	---	---
Hoop Flexural Modulus, psi x 10^6	2.5	---	---
Edgewise Compressive Strength, psi x 10^3 (hoop)	40,000	19,000	8,000
Edgewise Compressive Modulus, psi x 10^6 (hoop)	1.8	0.9	0.4
Interlaminar Shear Strength, psi	1,140	960	320
Shear Strength Across Plies, psi	7,000	6,500	4,800
Poisson's Ratio	0.25	---	---
Coefficient of Thermal Expansion (in/in/°F) x 10^{-6} Parallel	5.0	8.9	10.2
Perpendicular	8.0	11.4	13.1
Thermal Conductivity, BTU/in/sec/°F x 10^{-4}	0.0979	---	0.35
Specific Heat, BTU/lb/°F	0.29	---	0.25
Char Temperature, °F	N/A	875	N/A
Heat of Pyrolosis, BTU/lb of volatiles	N/A	650	N/A
Density, lb/in^3	0.053	---	0.044

TABLE VII

NOZZLE MATERIALS
PHYSICAL AND THERMAL PROPERTIES OF PLASTICS

Type of Material: Phenolic Resin Impregnated Graphite Fabric Tape per SB-SP-124

Supplier and Designation: U. S. Polymeric Chemicals, FM-5064

Material Form and Orientation: 45° Bias Tape, 45° Shingle Angle

Raw Material Description:

    (a)   Reinforcement   National Carbon's WCA Graphite Fabric per SB-SP-131, Type II

    (b)   Resin   U. S. P. 39 Phenolic Resin per SB-SP-117, Type I

    (c)   Resin Content   31 - 37 percent

    (d)   Filler and Percent   Carbonaceous, 3 - 14 percent

Physical and Thermal Properties:

Property	Values at Temperature		
	75°F	500°F	1,000°F
Hoop Tensile Strength, psi	8,650	7,900	5,650
Hoop Tensile Modulus, psi x 10^6	1.75	1.40	1.15
Hoop Flexural Strength, psi	12,800	---	---
Hoop Flexural Modulus, psi x 10^6	1.75	---	---
Edgewise Compressive Strength, psi (hoop)	25,000	9,000	5,600
Edgewise Compressive Modulus, psi x 10^6 (hoop)	1.7	.92	.40
Interlaminar Shear Strength, psi	1,000	---	---
Shear Strength Across Plies, psi	6,450	5,400	3,950
Poisson's Ratio	.25	---	---
Coefficient of Thermal Expansion (in/in/°F) x 10^{-6} Parallel	4.0	6.6	7.6
Perpendicular	7.0	9.2	10.6
Thermal Conductivity, BTU/in/sec/ °F x 10^{-4}	0.116	---	0.40
Specific Heat, BTU/lb/°F	0.24	---	0.22
Char Temperature, °F	N/A	875	N/A
Heat of Pyrolosis, BTU/lb of volatiles	N/A	650	N/A
Density, lb/in^3	0.054	---	0.043

TABLE VIII

NOZZLE MATERIALS
PHYSICAL AND THERMAL PROPERTIES OF PLASTICS

Type of Material: Phenolic Resin Impregnated Graphite Fabric Tape per SB-SP-124

Supplier and Designation: U. S. Polymeric Chemicals, FM-5064

Material Form and Orientation: 45° Bias Tape, 60° Shingle Angle

Raw Material Description:

     (a) Reinforcement   National Carbon's WCA Graphite Fabric per SB-SP-131, Type II

     (b) Resin   U. S. P. 39 Phenolic Resin per SB-SP-117, Type 1

     (c) Resin Content   31 - 37 percent

     (d) Filler and Percent   Carbonaceous, 3 - 14 percent

Physical and Thermal Properties:

Property	Values at Temperature		
	75 °F	500 °F	1,000 °F
Hoop Tensile Strength, psi	8,500	7,800	5,600
Hoop Tensile Modulus, psi $\times 10^6$	1.7	1.34	1.1
Hoop Flexural Strength, psi	12,000	---	---
Hoop Flexural Modulus, psi $\times 10^6$	1.7	---	---
Edgewise Compressive Strength, psi (hoop)	25,000	9,000	5,600
Edgewise Compressive Modulus, psi $\times 10^6$ (hoop)	1.7	.92	.40
Interlaminar Shear Strength, psi	1,000	---	---
Shear Strength Across Plies, psi	6,200	5,200	3,800
Poisson's Ratio	.25	---	---
Coefficient of Thermal Expansion (in/in/°F) $\times 10^{-6}$ Parallel	4.0	6.6	7.6
Perpendicular	7.0	9.2	10.6
Thermal Conductivity, BTU/in/sec/°F $\times 10^{-4}$	0.116	---	0.40
Specific Heat, BTU/lb/°F	0.24	---	0.22
Char Temperature, °F	N/A	875	N/A
Heat of Pyrolosis, BTU/lb of volatiles	N/A	650	N/A
Density, lb/in^3	0.054	---	0.043

TABLE IX

NOZZLE MATERIALS
PHYSICAL AND THERMAL PROPERTIES OF PLASTICS

Type of Material: Phenolic Resin Impregnated Graphite
Fabric Tape per SB-SP-124

Supplier and Designation: U. S. Polymeric Chemicals, FM-5064

Material Form and Orientation: 45° Bias Tape, 30° Shingle Angle

Raw Material Description:

(a) Reinforcement   National Carbon's WCA Graphite Fabric
per SB-SP-131, Type II

(b) Resin   U.S.P. 39 Phenolic Resin per SB-SP-117,
Type I

(c) Resin Content   31 - 37 percent

(d) Filler and Percent   Carbonaceous, 3 - 14 percent

Physical and Thermal Properties:

Property	Values at Temperature		
	75°F	500°F	1000°F
Hoop Tensile Strength, psi	8,800	8,000	5,700
Hoop Tensile Modulus, psi × 10⁶	1.80	1.46	1.2
Hoop Flexural Strength, psi	13,600	---	---
Hoop Flexural Modulus, psi × 10⁶	1.80	---	---
Edgewise Compressive Strength, psi (hoop)	25,000	8,500	5,600
Edgewise Compressive Modulus, psi × 10⁶ (hoop)	1.7	.90	.40
Interlaminar Shear Strength, psi	1,000	---	---
Shear Strength Across Plies, psi	6,700	5,600	4,100
Poisson's Ratio	.25	---	---
Coefficient of Thermal Expansion (in/in/°F) × 10⁻⁶ — Parallel	4.0	6.6	7.6
Perpendicular	7.0	9.2	10.6
Thermal Conductivity, BTU/in/sec/°F × 10⁻⁴	0.116	---	0.40
Specific Heat, BTU/lb/°F	0.24	---	0.22
Char Temperature, °F	N/A	875	N/A
Heat of Pyrolosis, BTU/lb of volatiles	N/A	650	N/A
Density, lb/in³	0.054	---	0.043

TABLE X

NOZZLE MATERIALS
PHYSICAL AND THERMAL PROPERTIES OF PLASTICS

Type of Material   Phenolic Resin Impregnated High Silica Tape per SB-SP-125

Supplier and Designation: Fiberite Corporation, MX-2600

Material Form and Orientation: Warp-Cut Tape, Parallel to Centerline

Raw Material Description:

    (a)   Reinforcement   HITCO Refrasil Fabric C-100-48 per SB-SP-132 Type II

    (b)   Resin   SC 1008 Phenolic Resin per SB-SP-117, Type II

    (c)   Resin Content: 29 - 35 percent

    (d)   Filler and Percent   Silica Dioxide, 6 - 10 percent

Physical and Thermal Properties:

Property	Values at Temperature		
	75°F	500°F	750°F
Hoop Tensile Strength, psi	8,000	6,400	5,200
Hoop Tensile Modulus, psi $\times 10^6$	2.6	1.8	1.7
Hoop Flexural Strength, psi $\times 10^3$	12.9	9.0	7.6
Hoop Flexural Modulus, psi $\times 10^6$	2.6	1.6	.95
Edgewise Compressive Strength, psi (longitudinal)	12,000	11,000	5,600
Edgewise Compressive Modulus, psi (longitudinal)	1.5	1.0	.70
Interlaminar Shear Strength, psi	2,100	1,000	600
Shear Strength Across Plies, psi	---	---	---
Poisson's Ratio	.20	---	---
Coefficient of Thermal Expansion (in/in/$^\circ$F) $\times 10^{-6}$ Parallel	4.66	5.5	6.32
Perpendicular	22.2	26.0	29.8
Thermal Conductivity, BTU/in/sec/$^\circ$F $\times 10^{-4}$	.041	---	.10
Specific Heat, BTU/lb/$^\circ$F	.24	---	.20
Char Temperature, $^\circ$F	N/A	N/A	750
Heat of Ablation, BTU/lb of volatiles	N/A	650	N/A
Density, lb/in^3	.063	---	.056

TABLE XI

NOZZLE MATERIALS
PHYSICAL AND THERMAL PROPERTIES OF PLASTICS

Type of Material: Phenolic Resin Impregnated Bidirectional Glass Tape per SB-SP-126

Supplier and Designation: Fiberite Corporation, MX-4600

Material Form and Orientation: Warp-Cut Tape, Parallel to Centerline

Raw Material Description:

    (a) Reinforcement   181 Bidirectional Glass Fabric, A1100 Finish, per MIL-C-9084, Type VIII

    (b) Resin   Polyamid Modified Reichold 5900 Phenolic Resin per SB-SP-117, Type IV

    (c) Resin Content   17 - 22 percent

    (d) Filler and Percent   None

Physical and Thermal Properties:

Property	Values at Temperature		
	75 F	500 F	750 F
Hoop Tensile Strength, psi	50,000	32,000	15,000
Hoop Tensile Modulus, pxi $\times 10^6$	3.4	2.3	1.9
Hoop Flexural Strength, psi	70,000	21,000	6,100
Hoop Flexural Modulus, psi $\times 10^6$	3.8	1.0	0.5
Edgewise Compressive Strength, psi (longitudinal)	65,000	20,000	7,100
Edgewise Compressive Modulus, psi $\times 10^6$ (longitudinal)	1.9	0.4	0.2
Interlaminar Shear Strength, psi	1,800	900	500
Shear Strength Across Plies, psi	---	---	---
Poisson's Ratio	0.20	---	---
Coefficient of Thermal Expansion (in/in/F) $\times 10^{-6}$ Parallel	11	12.5	13
Perpendicular	50	56	60
Thermal Conductivity, BTU/in/sec/F $\times 10^{-4}$	3.8	---	9.1
Specific Heat, BTU/lb/F	0.22	---	0 18
Char Temperature, F	N/A	N/A	700
Heat of Ablation, BTU/lb of volatiles	N/A	650	N/A
Density, lb/in^3	0.070	---	0.060

TABLE XII

SUMMARIZED COMPARISON OF NOZZLE ABLATIVE COMPONENT
ULTIMATE TENSILE STRENGTH (As Determined From In-Process Samples)
WITH SPECIFICATION REQUIREMENTS
(156-2C-1)

Component	Minimum Specification Requirement SB-SP-2C, psi	In-Process Test Results, psi, Mean Standard Deviation
Entrance Cone FM 5063	10,200	14,500/800
Forward Throat FM 5064	7,200	19,400/3,000
Mid-Throat FM 5064	7,200	17,400/1,300
Aft Throat FM 5064	7,200	13,700/1,300
Exit Cone MX 4926	17,000	25,000/1,300
Exit Cone MX 2600	6,800	11,700/1,000

TABLE XIII

SUMMARIZED COMPARISON OF NOZZLE ABLATIVE COMPONENT
ELASTIC MODULUS (As Determined From In-Process Samples)
WITH SPECIFICATION REQUIREMENTS
(156-2C-1)

Component	Minimum Specification Requirement SB-SP-2C, psi	In-Process Test Results, psi Mean Standard Deviation
Entrance Cone FM 5063	2.2×10^6	$2.4 \times 10^6/.16 \times 10^6$
Forward Throat FM 5064	1.5×10^6	$2.9 \times 10^6/.65 \times 10^6$
Mid-Throat FM 5064	1.5×10^6	$1.8 \times 10^6/.86 \times 10^6$
Aft Throat FM 5064	1.5×10^6	$1.7 \times 10^6/.21 \times 10^6$
Exit Cone MX 4926	2.6×10^6	$2.8 \times 10^6/.26 \times 10^6$
Exit Cone MX 2600	2.2×10^6	$2.7 \times 10^6/.12 \times 10^6$

TABLE XIV

SUMMARIZED COMPARISON OF NOZZLE ABLATIVE COMPONENT
FLEXURAL STRENGTH (As Determined From In-Process Samples)
WITH SPECIFICATION REQUIREMENTS
(156-2C-1)

Component	Minimum Specification Requirement SB-SP-2C, psi	In-Process Test Results, psi, Mean Standard Deviation
Entrance Cone FM 5063	21,600	31,042/628
Forward Throat FM 5064	11,000	26,896/995
Mid-Throat FM 5064	11,000	22,018/702
Aft Throat FM 5064	11,000	20,421/529
Exit Cone MX 4926	25,500	40,427/1,101
Exit Cone MX 2600	11,000	20,450/273

TABLE XV

SUMMARIZED COMPARISON OF NOZZLE ABLATIVE COMPONENT
MODULUS OF ELASTICITY (As Determined From In-Process Samples)
WITH SPECIFICATION REQUIREMENTS
(156-2C-1)

Component	Minimum Specification Requirement SB-SP-2C, psi	In-Process Test Results, psi, Mean Standard Deviation
Entrance Cone FM 5063	1.5×10^6	$2.4 \times 10^6 / .08 \times 10^6$
Forward Throat FM 5064	1.0×10^6	$1.9 \times 10^6 / .09 \times 10^6$
Mid-Throat FM 5064	1.0×10^6	$1.6 \times 10^6 / .04 \times 10^6$
Aft Throat FM 5064	1.0×10^6	$1.7 \times 10^6 / .03 \times 10^6$
Exit Cone MX 4926	1.9×10^6	$2.9 \times 10^6 / .09 \times 10^6$
Exit Cone MX 2600	2.2×10^6	$2.5 \times 10^6 / .03 \times 10^6$

The MX-4600 phenolic-glass laminates were vacuum bag cured for the 156-2C-1 nozzle. The density and physical properties were, therefore, slightly reduced from those defined in Table XI. Density of the laminates averaged 0.063 pounds per cubic inch. Laboratory test results showed the average tensile strength to be 48,600 psi and the average modulus of elasticity to be 3.1 $\times 10^6$ psi.

Tensile strength of the polyester-glass tie laminate of the 156-2C-1 nozzle was lower than indicated attainable by laboratory testing. Tested specimens from in-process control panels showed the tensile strength to be 38,300 psi.

The circumferentially wound roving developed a hoop tensile strength of 161,000 psi with a hoop tensile modulus of 6.2 $\times 10^6$ psi. These values were obtained from in-process control tests.

V. STRUCTURAL AND THERMAL ANALYSIS

The structural and thermal analysis for the large nozzle design was conducted at the Huntsville Division of Thiokol Chemical Corporation. The results of this analysis are presented in Volumes I and II of Huntsville Division Report "Thermal, Structural, and Dynamic Analysis of the Nozzle for the One-Half Length 260-Inch Diameter Space Booster Motor", dated August 1963. The analysis was based on the design as it existed at that time using the available ablative properties. The flange area of the large nozzle shell was analyzed in combination with the 156-inch case in a Huntsville Division report entitled, "Structural and Dynamic Analysis of the 156-2C-1 Inch Diameter Space Booster Motor Case", dated March 10, 1964. The analysis of the nozzle was accomplished in the following four phases:

    1. Convective heat transfer and jet separation analysis

    2. Thermal analysis

    3. Dynamic analysis

    4. Thermal and pressurization stress analysis

The following is a brief summary of the phases investigated. The details for each phase are presented in the analyses referenced above. For phase four, the method of analysis and margins of safety are discussed below:

    1. Convective heat transfer and jet separation analysis was divided into three areas of study:

        a. Computation of the convective heat transfer in nozzle during normal operation.

        b. Determination of the effects of the boundary layer of the nozzle flow.

        c. Computation of the pressure distribution in the nozzle during the time that flow was separating from the wall of the nozzle.

    2. Thermal Analysis

        This study was conducted to determine the thermal response characteristics of the nozzle during motor operation. As a part of the study, thermal data from previous experimental nozzle tests were analyzed. Based upon this experimental data, erosion and char profiles through various cross-sections in the Space Booster nozzle were predicted. Independent of this prediction (based upon experimental results) analytical predictions of char profiles and temperature gradients were also performed.

These char and erosion profiles were utilized to determine whether or not adequate insulation had been provided in the nozzle design.

Thermal gradients through the various cross-sections of the nozzle were predicted in support of the thermal stress calculations.

3. Dynamic Analysis

Three environmental conditions that could affect the dynamic behavior of the nozzle were investigated: (a) the sudden pressure rise during motor ignition, (b) thrust and internal pressure variations resulting from normal motor operation, and (c) pressure variation on the external surface of the nozzle caused by noise generated in the exhaust stream of the motor.

Three types of dynamic motion of the nozzle that could be excited by the above environments were investigated. These were: (a) lateral vibration of the nozzle exit cone as a cantilever beam, (b) radial vibration of circular sections along the length of the nozzle, and (c) flexural vibration of circular sections along the length of the nozzle.

4. Thermal and Pressurization Stress Analysis

As previously discussed, the large nozzle design for the 156 and 260-SL motors consists of structures of erosion and heat resistant, tape wound, phenolic impregnated plastic materials, bonded to a partial-length steel shell. The exit cone is also structurally connected to the shell with a bidirectional glass laminate. The tie laminate is locked to the shell with circumferentially wound glass roving. The structure is subjected to the action of internal pressure during static test. The magnitude of the pressure varies along the nozzle axis. Also, the structure undergoes loading resulting from the thermal expansion of the inner face caused by contact with the motor exhaust gases. Supplementary loading conditions include dynamic effects during static test, and handling and transportation loads. The effects of the loading conditions are documented in "Special Report - Thermal, Structural, and Dynamic Analysis of the Nozzle for the One-Half Length 260 Inch Diameter Space Booster Motor" dated August 1963, and prepared by the Thiokol Chemical Corporation Huntsville Division.

A three-dimensional rigorous solution for thermal
loading of conic elements is not available; it was
considered, however, that a reasonable analytical
technique would consist of representing the nozzle
cross-section, at several stations along its length,
by a series of radially symmetrical thick-walled
concentric cylinders of curvatures comparable to
the cones. The deflections at inner and outer
faces of each cylinder could then be determined as
a function of the cylinder's temperature change and
the interface pressures between it and the next
inner and next outer cylinders. (For the inner-
most and outermost cylinders, of course, the
nozzle internal and external pressures were used.)
By equating deflections of the two cylinders at each
interface, the interface pressures may be deter-
mined, hence the stresses throughout the model.
The advantage of using this type of analysis is that
the effects of a radial variation in material pro-
perties and temperature can be studied. The
radial temperature distribution was approximated
by assuming the temperature distribution in each
cylinder to be linear. By sub-dividing the nozzle
cross-section into very small cylinders (approxi-
mately 0.1-inch thick) the continuous radial tem-
perature distribution obtained from a heat transfer
and ablation analysis was approximated. The
radial variation in material properties (due to
variation in temperature) was approximated by
assuming the material properties constant for
each cylinder but using values at the average tem-
perature of each cylinder, a fairly good approxi-
mation since each cylinder was relatively thin.
All materials were considered to be linearly
elastic.

One of the more difficult problems in such an
analysis is the selection of material properties
which are representative of the insert materials.
The state of technology of manufacturing reinforced
plastic structural components is far in advance of
the mechanical characterization of these materials.
As the elastic properties of the tape wound graphite
and insulation materials are temperature depen-
dent, stress magnitudes are only as realistic as
the assigned mechanical properties. Further,
stated values for the material properties are
based on uniaxial stress fields. In order to deter-
mine the influence of material properties on the
calculated stresses, a short parametric study
was conducted of the effects of the coefficient of
thermal expansion of insert material and the

modulus of the charred material on the induced
thermal stresses, based on the predicted tem-
perature distribution at the nozzle throat at
20 seconds after ignition. (The material above
1000 F, for the entrance and throat sections and
750 F for the exit section was considered to be
charred.) It was determined that a variation in
the modulus of the charred material results in
an appreciable variation in the hoop stress at
the inside diameter of the nozzle; however, the
hoop stresses at the char line (1000 F) and at
the outside diameter of the graphite insert are
not appreciably affected. Therefore, it appeared
that with reasonable mechanical property values
for the material below 1000 F reasonable evaluations
would be obtained of stresses in the uncharred
material without having precise mechanical pro-
perty values for the charred material. However,
if the coefficient of thermal expansion of the in-
sert material were doubled the hoop stress also
would be doubled. This illustrates the importance
of selecting an insert material with a low coeffi-
cient of thermal expansion.

This analytical technique was applied for various
times during static firing. At ignition, the ma-
terials were assumed to be at ambient temper-
ature in order to obtain maximum tensile stress
magnitudes; predicted thermal conditions at
later times during the firing were employed. Fur-
ther analyses were performed to determine the
effects of geometric discontinuities in the nozzle
shell. These analyses employed essentially the
same technique which was used for discontinuities
in the case.

Margins of safety for the steel components were
evaluated for the design value of 875 psi maximum
expected instantaneous pressure level coupled with
the associated erosion, ablation and thermal gra-
dients at various intervals from ignition to 135
seconds burning time. In addition, stresses due
to the dynamic environment have been judiciously
combined with those due to thermal pressurization
loading where applicable. These margins are
tabulated below for the 156-inch motor, where the
nozzle shell was attached directly to the case aft
dome, and for the 260-inch motors where an
adapter section was to be used between the nozzle
and the case aft dome.

SAFETY MARGINS FOR
STEEL COMPONENTS

	156-Inch Motor	260-Inch Motor
Nozzle Membrane	+ .61	+ .497
Nozzle Shear Lip	+ 3.93	+ 2.75
Bolts-NAS 632-3/4-Inch Diameter 180 Ksi ult.	+ .60	+ 1.24 nozzle to adapter + .615 adapter to case
Adapter membrane to nozzle	--	+ 1.33
Adapter membrane at case	--	+ 2.19
Adapter shear lip	--	+ .533

For the 260-inch motors, these margins are based
on identical aft dome and adapter configurations;
separate checks were performed to assure, for the
first 260-inch case, that minor increases of adapter
membrane thickness would have no significant effect.

The nozzle exit cone section was checked for elastic
stability during jet separation at tail-off. Using
average separation pressures to compute normal
radial pressure loadings over the entire effective
length of the exit cone, an extremely conservative
assumption, a positive margin of + 16 percent was
determined.

Due to thermal and internal pressurization combined,
at an action time of 135 seconds, the minimum mar-
gins of safety in the nozzle ablatives lie at the char
line, assumed to be at a constant temperature of
1000°F for entrance and throat sections, and 750°F
for the exit section, and were determined to be:

Station 2 (Nozzle Entrance Section): +15%, based
on axial compression of the carbon tape.

Station 3 (Fwd. of the Throat Section): +25%, based
on axial compression of the graphite tape.

Station 4 (Throat Section): +32%, based on hoop
compression of the graphite tape.

Station 5 (Aft of the Throat Section): +31%,
based on hoop compression of the carbon tape.

Station 6 (Nozzle Exit Plane): +12%, based on
axial compression.

Note: In computing this margin, a material
property value of 5600 psi at 750°F
was used for the High Silica Phenolic
Resin System insulation. This value
is extremely conservative.

It should be noted that these margins of safety are
are based on an assumed "char line" of the in-
sulation materials which is a few mils thick and
at a stagnation temperature of 1000°F (or 750°F
depending upon the materials and the locations
where they are used). These char line stresses
are both hoop and axial compression. Due to the
steep thermal gradients, the stress magnitudes
vary rapidly to both hoop and axial tension on the
O.D. of the insulation materials. It is difficult
to see how even localized compression yielding
over a few mils thickness at the char line could
predicate component "rupture". The stated mar-
gins of safety, based on component failure are
thus believed to be conservative.

Calculated stresses in the charred graphite ma-
terial on the throat I.D. were in excess of 25,000
psi hoop compression. This value greatly exceeds
the quoted char strength at ambient temperature.
However, as the charred layer is highly porous and
not isotropic and elastic, this value is fictitious;
compressive loads can compress the cellular struc-
ture, relieving its stresses as well as those in the
adjacent non-charred material.

VI. FABRICATION

A.   156-2C-1 NOZZLE FABRICATION

1. Steel

a. Fabrication Approach

When fabrication on the nozzle and nozzle adapter shell was initiated, the following sequence of operations was the planned fabrication approach:

1. Each conical section of the shell would be fabricated by longitudinally welding together six segments of plate which had been cold formed to the correct contour.

2. Each attachment flange would be made from a rolled-ring forging.

3. The attachment flanges and the conical sections would be joined by circumferential welds.

4. All welds would be deposited using the two-pass submerged-arc process for which Rohr had been qualified (see Section IX. A. 5. of this report for welding parameters and properties obtained).

5. The welded assembly would then be nondestructive tested and aged to obtain 230, 000 psi yield in the parent metal.

6. The aged component would then be machined to the configuration shown on Thiokol drawing 1S 11004 or 1S 11005 as applicable.

After several longitudinal welds had been deposited in the first unit and the first couple of conical rings had been fabricated, the following problem areas developed:

1. The high heat, developed by the high energy input, of the second weld pass caused a massive heat-affected zone in the as-deposited first pass weld metal. The high stresses in the heat affected zone (HAZ) resulted in cracking of the first pass.

2. The material distortion, due to the high energy in the two-pass submerged-arc weld, was much higher than anticipated at the time of material purchase; hence, the thickness was not adequate for clean-up of the final part.

3. The sub-arc weld repair procedures which had been
successfully proven during the welding qualification
program would not work on a production weld with
the weld metal in the as-welded condition.

4. A portion of the first weld pass, in the submerged-
arc two-pass weld, in material approaching the 1.5-
inch thickness range would not attain the mechanical
properties required when aged. This condition was
caused by the reverted portion of the HAZ in the first
pass as a result of the energy of the second pass.

NOTE: The four problem areas listed above will be
discussed in detail along with other steel
problems in Section IX. A. 5. of this report.

The following actions were taken in an effort to solve or work around the
problems listed above:

1. To prevent the second pass HAZ from cracking the
first pass, the part was reverted after welding the
first pass. This reversion was accomplished at
1250° F with a one-hour soak at temperature.

   In addition to reversion, pre and post-heat were
   added to the welding sequence. This was done to
   insure against hydrogen pick-up which could cause
   transverse weld cracking.

2. In order to counteract the distortion due to the weld-
ing and the reversion cycle added by Item 1., above,
and to return the material to a condition where it
could be aged, it was necessary to add an anneal
cycle. The addition of the revert and anneal cycles
resulted in material shrinkage (see Section IX. A. 5.
of this report), which had not been accounted for in
the original part design. Since the shrinkage would
result in a lack of clean-up stock, an anneal and size
cycle was added as an attempt to regain the original
configuration.

3. The attempts to repair a production part with sub-
arc welding resulted in cracks being formed in
previously sound weld metal. The sub-arc weld
repair was discontinued for all defects other than
a long area of lack of fusion or lack of penetration,
and a procedure was established for repairing by the
tungsten inert gas (TIG) process.

4. The addition of the reversion cycle between weld
passes made an anneal cycle necessary after all
welding had been accomplished. The final anneal
cycle removed an additional problem area, namely

the reverted zone in the first pass which
previously had not responded to aging.

After the problem areas discussed above had been resolved, the fabrication
approach for the nozzle shell and nozzle adapters was revised to reflect the
following:

1. Six or more segments of the required plate
thickness were cold or hot formed to the
correct contour (the entrance cone segments
of the nozzle shell were hot formed and all
others were cold formed).

2. After all segments were longitudinal weld
prepped, they were placed on a weld jig with
start and run-off tabs welded in place. All of
the outside longitudinal weld passes were de-
posited.

3. The conical ring was then placed in a furnace
and maintained at 1250° F for one hour.

4. The second pass side of each joint was then
prepared for welding by arc-air gouging or
machining and the second weld pass was de-
posited.

5. The conical section was then subjected to one or
more anneal and size operations to obtain the
correct dimensions in order to allow the cir-
cumferential weld joints to be machined on each
end. The part was sized by placing it over the
welding fixture immediately on removal from
the furnace.

6. Nondestructive radiographic and dye penetrant
testing of the longitudinal welds was conducted
at this time.

7. For nozzle shell fabrication, all of the three con-
vergent cones and the flange forging were stacked
and the outside circumferential weld pass deposited.
The unit was then reverted and the inside of the
same joint was prepared and welded. The unit was
annealed, sized, and then prepared for welding to
the divergent cone section. The outside pass of
this weld was then deposited, torch reverted, pre-
pared for welding, and welded on the inside without
cooling down.

8. Each of the components was then annealed and sized
to obtain the correct dimensional control.

9. The unit was then subjected to complete non-destructive testing consisting of radiographic, ultrasonic, and dye penetrant inspections.

10. The component was then aged to obtain the required properties.

11. The aged assembly was machined on both the inside and outside to obtain the configuration shown on Thiokol drawing 1S 11004 or 1S 11005, as applicable.

12. After the machining, all the welds were given radiographic, ultrasonic, and dye penetrant inspection.

13. When the component was completely acceptable, the holes were drilled and tapped, as required.

14. The part was then prepared for shipping or assembly.

b. Material Acceptance and Properties

All plate and forging materials purchased for use in the Unit No. 1 and No. 2 nozzle shell were accepted on the basis of Thiokol specification SB-SP-174. Tables XVI and XVII show a breakdown of the plate and forging materials going into each component and a summary of the properties of each plate or forging. As indicated by the tables, most of the material had to be solution annealed one or more times in order to obtain reproducible properties in the longitudinal and transverse directions; however, as the fabrication approach was resolved, all of the material actually received one or more additional anneals after it had been welded into the component.

The weld wire used in the submerged-arc processes was purchased to Thiokol specification SB-SP-7 with a titanium content which was changed after fabrication had been initiated in an effort to improve the fracture toughness of the weld. During fabrication the titanium content was changed from an initial level of 1.2% to the 0.55 to 0.70% range. The wire used for all TIG repairs was in the 0.40 to 0.50 titanium content range.

The flux used throughout all welding was Linde 105 Lo-Sil. This flux was developed especially for welding maraging steel. With the high energy input required by the section thickness, it was impossible to use the Linde 105 special No-Sil No-Mn flux used for a time in case fabrication.

After the fabrication of the Unit No. 1 nozzle shell had progressed through all the required repair cycles, which included a reversion cycle to stop crack propagation, it was annealed twice to obtain the correct dimensional control and then aged. Considerable difficulty was encountered in controlling the furnace at the desired temperature rise rate and tolerance ranges. Figure 5 shows the various welds which form the Unit No. 1 nozzle shell. Table XVIII presents a comparison of the tensile and fracture

TABLE XVI

PLATE

Material Used for Fab. of	Plate No.	Heat No.	Direction	Yield (ksi)	Ultimate (ksi)	Percent Elongation	Percent R/A	Fracture Toughness ☆
Unit No. 1 Nozzle Shell	197052 Note 1	USS X53089	Long. / Tran.	231.2 / 234.1	241.8 / 241.8	11.8 / 9.8	47.1 / 39.0	W/A = 782 / W/A = 827
Units No. 1 and 2 Nozzle Shell	197058 Note 1	USS X53089	Long. / Tran.	235.2 / 229.5	244.4 / 239.2	13.7 / 11.0	48.1 / 46.8	W/A = 1001 / W/A = 804
Units No. 1 and 2 Nozzle Shell	197059A Note 1	USS X53089	Long. / Tran.	240.0 / 239.0	250.7 / 247.2	10.1 / 8.8	36.3 / 36.3	W/A = 1073 / W/A = 904
Units No. 1 and 2 Nozzle Shell	197059B Note 1	USS X53089	Long. / Tran.	236.1 / 241.0	244.8 / 247.3	12.0 / 12.7	46.1 / 42.4	W/A = 962 / W/A = 834
Units No. 1 and 2 Nozzle Shell	41707 Note 1	USS X53471	Long. / Tran.	239.8 / 240.2	248.9 / 249.5	10.9 / 11.0	44.5 / 47.0	C_L = 0.240 / C_L = 0.208
Unit No. 1 Nozzle Adapter	41705 Note 2	USS X53471	Long. / Tran.	239.4 / 241.7	248.8 / 250.0	11.3 / 10.5	45.5 / 44.5	C_L = 0.240 / C_L = 0.200
Unit No. 2 Nozzle Shell	N-5 Note 4	Cameron 50236-3	Long. / Tran.	231.8 / 234.3	241.1 / 244.4	12.9 / 12.5	52.8 / 49.9	C_L = 0.250
Unit No. 2 Nozzle Adapter	RO-2 Note 3	Cameron 50339-B2	Long. / Tran.	250.3 / 250.5	257.6 / 258.9	10.5 / 10.8	44.7 / 44.1	C_L > 0.265
Unit No. 2 Nozzle Shell	4 A-1 Note 5	USS X53541	Long. / Tran.	232.0 / 231.3	240.0 / 239.7	11.5 / 11.0	48.0 / 44.0	C_L > 0.250

☆ Fracture toughness - W/A in lb/in^2) obtained from pre-cracked Charpy bars; C_L (inch) obtained from partial crack tensile bars.

NOTES: 1. Plates received one re-solution anneal at 1650°F for one hour per inch thickness. These properties represent plate after anneal.
2. These properties represent this plate after one anneal at 1650°F and a final anneal at 1500°F.
3. Plates received double anneal at 1650°F.
4. Plates received double anneal, 1650°F and 1600°F.
5. Plates received three anneals 1650°F, 1550°F, and 1510°F.
6. All aging cycles three hours at 900°F except for plate 4 A-1 which received four hours at 835°F.
7. Values for tensile properties and W/A are average of a minimum of three tests.

35

TABLE XVII

FORGINGS

Material Used for Fab. of	Forging Identification	Specimen Orientation	Specimen Location (degrees)	Yield Strength (ksi)	Ult. Tensile Strength (ksi)	Elongation (percent)	Reduction of Area (percent)	W/A PCl (in-lbs/in^2)
Unit No. 1 and Unit No. 2 Nozzle Shell	IS 11004-806 No. 1 and No. 2 Note 1	Circumferential	0	238.1	249.9	10	49	629
			180	236.9	249.3	10	49	639
		Axial	0	239.4	248.1	6	30	576
			180	238.0	249.5	7	35	579
		Radial	0	235.5	245.4	8	32	481
			180	232.0	242.3	8.5	36	579
Unit No. 1 Adapter	IS 11005-804 Unit No. 1 Large Attachment Flange	Circumferential	0	248.1	260.1	11	53	573
			180	246.1	257.1	10	50	568
		Radial	0	248.0	258.1	5	20	357
			180	248.0	257.5	4.5	21	324
	IS 11005-805 Unit No. 1 Small Attachment Flange	Circumferential	0	251.2	262.5	10	49	541
			180	248.9	260.4	10.5	50	408
		Radial	0	246.0	258.3	2.5	9	391
			180	247.5	261.5	4.5	16	369
		Axial	0	246.2	256.3	7	33	471
			180	248.4	257.5	7	30	483
Unit No. 2 Adapter	IS 11005-804 Unit No. 2 Large Attachment Flange	Circumferential	0	241.4	251.7	10	49	740
			180	241.2	250.7	11	51	733
		Radial	0	240.6	250.0	5.5	24	391
			180	240.0	250.6	9	25	401
		Axial	0	236.9	246.7	5	20	487
			180	237.0	247.8	5.5	25	524
	IS 11005-805 Unit No. 2 Small Attachment Flange	Circumferential	0	240.2	249.9	10	44	693
			180	240.6	250.5	9.5	40	731
		Radial	0	239.5	249.1	6	22	376
			180	238.7	248.3	4.5	17	376
		Axial	0	236.7	246.7	5.5	25	513
			180	237.2	246.2	6	24	580

NOTE:

1. All specimens double annealed at 1650°F.
2. All specimens aged at 900°F for three hours.
3. All tensile values represent an average of two bars.
4. All W/A values represent an average of three tests.

36

NOTE:
 1. CIRCUMFERENTIAL WELDS ARE J, K, L, AND M
 2. LONGITUDINAL WELDS ARE A, B, C, AND D
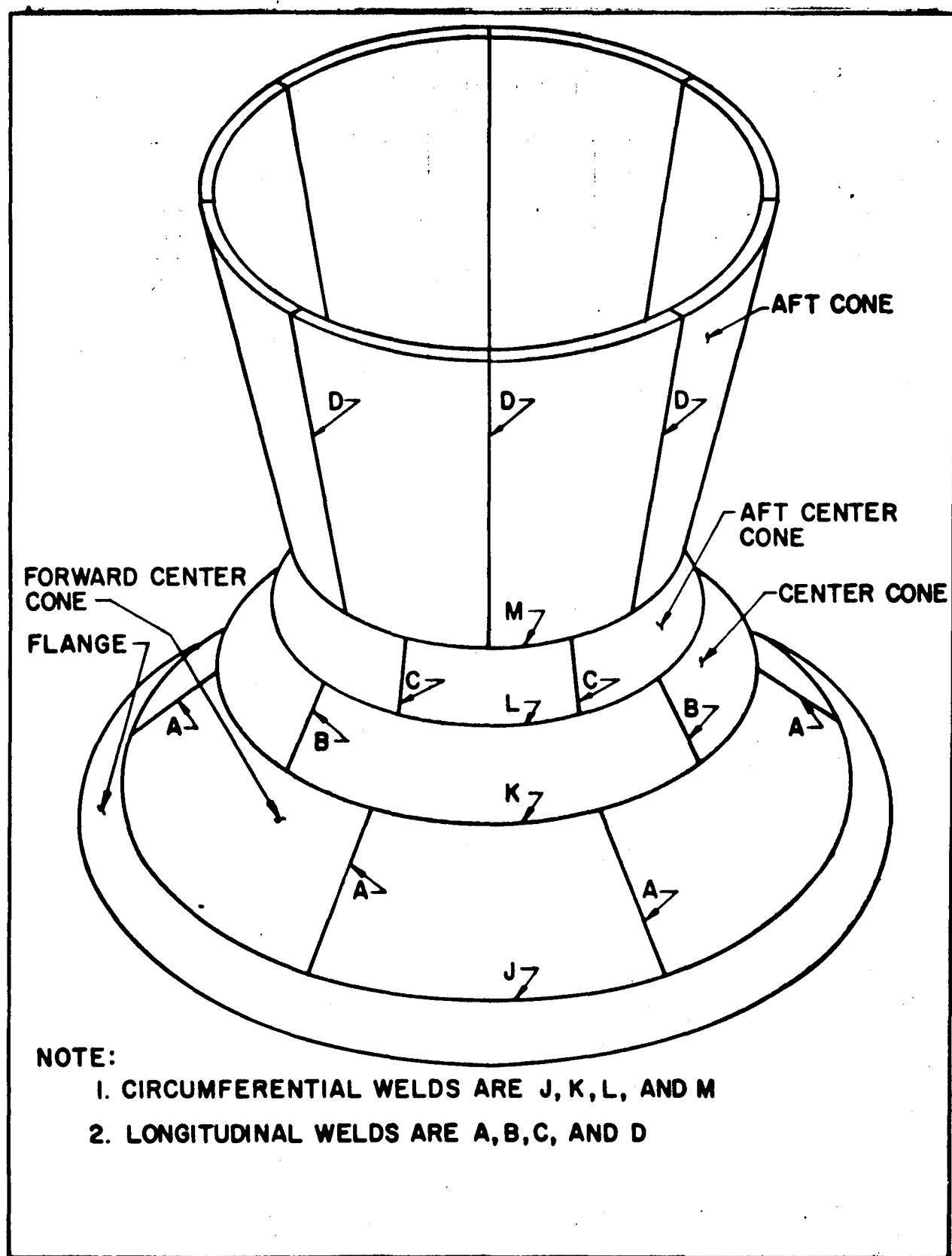
Figure 5 - 156-2C-1 Nozzle Steel Shell Circumferential and Longitudinal Welds

37

TABLE XVIII

COMPARISON OF 156-2C-1 NOZZLE AGED STEEL SHELL PROPERTIES

Plate Identification	Test Direction	Yield Strength (ksi)	Ult Tensile Strength (ksi)	Elongation (%)	Reduction of Area (%)	Fracture Toughness W/A (In. lb/in.^{2})
Heat X53089 Plate 197052	Parent material 0.505 inch dia.	220.7 218.5 221.9	236.1 237.4 237.1	8.5 8.5 9.0	35.6 35.7 37.3	N/A N/A N/A
Forward center cone	Weld-A longitudinal 0.505 inch dia.	223.4 222.7 220.3	237.2 236.4 235.7	7.5 7.5 7.5	29.3 33.7 33.0	321 325 380
	0.252 inch dia.	225.8 226.0 224.0 225.3	233.0 234.0 236.0 234.1	7.8 9.0 8.0 5.1	35.4 40.5 31.0 22.8	414 411 399
	Weld-J circumferential 0.505 inch dia.	220.6 218.1 219.8	234.4 233.8 235.7	5.5 6.5 6.0	21.3 26.3 21.8	250 244 249
	0.252 inch dia.	217.2 218.9 225.8 229.4	224.0 226.0 233.0 234.0	6.0 8.0 5.5 7.0	25.5 34.7 23.4 27.6	262 254 226
Heat X53471 Plate 041707	Parent material 0.505 inch dia.	225.3 218.1 219.8	238.7 235.1 234.9	9.5 10.5 10.8	41.6 43.0 42.7	N/A N/A N/A
Center cone	Weld-B longitudinal 0.505 inch dia.	227.3 217.2	241.0 233.1	7.5 ☆	19.5 ☆	N/A N/A
	Weld-K circumferential 0.505 inch dia.	218.3 216.8 217.4	232.2 231.9 232.5	3.5 6.0 7.0	8.6 19.7 24.9	243 266 242
	0.252 inch dia.	225.0 225.8 223.0 220.9	232.1 233.0 232.1 231.1	5.0 7.0 7.0 8.5	19.7 21.9 25.6 32.1	405 273 246
Heat X53089 Plate 197058	Parent material 0.505 inch dia.	217.9 220.1 217.5	233.5 236.2 233.7	10.0 7.5 9.0	38.4 30.3 37.5	N/A N/A N/A
Aft center cone	Weld-C longitudinal 0.505 inch dia.	222.7 221.9 222.3	235.1 234.5 235.9	7.0 4.0 9.5	30.4 13.4 42.7	277 243 239
	0.252 inch dia.	228.3 233.4 228.6 225.9	236.3 239.9 237.9 235.4	2.5 6.0 9.0 7.0	37.8 29.9 33.2 26.8	301 297 246
	Weld-L circumferential 0.505 inch dia.	222.3 219.4	240.2 237.9	5.5 8.2	18.7 31.0	276 272 269'
	0.252 inch dia.	228.9 234.9 231.3 231.4	240.2 242.2 241.7 240.7	5.5 5.0 6.5 6.5	22.8 14.0 22.8 24.4	248 229 267
Heat X53089 Plate 197059	Parent material 0.505 inch dia.	213.8 218.1 214.3	232.6 235.9 234.0	10.0 9.5 11.0	37.8 38.4 37.1	
Aft cone	Weld-D longitudinal 0.505 inch dia.	215.4 215.9 212.9	233.0 231.0 230.0	9.5 7.0 8.5	38.7 29.6 29.2	
	0.252 inch dia.	221.9 222.7 223.4 225.4	236.2 233.3 233.5 233.5	3.0 1.5 8.5 8.0	8.7 4.0 28.0 30.6	
	Weld-M circumferential 0.505 inch dia.	218.1 221.0 216.7	228.8 234.7 233.1	1.0 10.5 10.0	2.0 41.5 42.1	207 219 231
	0.252 inch dia.	228.6 226.5 232.4 223.0	237.0 235.5 240.9 234.2	4.0 5.0 9.0 3.5	8.3 13.0 9.0 16.9	227 216 220

☆ Failed outside of gage length

toughness properties obtained for the steel shell parent material and weld metal. The properties shown indicate the part aged more than intended and it is believed this condition resulted from too long a heating time above the range of 675 - 700°F.

A further discussion of heat treatment problems in connection with the adapter is found in Section VIII, and other problems and their solutions during fabrication of the Unit No. 1 nozzle steel shell are discussed in Section IX. F.

2. Ablatives

a. Fabrication Approach

The ablative components were fabricated using phenolic tape impregnated materials wrapped on an inside mandrel. The mandrels were fabricated from rolled and welded sections of boiler plate steel. The entire series of mandrels were match-machined in order to obtain the required inside contour on the ablative. The detail of the mandrel design is shown on Thiokol tooling drawing ST 20206. Figure 6 shows the assembled mandrel used for wrapping the 156- and 260-inch ablative exit cones.

Each of the ablative components was wrapped on its respective mandrel section with wrapping head designs which were developed along with the wrapping technique which will be described elsewhere in this report. The wrapping heads for these ablatives contain all the necessary equipment for applying temperature, pressure and tension to the tape as it passes through the head. Three of these wrapping heads were purchased from Edwards Enterprises of San Carlos, California, per the wrapping requirements as they were known at the time of purchase and to the configuration shown on the following drawings:

1. ST 20241 WRHD - Head for wrapping warp-cut tape parallel to centerline, (Figure 7).

2. ST 30205 WRHD - 1 and -2 - Heads for wrapping of bias-cut tapes at angles of 30 to 60 degrees to centerline, (Figure 8).

Figures 7 and 8 show the heads being used for experimental wrapping operations. Extensive modifications were required on all three heads to adapt them to the specific processes used in fabrication of the 156- and 260-inch ablative components. The method and parameters for tape wrapping are covered in detail in Section IV. C and E of RPL-TDR-64-101.

Following the completion of wrapping, the components were bagged and placed in a hydroclave for cure. Figure 9 shows the entrance cone ablative for the 156-inch nozzle being prepared for cure in the 175-inch-diameter, 350-inch deep hydroclave at the Rohr facility. The entrance cone, exit cone, and forward throat ablatives for the 156- and 260-inch motor nozzles were cured in this hydroclave while the mid and aft throat ablatives for these nozzles and all 65-inch subscale ablatives were cured in a smaller hydroclave.
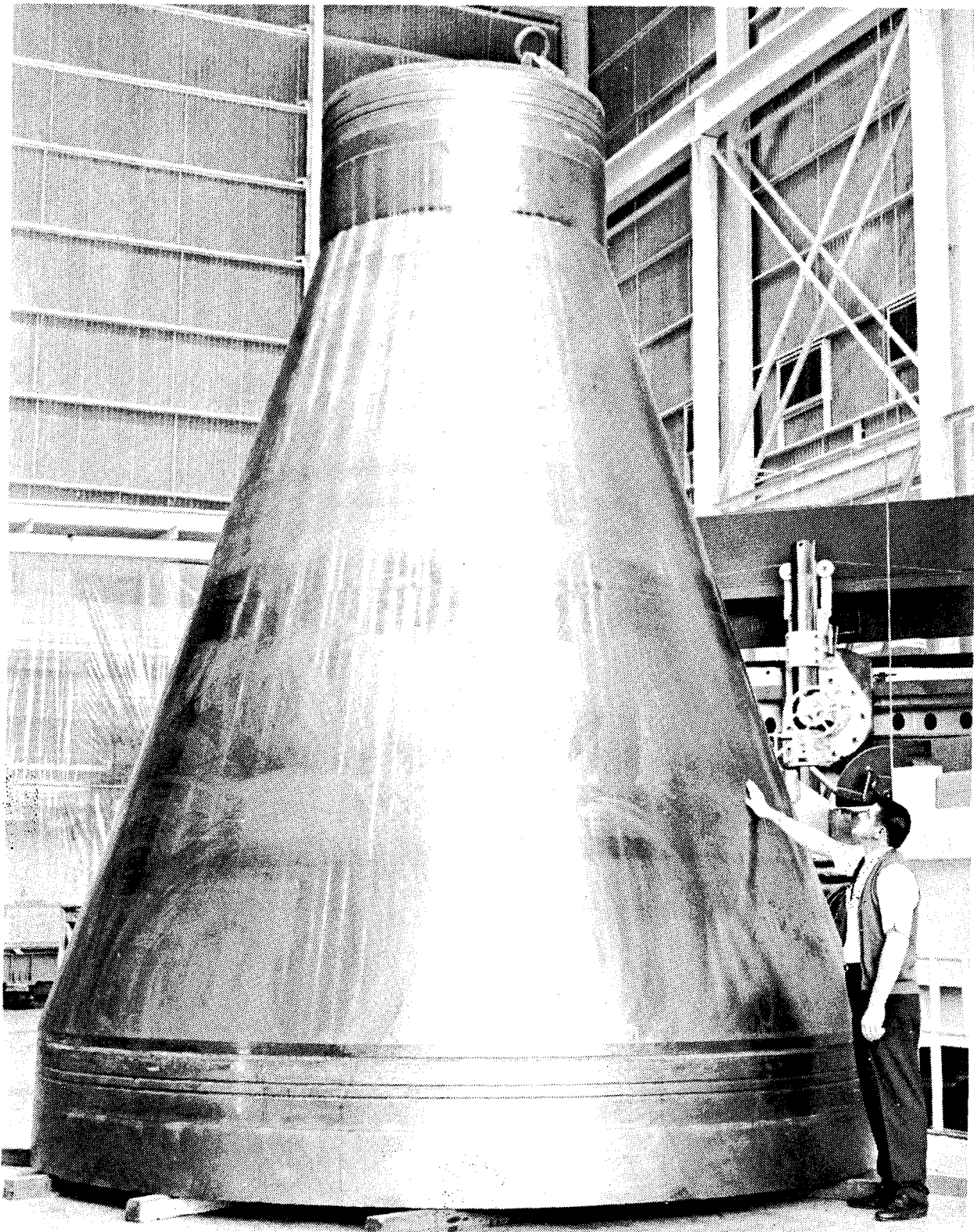
Figure 6 - Mandrel for Wrapping of Exit Cone
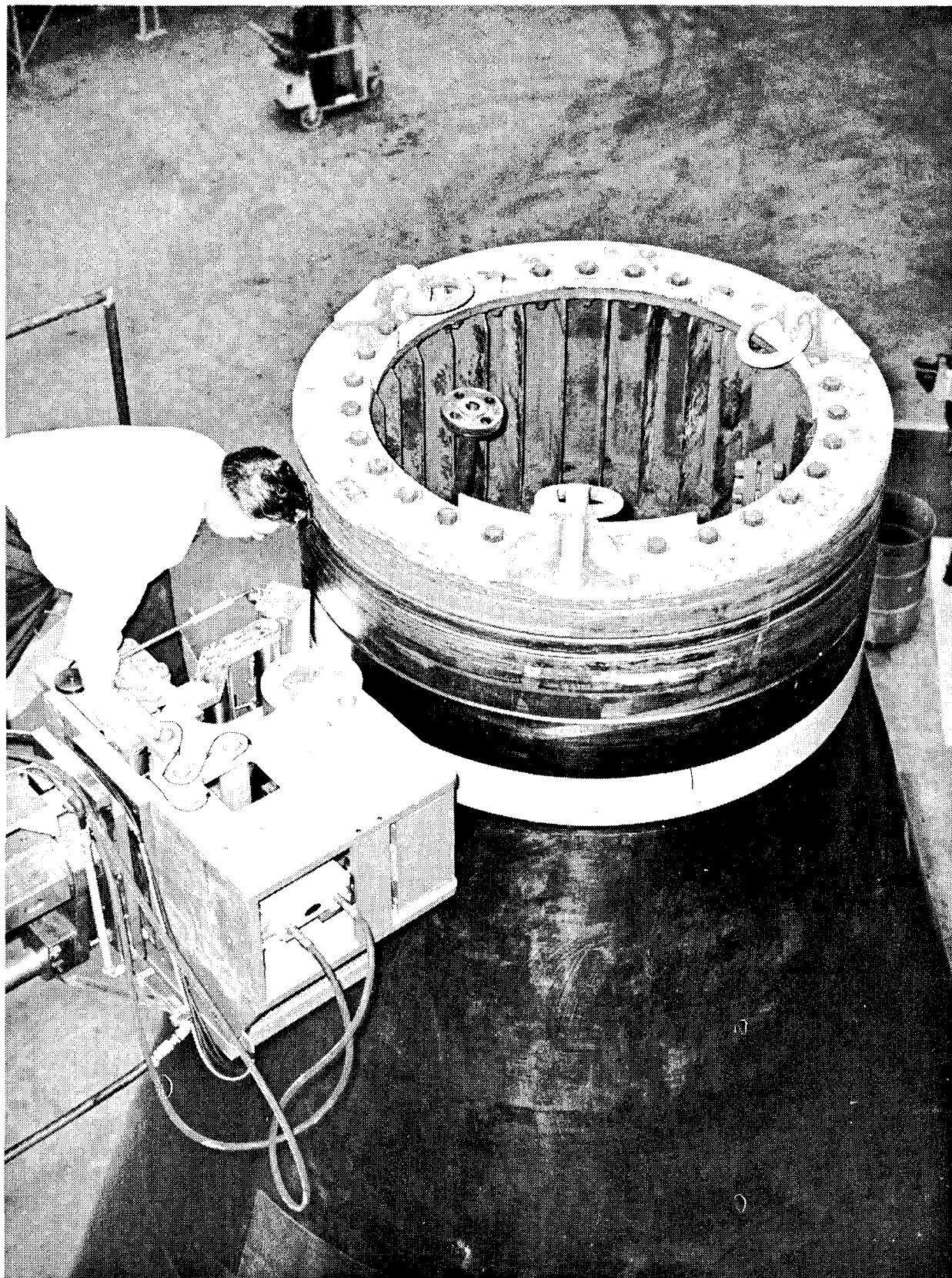
Figure 7 - Tryout of the Parallel to Centerline Wrapping Head on the Exit
Cone Mandrel

41
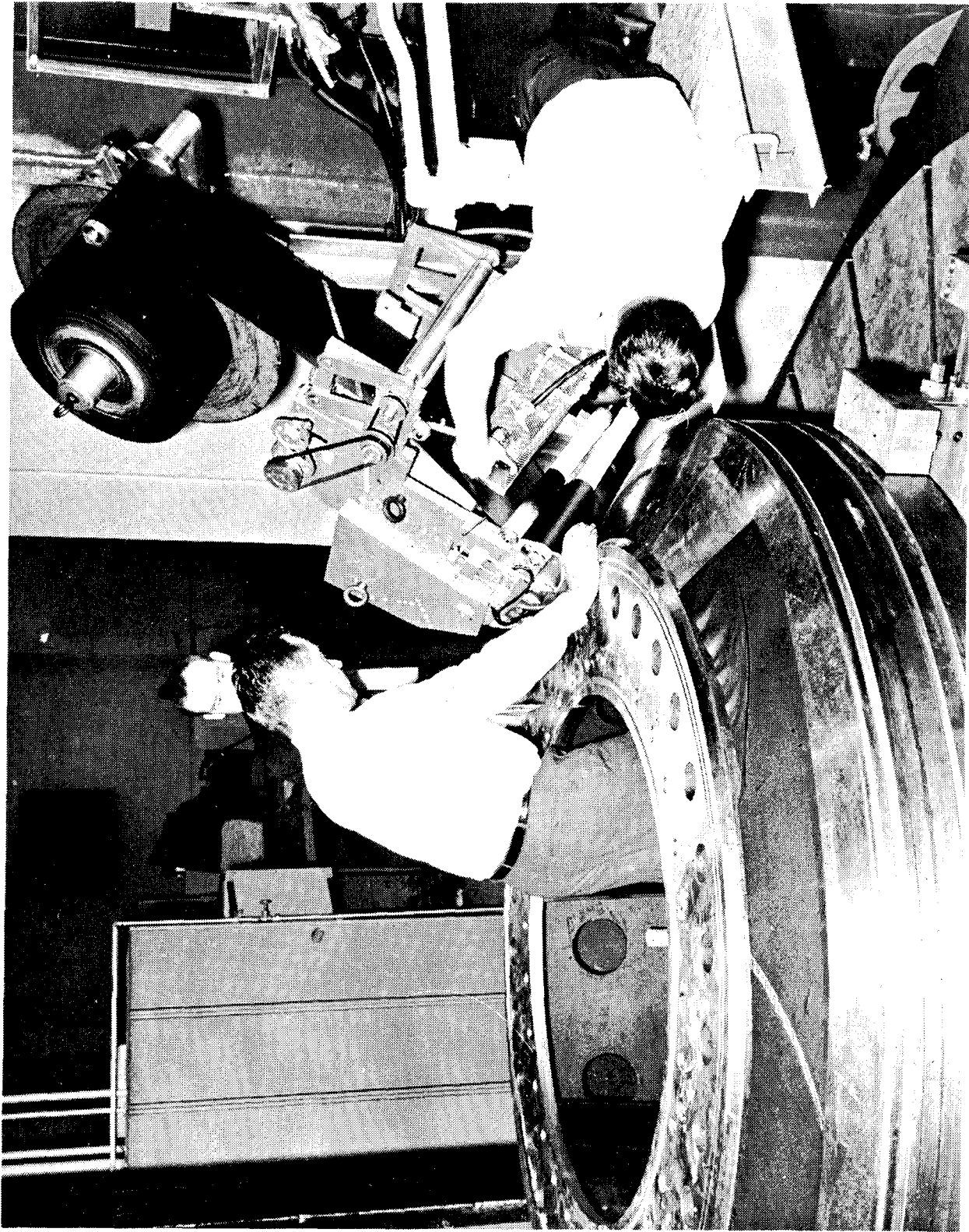
Figure 8 - Wrapping Head
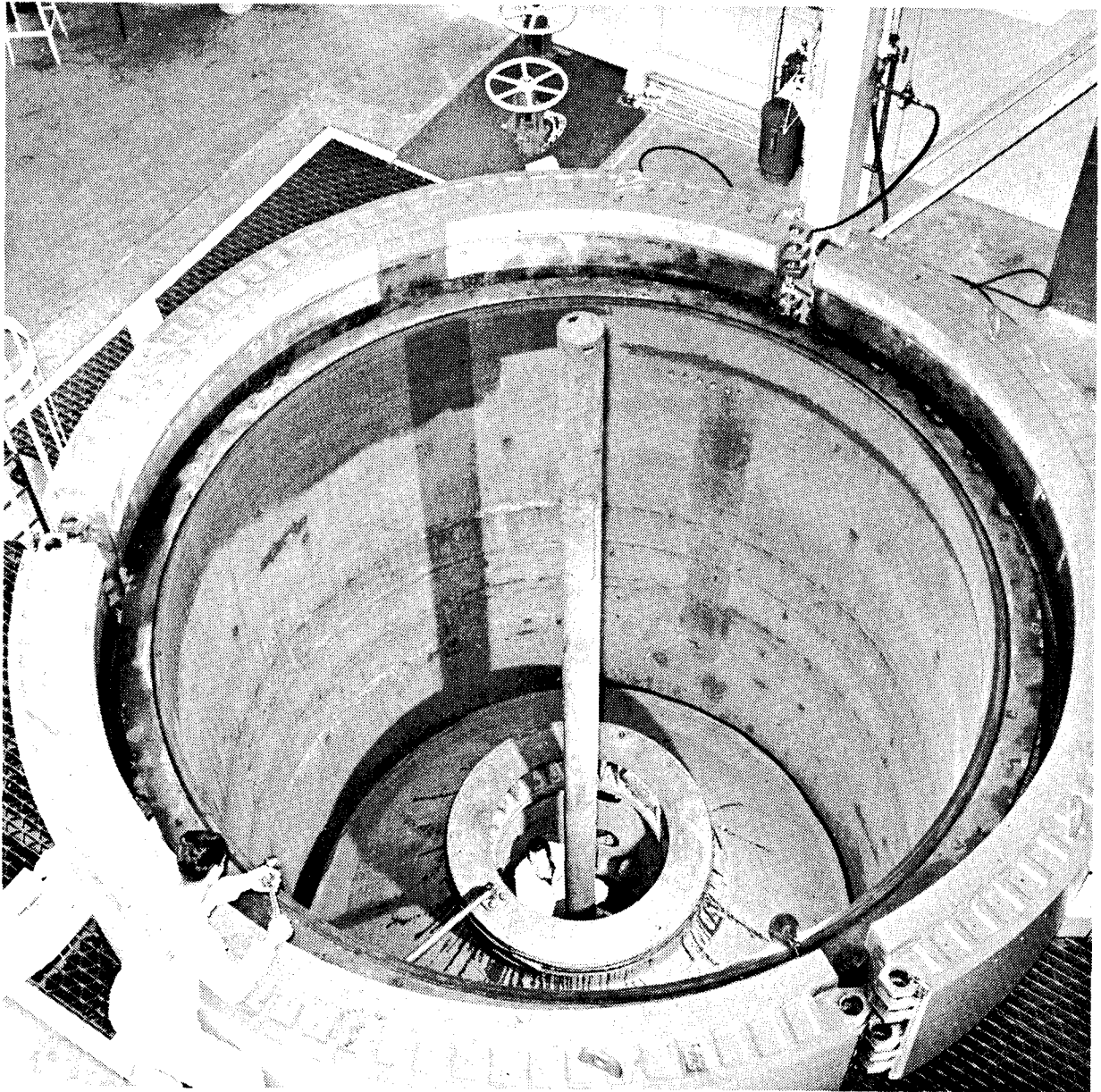
Figure 9 - Preparation for Cure on Hydroclave

The cure of the ablative in most instances was followed by a post-cure cycle in an oven atmosphere or by the extension of the hydroclave cure time. Following cure, the ablatives were machined, quality control samples were removed and tested to determine the percent of acetone extractables, and the glass laminates were applied and cured.

Following the glass laminate cure, the ablative assemblies were machined on the outside to clean-up only, to remove wrinkles in the glass overlay, and then were removed from the mandrels and subjected to the NDT described in Section IX. D of this report.

After the ablative assemblies had been accepted by NDT and the mechanical properties and state of cure of the component had met the specification requirements, the component was machined to the final configuration on all surfaces except the outside of the glass laminate.

b. Material Acceptance and Properties

The individual ablative materials discussed in Section IV were purchased to specifications for fabrication of the 156-2C-1 nozzle. The performance of these materials can best be summarized by Tables XIX and XX. These tables show a comparison of the "as received" material properties and the "in-process" material properties. The problems encountered with these materials during fabrication are discussed in Section IX. A.

c. Full-Scale Tape Wrapping

Development of parameters for tape wrapping of components for the 156-2C-1 and 260-SL-1 nozzle components was accomplished through trial wrappings of test rings for each component. For these trial wrappings and for tape wrapping of all components, a tape wrapping head was used which contained units for heating the tape, tensioning the tape, compressing the tape during application, and cooling the tape after application.

Whereas the subscale components were fabricated using heat guns as the source of heat for wrapping, full-scale component tape heating was done with quartz heating lamps. This produced a controllable radiant heat instead of the more variable convective heat provided by the heat guns. Banks of quartz lamps mounted at fixed locations heated both the top side and the tack side of the feed-in ply. Number of lamps, distance of lamps from the moving tape, and power input to the lamps all controlled the tape temperature achieved.

Tape tensioning, found to be of secondary importance to attaining the end results, was achieved by means of Dynamatic AB-701 electric brakes for warp cut tape. Because bias tape exhibits weave distortion when tensioned, true tension could not be applied. The tape was fed to the mandrel using a Graham N28AK variable speed drive.

TABLE XIX

AS RECEIVED RAW MATERIAL PROPERTIES 156-2C-1

COMPONENT 1. NAME 2. P/N 3. MATERIAL	COMMERCIAL DESIGNATION	UNCURED		CURED				
		RESIN CONTENT %	VOLATILE CONTENT %	TENSILE STRENGTH PSI	ELASTIC MODULUS PSI × 10⁶	FLEXURAL STRENGTH PSI	MODULUS ELASTICITY PSI × 10⁶	DENSITY g/cc
1. EXIT CONE 2. IS 11004-01-01 3. HIGH-SILICA	MX-2600	29.0 - 33.1	2.8 - 5.1	13,200 - 15,700	2.48 - 2.85	18,500 - 25,800	2.30 - 2.98	1.71 - 1.83
1. EXIT CONE 2. IS 11004-01-01 3. CARBON	MX-4926	31.7 - 36.8	4.2 - 6.0	17,900 - 30,400	2.37 - 3.45	33,000 - 49,600	2.08 - 2.86	1.40 - 1.46
1. AFT THROAT 2. IS 11004-01-02 3. GRAPHITE	FM-5064	31.0 - 34.9	3.9 - 5.2	13,500 - 17,800	1.80 - 2.28	23,300 - 25,600	1.61 - 1.81	1.43 - 1.46
1. MID THROAT 2. IS 11004-01-04 3. GRAPHITE	FM-5064	31.2 - 35.6	4.5 - 5.5	9,680 - 13,600	1.47 - 1.78	17,900 - 22,600	1.71 - 1.98	1.45 - 1.49
1. FORWARD THROAT 2. IS 11004-01-05 3. GRAPHITE	FM-5064	31.0 - 36.0	3.9 - 5.4	10,200 - 17,800	1.50 - 2.28	19,600 - 25,600	1.61 - 2.11	1.43 - 1.46
1. ENTRANCE CONE 2. IS 11004-01-06 3. CARBON	FM-5063	32.1 - 37.0	2.7 - 5.7	16,000 - 27,400	2.66 - 3.19	24,000 - 43,600	2.13 - 2.84	1.45 - 1.49
1. ALL 2. ALL > Reinforcement Laminates 3. GLASS	MX-4600	19.0 - 22.0	2.2 - 3.4	62,000 - 72,000	✕ NOTE 1	87,500 - 106,000	3.83 - 4.26	2.06 - 2.10

NOTE 1: Not required by specification.

45

TABLE XX

IN-PROCESS CONTROL TEST RESULTS (56-2C-1

COMPONENT 1. NAME 2. P/N 3. MATERIAL	ANGLE OF WRAP TO ¢	DENSITY g/cc	CURED				
			TENSILE STRENGTH PSI (AVG.)	ELASTIC MODULUS PSI × 10⁶ (Avg)	FLEXURAL STRENGTH PSI (AVG.)	MODULUS ELASTICITY PSI × 10⁶ (Avg.)	ACETONE EXTRACTABLES % (AVG.)
1. EXIT CONE 2. IS 11004-01-01 3. HIGH-SILICA	0°	1.766	11,656	2.663	20,449	2.515	0.430
1. EXIT CONE 2. IS 11004-01-01 3. CARBON	0°	1.444	25,132	2.752	40,426	2.910	0.210
1. AFT THROAT 2. IS 11004-01-02 3. GRAPHITE	29° – 31°	1.443	13,740	1.717	20,420	1.631	1.8143
1. MID THROAT 2. IS 11004-01-04 3. GRAPHITE ‡REPAIR	43° – 46.5°	1.430 1.427☆	17,357 9,999☆	1.795 1.584☆	22,018 17,628☆	1.604 1.372☆	4.316 4.305☆
1. FORWARD THROAT 2. IS 11004-01-05 3. GRAPHITE	58.5° – 59.5°	1.422	19,369	2.928	26,868	1.936	3.555
1. ENTRANCE CONE 2. IS 11004-01-06 3. CARBON	59.5° – 62°	1.488	14,531	2.362	31,042	2.362	4.492
1. ALL 2. ALL 3. GLASS ⟩ Reinforcement Laminates	NOTE 1	1.739	NOTE 1	✕	58,140 NOTE 2	NOTE 1	NOTE 1
1. EXIT CONE 2. IS 11004-01-01 3. ROVING	NOTE 1	2.120	196,014	6.305	NOTE 1	NOTE 1	NOTE 1

NOTE 1: Not required by specification.

NOTE 2: Average reported based on values obtained after repair of mid throat component. At time of fabrication of other components, flexural strength parameter was not a specification requirement.

46

Debulking of the tape materials during the winding process was accomplished to minimize tape movement and subsequent wrinkling that could occur during hydroclave curing under high pressures. An as-wrapped debulk factor of 80 percent minimum was established as a processing requirement to prevent serious wrinkling during cure. This corresponded to an as-wrapped density of 85 percent of the density achieved in a 1,000 psi hydroclave cure.

The debulking factor was defined as the ratio of the difference in thickness of as-purchased material and as-wrapped material to the difference in thickness of as-purchased material and as-cured material. The debulking factor was used as an in-process check on the wrapping operation, whereas as-wrapped density was also checked during trial ring wrappings.

A hydraulically actuated, large-diameter steel roller was used to achieve debulking of the tape during application. This roller rotated against the moving mandrel and was driven by it so that tape feeding into the mandrel was compressed by a wringing action. The load exerted on the debulking roller by the hydraulic actuation system, measured in pounds per inch of tape width, determined the amount of compression of the tape material. Bias tape wrapping heads had a ring-segmented debulking roller so that compensation of differences in surface speed between ID and OD of the applied tape sections could be accommodated without significant slipping of the roller over the material.

It was necessary to cool the tape after it had passed under the debulking roller to prevent springback of the material. The cooling of the wrapped tape tended to set the material and prevent subsequent movement and loss of compression. The cooling method used on the subscale components was that of blowing air through a drum of dry ice, thereby chilling the air. The chilling, however, reduced the temperature of the air below the dew point, causing moisture to be condensed and blown onto the part being wrapped. For full-scale components, the cooling method was changed to prevent possible contamination of the material by condensation. Compressed air was expanded through small air jets placed adjacent to the debulking roller and oriented to blow onto the part. This cooling, in conjunction with the cooling provided by the mass of the part and tooling, provided satisfactory results.

Initially, a tape wrapping speed of five feet per minute was considered to be the maximum application rate compatible with attainment of satisfactory debulking factors. This rate was found to be the state-of-the-art capability in nozzle tape wrapping at the start of the program. The number of miles of ablative tape required for the large nozzle, if wrapped at a speed of only five feet per minute, would have required an excessively long fabrication period. It was, therefore, concluded that parameters would have to be established which would permit faster material application rates. A target wrapping speed of 10 fpm for bias tape components and 15 to 20 fpm for warp tape components was established.

By a series of trial ring wrappings beginning at the established state-of-the-art speed of five feet per minute and advancing incrementally in application speed, parameters were established for wrapping full-scale components. Table XXI summarizes the parameters established for each component and material, and presents the level of as-wrapped density achieved for each test ring. These data were typical of results achieved in wrapping the actual nozzle components.

TABLE XXI

SUMMARY OF TAPE WRAPPING PARAMETERS FOR FULL SCALE ABLATIVES

Component	Material	Input Tape Temperature F	Wrapped Mass Temperature F	Debulking Roller Force lb/in of width	Wrapping Speed ft/min	As-Wrapped Density, % of Theoretical
Entrance Cone	Carbon-Phenolic FM-5063, Biased	220-260	90-110	150	12	87.9-94.4
Forward Throat	Graphite-Phenolic FM-5064, Biased	200-240	80-100	300	10	86.2-94.6
Midthroat	Graphite-Phenolic FM-5064, Biased	180-220	80-100	210	10	83.4-95.2
Aft Throat	Graphite-Phenolic FM-5064, Biased	160-200	80-100	150	10	84.5-85.3
Exit Cone	Carbon-Phenolic MX-4926, Warp	250-280	95-120	260	20	90.6-93.1
Exit Cone	Silica-Phenolic MX-2600, Warp	280-300	95-120	300	13	94.0-97.2

48

3. Assembly

a. Assembly Approach

The initial assembly sequence for the large nozzle was as follows:

1. Bond the aft throat ablative to the exit cone ablative with a phenolic resin, apply the structural laminate to the O. D., then cure and final machine.

2. Bond the divergent cone assembly to the steel shell with Epon 820, place the assembly in the horizontal position in an autoclave and cure the bond.

3. Place the phenolic prepreg glass tie laminates on the outside of the steel shell and divergent cone, place assembly in the hydroclave and cure at 1000 psi.

4. Add the prepreg rovings on the O. D., in the throat area and at the exit plane, place in the autoclave and cure the roving bands.

5. Fit and bond the mid throat ablative to the nozzle subassembly, autoclave cure the bond line.

6. Fit and bond the forward throat ablative to the nozzle subassembly, autoclave cure the bond line.

7. Fit and bond the entrance cone ablative to the nozzle subassembly, autoclave cure the bond line.

The following is a list of some of the major problems existing in the assembly method described above whose solution eventually led to improvements in the assembly technique.

1. The temperature cure required by the Epon 820 bond autoclave cure caused a problem because the steel shell would enlarge due to thermal expansion slightly more than the ablative component, and consequently could cause a strain in the adhesive and possibly bond line failure. The large diameters of the nozzle made the differential expansion a much more difficult problem than on previous designs. In order to overcome this

49

problem, tooling would be required which would permit movement during the autoclave heatup in order to keep the ablative properly seated. These tools would make use of the autoclave pressure for seating loads.

2. This method of assembly requires approximately seven cycles in the autoclave or hydroclave to complete the nozzle. Each of the autoclave cycles requires the nozzle to be rotated to the horizontal position. Each cycle would subject the previously cured bond lines to an elevated temperature condition while they were under stress due to the horizontal attitude. The hydroclave cycle for cure of the tie laminates would subject the epoxy bond line of divergent cone assembly to 300° F temperature, which would weaken the strength of the bond considerably.

3. Tooling would be required for handling the nozzle at several subassembly configurations.

4. The mandrels would have to be capable of handling the entire weight of the nozzle in the horizontal position with a minimum of deflections.

To eliminate these and other problems associated with assembly, four major changes were made to the materials used in the assembly of the nozzle.

1. The adhesive for bonding the ablatives to the nozzle shell was changed from a temperature-cured Epon 826 to Shell Chemical Company ambient-cured Epon 913.

2. The tie laminate material for the nozzle assembly was changed from a phenolic prepreg glass MX-4600 to a bidirectional glass fabric which was wet-dip impregnated at the time of application with a Selectron 5003 polyester resin.

3. The filament winding in the throat area and at the exit plane of the nozzle was changed from a temperature-cured prepreg to an ambient-cured wet-dip roving.

4. The joint filler material was changed from a phenolic resin with organic filler to a zinc chromate putty which requires no cure.

b. Assembly Procedure

Following these changes in materials, the assembly procedure was revised and the new procedure was successfully used in assembly of the 156-inch

nozzle. **The following is a summary of the assembly sequence used on this nozzle:**

1. Each ablative assembly was finish machined on all surfaces except for the outside glass, which was to mate with the steel shell.

2. The ablative components were then stacked on their respective mandrels to form the convergent and divergent stacks. Each stack was made up as follows:

    a. Convergent Stack

       (1) Entrance cone ablative

       (2) Forward throat ablative

       (3) Mid throat ablative

    b. Divergent Stack

       (1) Aft throat ablative

       (2) Exit cone ablative

    The inside contour of these two stacks represented the finished inside contour of the nozzle. Zinc chromate putty was placed in each ablative-to-ablative joint as the stack progressed.

3. Following the stacking operation, the outside surface of both stacks was finish machined to match the inside contour of the steel shell.

4. Pads of playdough between sheets of nylon were then placed at intervals on the surface of the shell as shown in Figure 10. The convergent ablative stack was then lowered in place on the steel shell to form the playdough. The shell and forward stack were then lowered in place on the divergent cone stack. The assembly was broken down and all the pads were collected and measured in order to determine the amount of adhesive to be applied.

5. All components were then thoroughly solvent cleaned. With the convergent stack positioned with the large diameter end up, the Epon 913 adhesive was applied as shown in Figure 11. Adhesive was then applied to the inside surface of the shell as shown in Figure 12, and the outside surface of the divergent cone as shown in Figure 13.
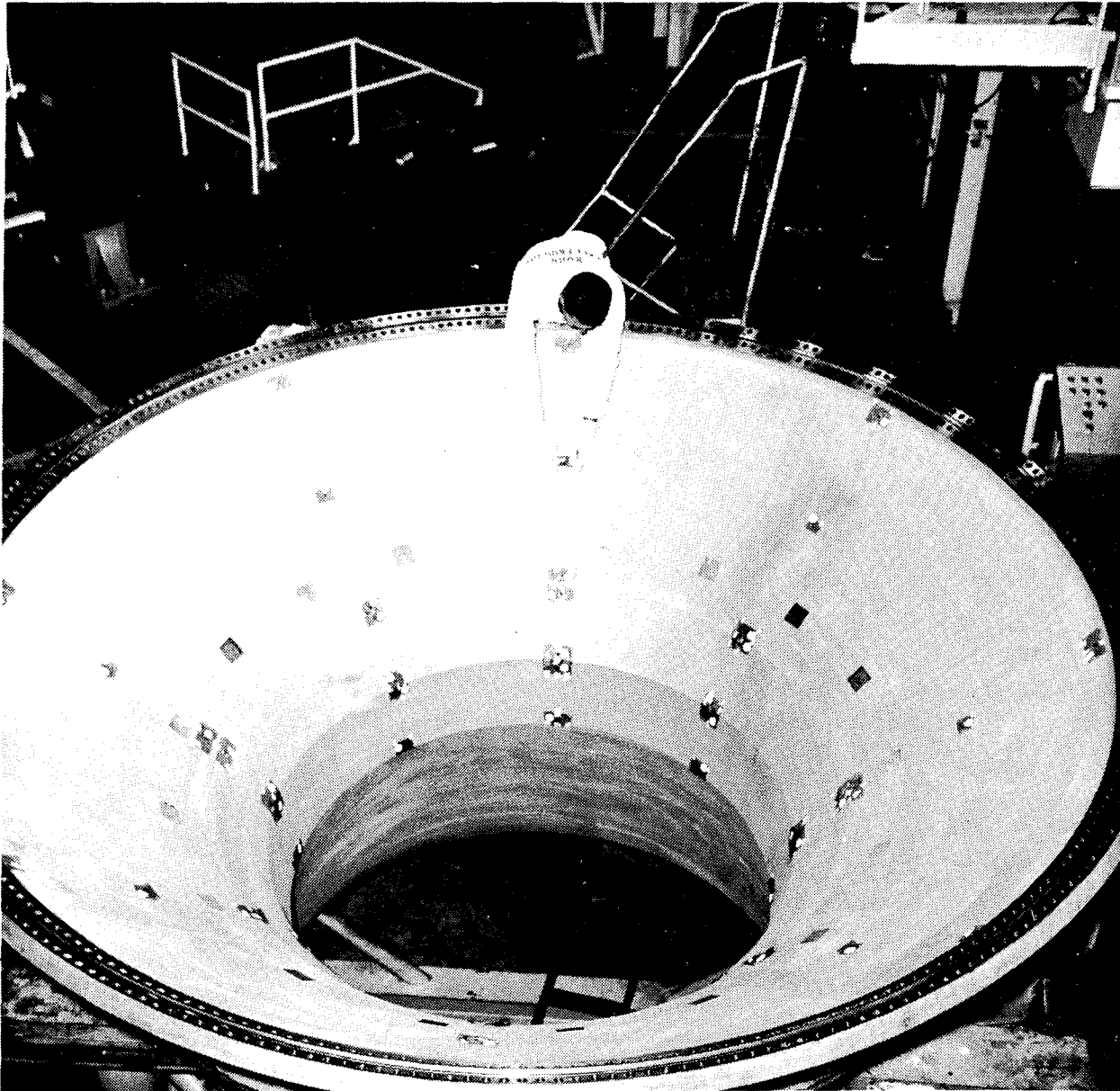
Figure 10 - Preparation of Shell for Dryfit
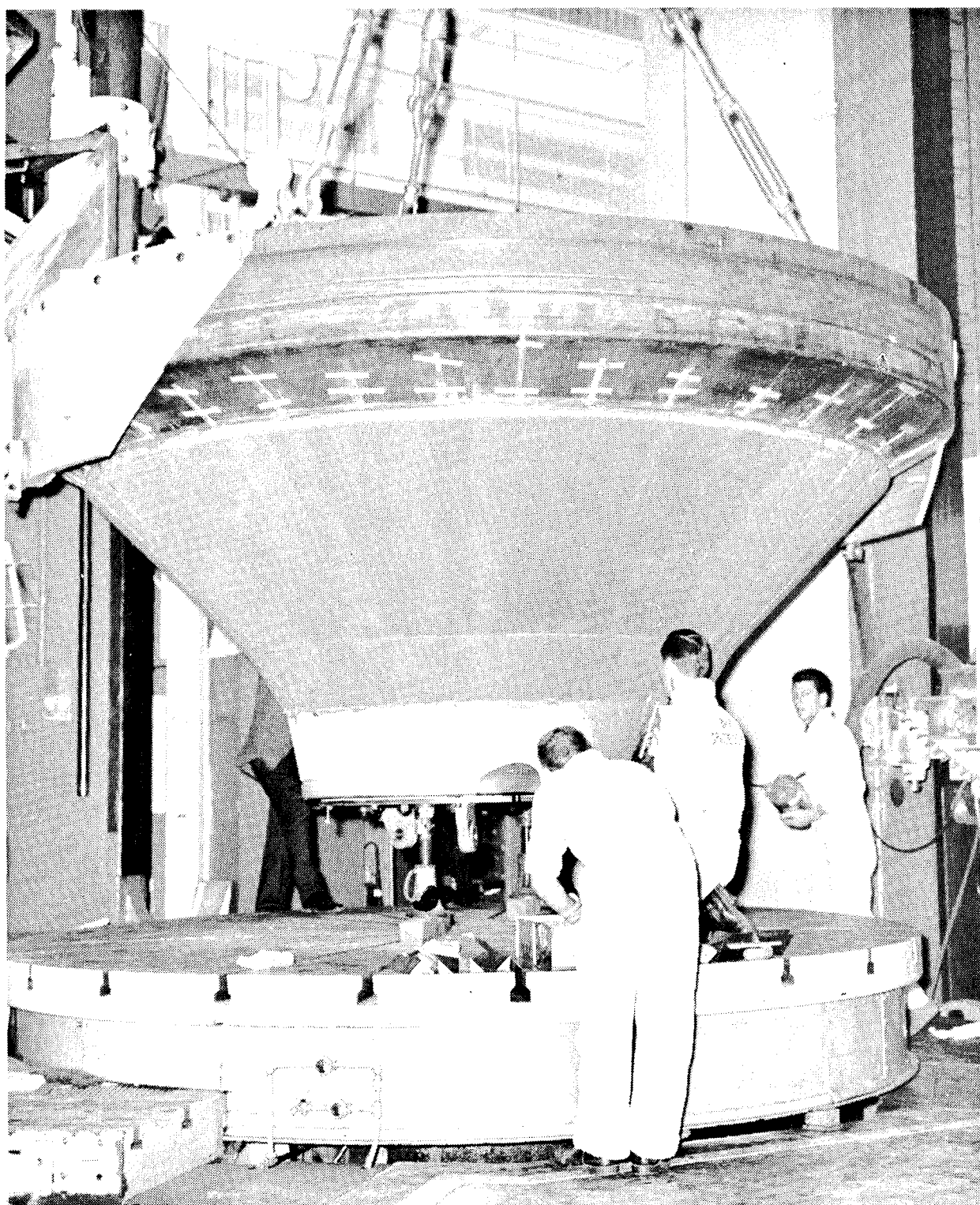
Figure 11 - Application of Adhesive
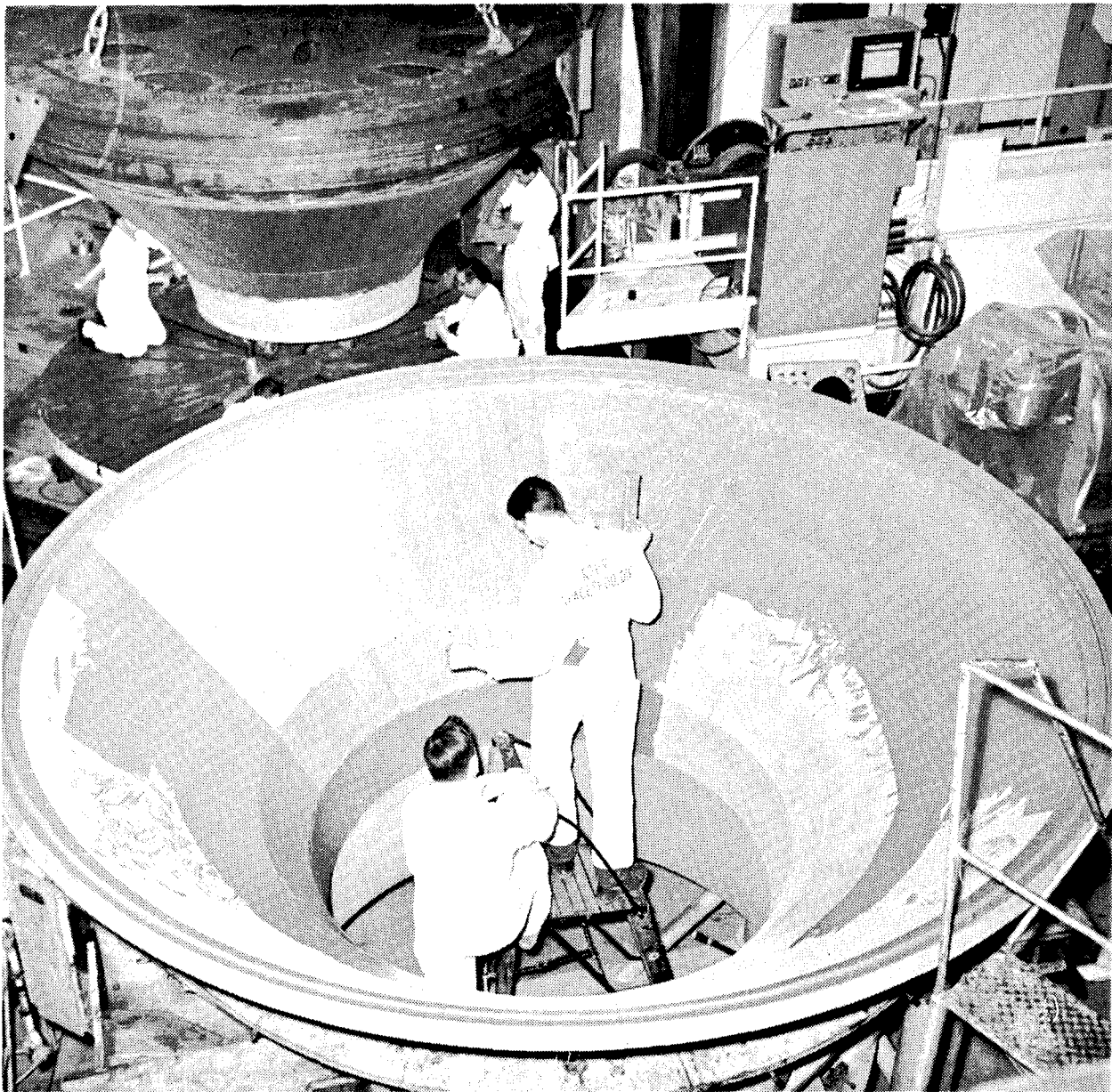
Figure 12 - Adhesive Application to Steel Shell
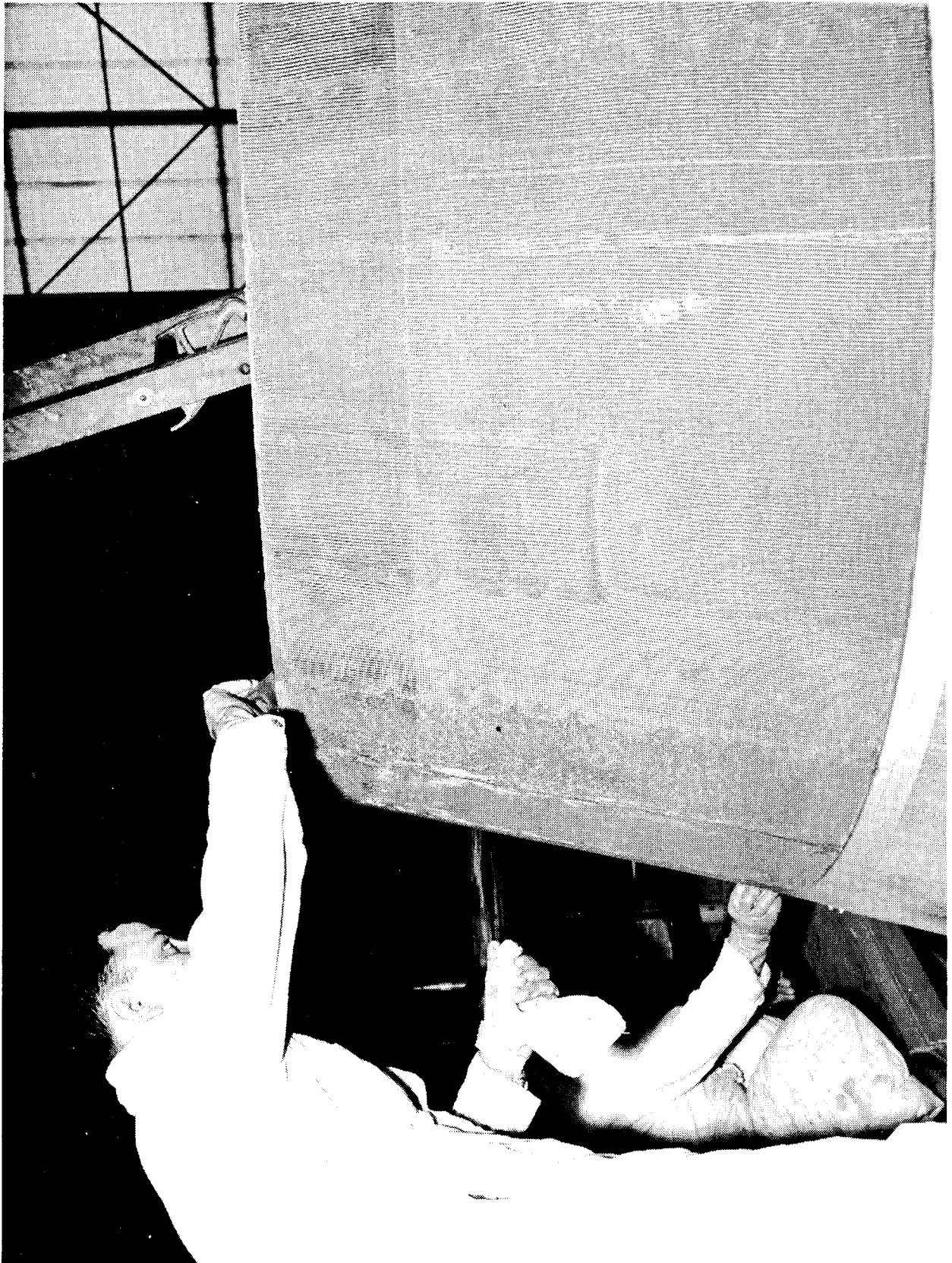
Figure 13 - Application to Divergent Cone

6. The covergent stack was then lowered into the steel shell, Figure 14, and the stack and shell were then locked together and placed on top of the divergent cone assembly as shown in Figure 15.

7. The tie laminate impregnated with the Selectron 5003 resin-ultraviolet catalyst mixture was applied to the assembly in the throat area and at the end of the steel shell as shown in Figure 16.

c. Assembly Loading Requirements

The initial concept was to assemble the ablative components to the shell, one at a time, with a temperature-cured bond. This concept also encompassed the use of the autoclave pressure as a loading mechanism for the seating of the ablative against the steel shell. When the change was made to an ambient cure adhesive and thus a one-step assembly, the loading concept was changed to one which required the entire mandrel stack to be assembled in order to seat the ablatives against the steel shell. Previous adhesion tests had shown that a minimum bond pressure of 6 psi would be required to properly bond the components. Since the angle of the -9 cone was the smallest, the bond pressure of 6 psi plus a frictional force of 0.4 psi was assumed for the bond line in this area and the axial component of bond pressure for the convergent section of the nozzle was based on this cone. The resulting bond pressure on the other convergent cone can be seen on Figure 17. Since the divergent cone must react the load placed on the convergent over a considerably smaller area, the resulting bonding pressure in this area was higher (46 psi) than for any other area.

These loads were applied to the ablatives by the mandrels which were, in turn, loaded by torquing 1.25 inch diameter bolts at the joint of the aft throat and mid-throat mandrel. To insure that the mandrels did not tend to seat on each other before adequate bonding pressure had been applied, the mating surfaces of the ablative and steel were coated with sufficient adhesive to completely fill the gap measured during the dry fit. Air entrapment would tend to further increase the bond line thickness. The 0.050-inch shim which was used between the aft throat and mid-throat mandrel during the dry fit was reduced to 0.020-inch to allow more travel before mandrel seating.

The 30 bolts in the mid-throat to aft throat mandrel were torqued in sequence in steps of 350 to 400 inch/lbs to obtain a torque of 1100 inch/lbs required to produce the seating load of 366,700 pounds.

d. Nozzle Handling

The handling of a nozzle with such large diameters and massive weight created many unique handling situations. Special tooling was required to prevent damage to the ablatives or the assembled nozzle. Because most of the ablative manufacturing was done in the vertical position using the mandrel, the mandrel was used during the majority of ablative handling. This was particularly true of the entrance and exit cones which were removed from their mandrels only once for nondestructive testing. Two lifts were made with three-legged support
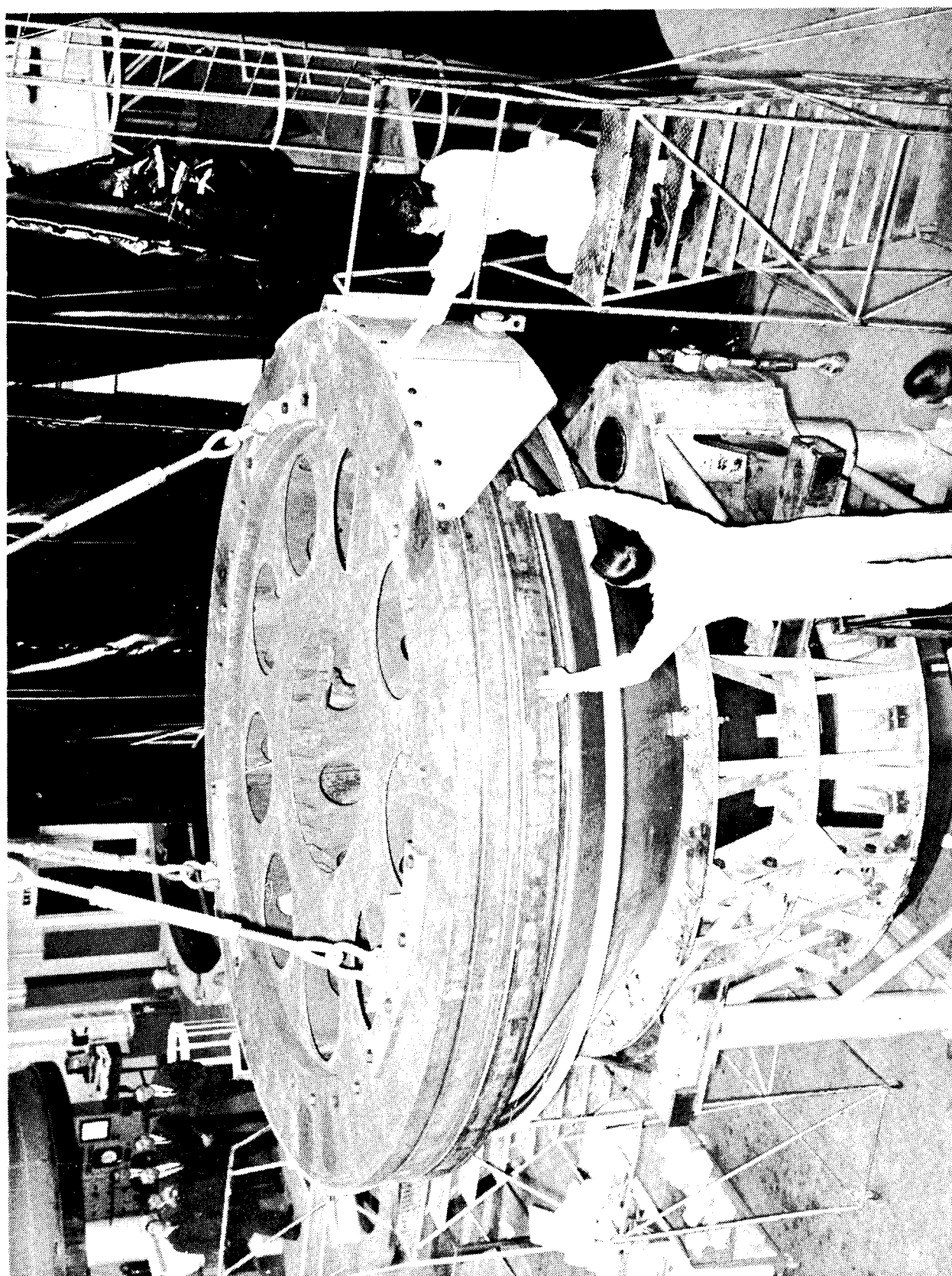
Figure 14 - Bonding Assembly
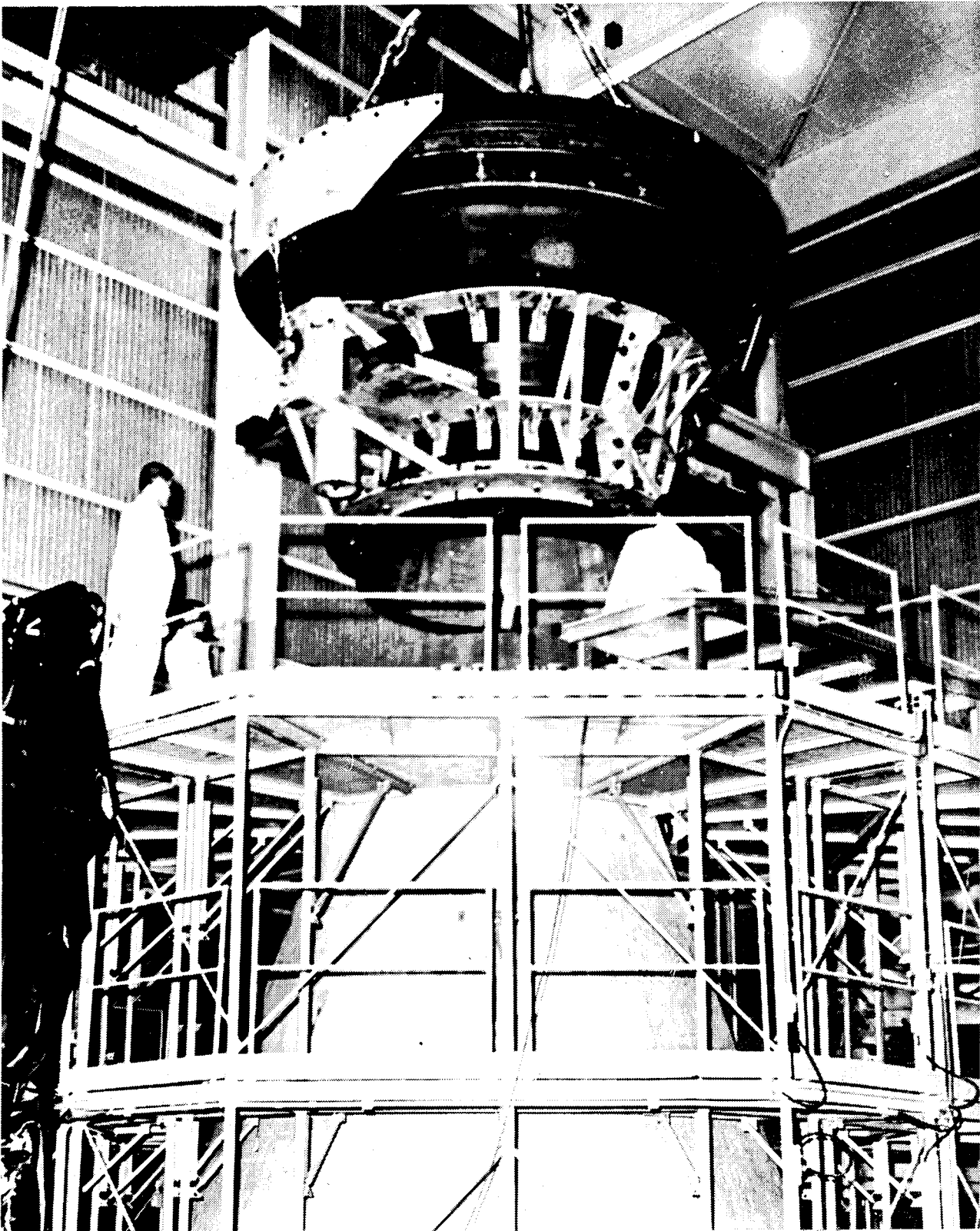
Figure 15 - Bonding Assembly - Shell to Divergent Stack

Figure 16 - Application of Tie Laminate

CONE	θ	BONDING PRESSURE P (PSI)	AXIAL COMPONENT OF BOND PRESSURE A (PSI)	FRONTAL AREA	AXIAL LOAD (LB X 10-3)
-7	44°21'	8.5	32.8	9223	302.5
-8	31°50'	17.3	32.8	1476	48.4
-9	11°15'	6.4	32.8	483	15.8
-10	15° 0'	46.0	177.7	2064	366.7
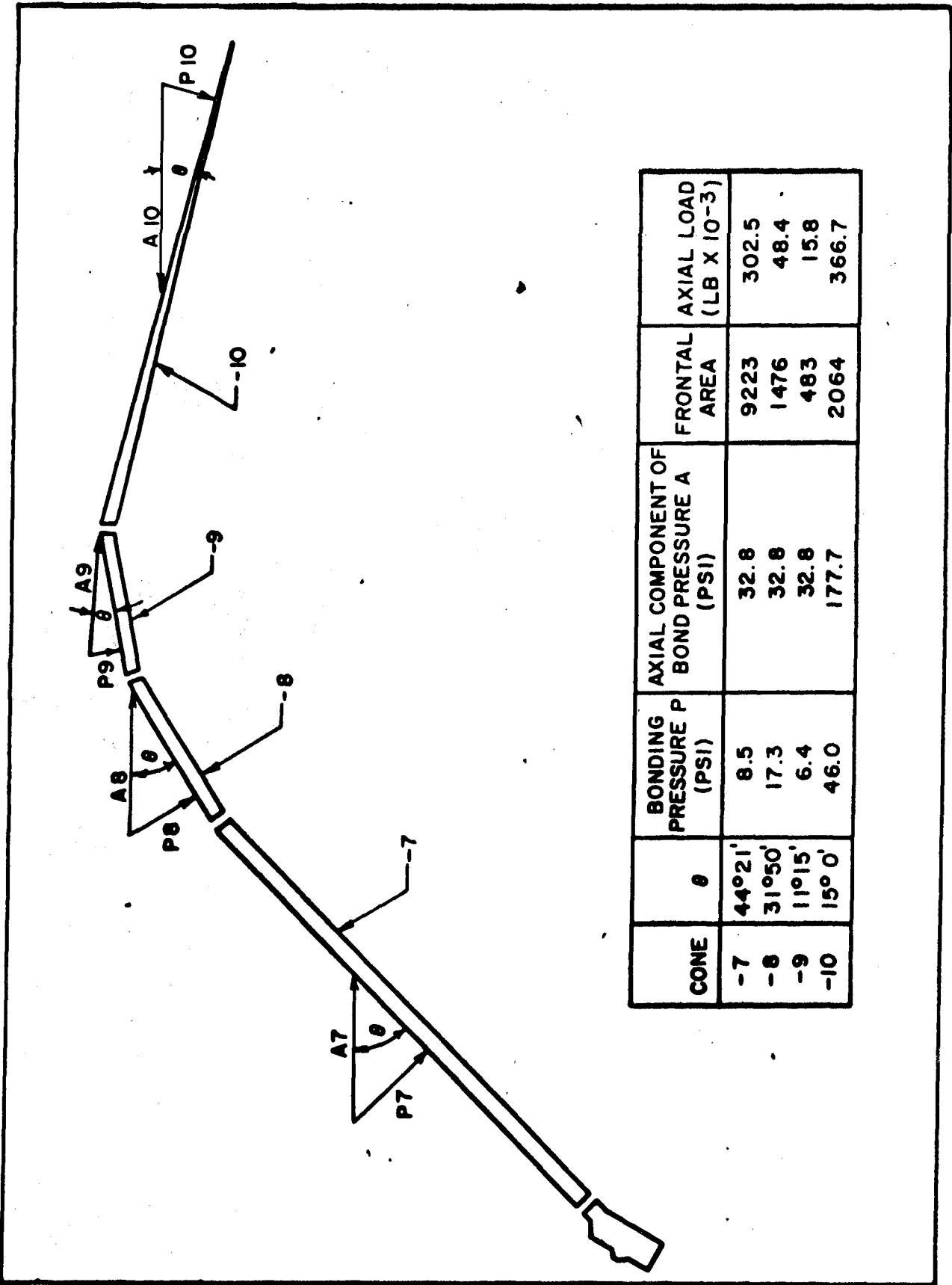
Figure 17 - Bond Pressure - Convergent Cone

which applied little or no load to the ablative except for the weight of the ablative itself. Figure 18 shows the completed nozzle assembly being removed from the mandrel with a special handling collar.

e. Shipment of the 156-Inch Nozzle

The 156-2C-1 nozzle was shipped from Riverside, California to Ontario, California by truck, then from Ontario, California to Brunswick, Georgia via the "Pregnant Guppy," and to the Camden County Plant Site by truck. Figure 19 shows the completed nozzle on the shipping buck ready to leave the Rohr facility. The shipping harness and pallet shown in the figure were designed, stressed, and submitted for FAA approval prior to fabrication. Complete details of the shipping fixture and handling sequence are available on Thiokol tooling drawing ST 10203.

f. Assembly to Motor

Upon delivery to the Camden County Plant Site, the nozzle assembly was rotated to the vertical position using the shipping pallet as a strong-back. The nozzle was then placed in inspection and a complete visual and contour inspection performed. The completed assembly was then dryfit checked on the motor and assembled to the motor with the zinc chromate putty joint filler and the required bolts.
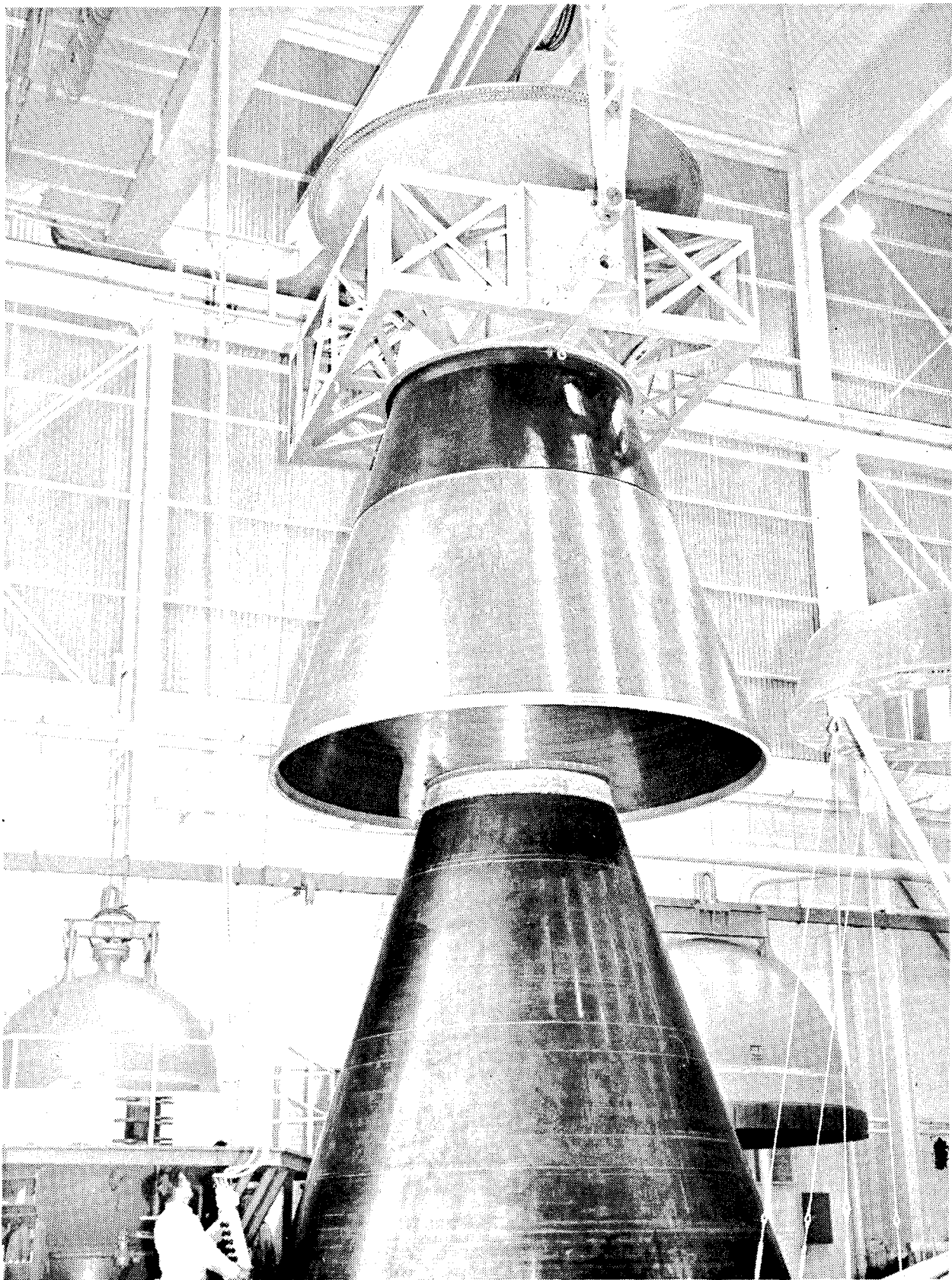
Figure 18 - Removal of Nozzle Assembly
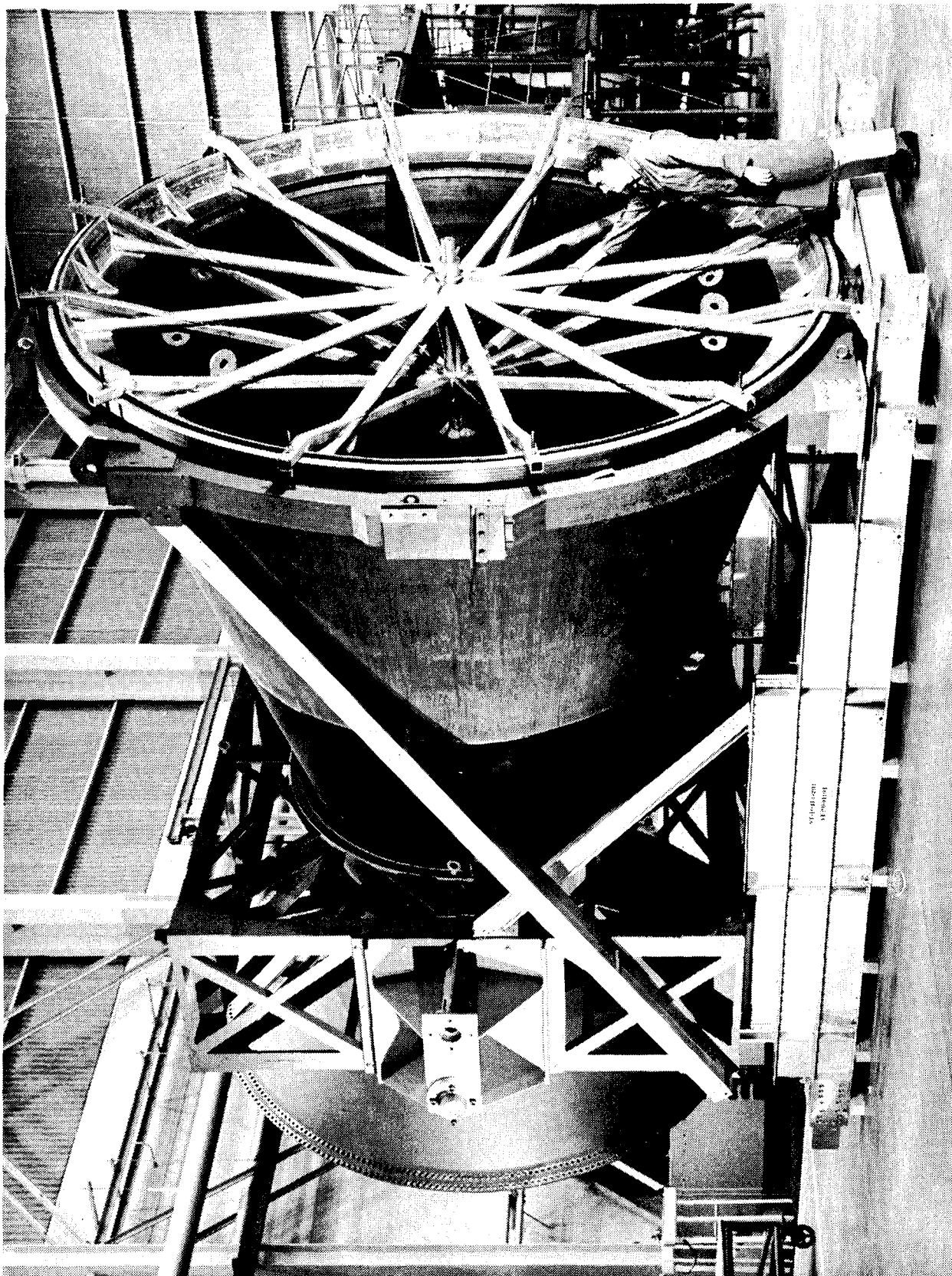
Figure 19 - Preparation for Shipment

B. 260-SL-1 ABLATIVE FABRICATION

The 260-SL-1 ablative materials were purchased to a series of Thiokol Specifications. Tables XXII and XXIII show a comparison of the "as received" material properties and the "in-process" material properties.

The following summarizes, by 260-SL-1 ablative areas, fabrication comparisons with the 156-2C-1 nozzle unit and the end-of-program status of these ablatives:

1. Entrance Cone

  a. Fabrication parameters were basically the same as the 156-2C-1 nozzle.

  b. Tape width was reduced from 13.5" to 12" since 13.5" proved to be unnecessary on the 156-2C-1 nozzle.

  c. End of program status - ready for assembly stacking.

2. Forward Throat

  a. Fabrication parameters were the same as the 156-2C-1 nozzle.

  b. End of program status - ready for assembly stacking.

3. Mid Throat

  a. Fabrication parameters were basically the same as the 156-2C-1 nozzle.

  b. Component was given a second post cure (32 hours in oven) to reduce acetone extractables.

  c. End of program status - ready for assembly stacking.

4. Aft Throat

  a. Fabrication parameters were basically the same as the 156-2C-1 nozzle.

TABLE XXII

AS RECEIVED RAW MATERIAL PROPERTIES - 260-SL-1

COMPONENT 1. NAME 2. P/N 3. MATERIAL	COMMERCIAL DESIGNATION	UNCURED				CURED		
		RESIN CONTENT %	VOLATILE CONTENT %	TENSILE STRENGTH PSI	ELASTIC MODULUS PSI × 10⁶	FLEXURAL STRENGTH PSI	MODULUS ELASTICITY PSI × 10⁶	DENSITY g/cc
1. EXIT CONE 2. IS 11004-01-01 3. HIGH-SILICA	MX-2600	29.0 - 34.9	2.2 - 5.2	14,800 - 15,800	2.53 - 2.63	21,000 - 23,700	2.44	1.73 - 1.77
1. EXIT CONE 2. IS 11004-01-01 3. CARBON	MX-4926	32.7 - 36.5	4.0 - 5.1	20,100 - 34,300	2.43 - 2.91	38,600 - 43,600	1.98 - 2.46	1.47 - 1.51
1. AFT THROAT 2. IS 11004-01-02 3. GRAPHITE	FM-5064	32.2 - 33.3	1.9 - 3.8	11,300	1.80	23,900	1.91	1.49
1. MID THROAT 2. IS 11004-01-04 3. GRAPHITE	FM-5064	31.2 - 34.3	4.5 - 5.1	12,400 - 13,600	1.53 - 1.65	19,400 - 22,600	1.63 - 1.93	1.43 - 1.49
1. FORWARD THROAT 2. IS 11004-01-05 3. GRAPHITE	FM-5064	33.9 - 35.6	3.2 - 3.9	12,400	1.88	29,900	2.08	1.44
1. ENTRANCE CONE 2. IS 11004-01-06 3. CARBON	FM-5063	32.2 - 36.8	2.1 - 5.5	17,400 - 23,900	2.53 - 2.83	28,000 - 35,800	1.91 - 2.64	1.46 - 1.50
1. ALL — Reinforcement 2. ALL — Laminates 3. GLASS	MX-4600	17.1 - 22.1	1.98 - 3.44	55,000 - 72,000	NOTE 1	77,500 - 106,000	3.82 - 4.48	2.06 - 2.10

NOTE 1:   Not required by specification.

TABLE XXIII

IN-PROCESS CONTROL TEST RESULTS

260-SL-1

COMPONENT 1. NAME 2. P/N 3. MATERIAL	ANGLE OF WRAP TO ℄	CURED					
		DENSITY g/cc	TENSILE STRENGTH PSI (AVG.)	ELASTIC MODULUS PSI × 10^6	FLEXURAL STRENGTH PSI (AVG.)	MODULUS ELASTICITY PSI × 10^6 (AVG.)	ACETONE EXTRACTABLES %/o (AVG.)
1. EXIT CONE 2. 1S 11004-01-01 3. HIGH-SILICA	0°	1.744	12,679	2.208	20,911	2.230	0.3333
1. EXIT CONE 2. 1S 11004-01-01 3. CARBON	0°	1.430	21,477	2.668	31,405	2.033	0.4122
1. AFT THROAT 2. 1S 11004-01-02 3. GRAPHITE	30°	1.432	12,388	1.972	23,450	2.183	1.4963
1. MID THROAT 2. 1S 11004-01-04 3. GRAPHITE	43° - 46.5°	1.434	14,500	2.106	20,909	1.564	5.0526☆ 2.4817 NOTE 3
1. FORWARD THROAT 2. 1S 11004-01-05 3. GRAPHITE	58° - 60°	1.454	17,794	1.902	14,802	1.288	4.3613
1. ENTRANCE CONE 2. 1S 11004-01-06 3. CARBON		1.464	16,791	2.442	35,875	2.465	4.395
1. ALL 2. ALL 3. GLASS Reinforcement Laminates	NOTE 2	1,740 NOTE 1	NOTE 2	NOTE 2	59,409 NOTE 1	NOTE 2	NOTE 2

NOTE 1: Average shown based on test results from mid throat component only. Sufficient excess material was not available to perform tests, from other components.

NOTE 2: Not required by specification.

NOTE 3: Starred (☆) value represents average acetone extractables, after initial cure and post cure. Unstarred value represents results after re-post cure.

66

b. Component was given a second post cure (32 hours in oven) to reduce acetone extractables.

c. End of program status - requires I. D. machining and end trim prior to assembly stacking.

5. Exit Cone

a. Fabrication parameters were basically the same as the 156-2C-1 nozzle.

b. Glass stiffener was added to the O. D. opposite carbon/ silica interface as a result of new erosion prediction made after the 156-2C-1 static test.

c. End of program status - requires end trim prior to assembly stacking.

C. 260-SL STEEL SHELL FABRICATION

The 260-SL-2 steel shell fabrication closely paralleled fabrication of the 156-2C-1 steel shell. As previously reported, after the 156-2C-1 static test, it was decided to use the fired steel shell for the 260-SL-1 nozzle. Hence, the unit undergoing fabrication at that time was earmarked for the 260-SL-2 motor.

During fabrication of this unit, welding processes were greatly improved. The practice of reverting between weld passes was instituted and, as a result, the frequency of weld repair was reduced.

The same steel, weld wire, and flux was used for this unit as had been used for the first unit. Also, the welding parameters remained the same.

One anomaly that occurred during fabrication was the distortion and shrinkage of the -07 cone. The cone was run through 17 anneal and revert cycles. The resultant part was undersized. To compensate for the condition, an extension cone was fabricated, thus an extra weld was necessary for the assembly.

At termination of the program, the nozzle shell unit lacked one weld. The depositing of weld "M" (see Figure 5) remained before the unit would have been ready for the final anneal, age cycles and machining.

VII. 156-2C-1 TEST RESULTS

A. NOZZLE STATIC TEST RESULTS

The complete details of the nozzle static test and the condition of the components after firing are reported in Thiokol Chemical Corporation, Space Booster Division report SBR-84.565 entitled, "Final Test Results of the 156-2C-1 Motor Firing." The following is a summary of the results taken from that report.

The external surface of the nozzle was little changed from the before firing condition. The Dyna-Therm coating over the rounding ring at the exit plane was covered with soot, and in two areas 180-degrees apart and adjacent to this rounding ring, phenolic-glass laminates were scorched for a maximum longitudinal distance of about two feet.

Interior sections of the nozzle exit cone and throat were uniform and regular in appearance. The throat was round and without the grooves and gouges. The carbon tape in the entrance and exit section appeared uniformly eroded. However, as noted later, the entrance section was actually gouged in areas corresponding to propellant star valleys. Erosion of the silica tape exit cone section was uniform and did not contain delaminations.

After removing the nozzle from the motor, examination of ablative-to-ablative interfaces showed that post-fire shrinkages of the charred plastic components had increased the joint gaps. Average joint gaps at the time of the examination were less than 0.100 inch. Zinc chromate putty joint filler was intact below the heat-affected zone of the ablative components. Erosion pattern in the vicinity of the joints showed no evidence of unusual or turbulent flow conditions. The fragile char produced by the zinc chromate putty was intact at all joints, indicating that the joints were tight during firing.

Joint	Sealed Pre-Firing Joint Depth (in.)	Unsealed Post-Firing Joint Depth (in.)
Entrance cone-forward throat	6.0	0.70
Forward throat - mid-throat	4.5	3.0
Mid-throat repairs at ring joint*	3.5	3.1
Mid-throat - aft throat	3.5	0.65
Aft throat - exit cone	4.0	0.20

NOTE: *The repair joint was bonded with a phenolic resin.

Delaminations were observed in the carbon-phenolic sections of the entrance and exit cones. One delamination was found in the phenolic-impregnated graphite tape mid-throat; no delaminations were found in the silica-phenolic portion of the exit cone. Exit cone delaminations occurred at regular inter- vals, approximately every four to five inches in the carbon tape segment. The typical depth of delamination, measured parallel to the plies, ranged from 1.2 inches in the forward section near the throat to about 0.70 inch near the silica tape section. Delaminations of the entrance section were shorter in length, being about 0.50 inch. The mid-throat delamination was narrow and extended to a depth of approximately two inches.

Formation of the delaminations was apparently the result of greater material shrinkage in the charred portion of the ablative components during quench and cooldown.

1. Ablative Performance

Measurements were made by directly scaling thicknesses from longitudinal strips cut from each ablative section such that the measured face originally coincided with a plane passing through the nozzle centerline.

Remaining wall thicknesses varied significantly in carbon-phenolic entrance cone regions between propellant valleys and star points. At the 2.0 entrance area ratio, an average erosion depth of 0.74 inch occurred in line with the propellant valleys and 0.37 inch in line with the propellant points. At the 4.0 entrance area ratio, the magnitude of erosion was reduced, but the factor of difference between valley and star locations was still evident. At an entrance area ratio of 1.35, the first measured station in the graphite-phenolic mat- erial, the average star point erosion was 0.37 inch and the average valley erosion was within 0.04 inch of this value. Throughout the rest of the throat areas, no significant difference in star point and valley erosion was found. Average throat erosion depth was 0.61 inch, approximately 90-percent great- er than the design prediction. However, dimensionally the throat diameter measurements were as uniform as when received from the fabricator. Table XXIV presents data confirming this condition.

In the divergent cone, the erosion depth reduced through the graphite-phenolic aft throat section and into the carbon-phenolic exit cone section. Near the 3.0 exit area ratio, erosion was not measurable in the carbon-phenolic mat- erial. At the transition from carbon-to-silica-reinforced ablative, however, erosion increased rapidly, achieving an average depth of 0.53 inch at an area ratio of approximately 3.40. The severity of the erosion was gradually dim- inished such that at an area ratio of 4.0, the average eroded depth was about 0.38 inch. Figure 20 depicts average erosion depths versus area ratios for star point and valley locations. Tables XXV and XXVI tabulate predicted and actual char and erosion depths.

Nozzle performance during the 156-2C-1 static test firing demonstrated the acceptability of the design concepts for three-million-pound thrust motors. Structural integrity and the ability to withstand operation-induced vibrations were demonstrated successfully. Performance of ablative-to-ablative joints and structural adhesive bond lines throughout the nozzle was considered sat- isfactory. As indicated in Table XXV the erosion rates for the ablatives were generally higher than predicted except for the higher Mach number
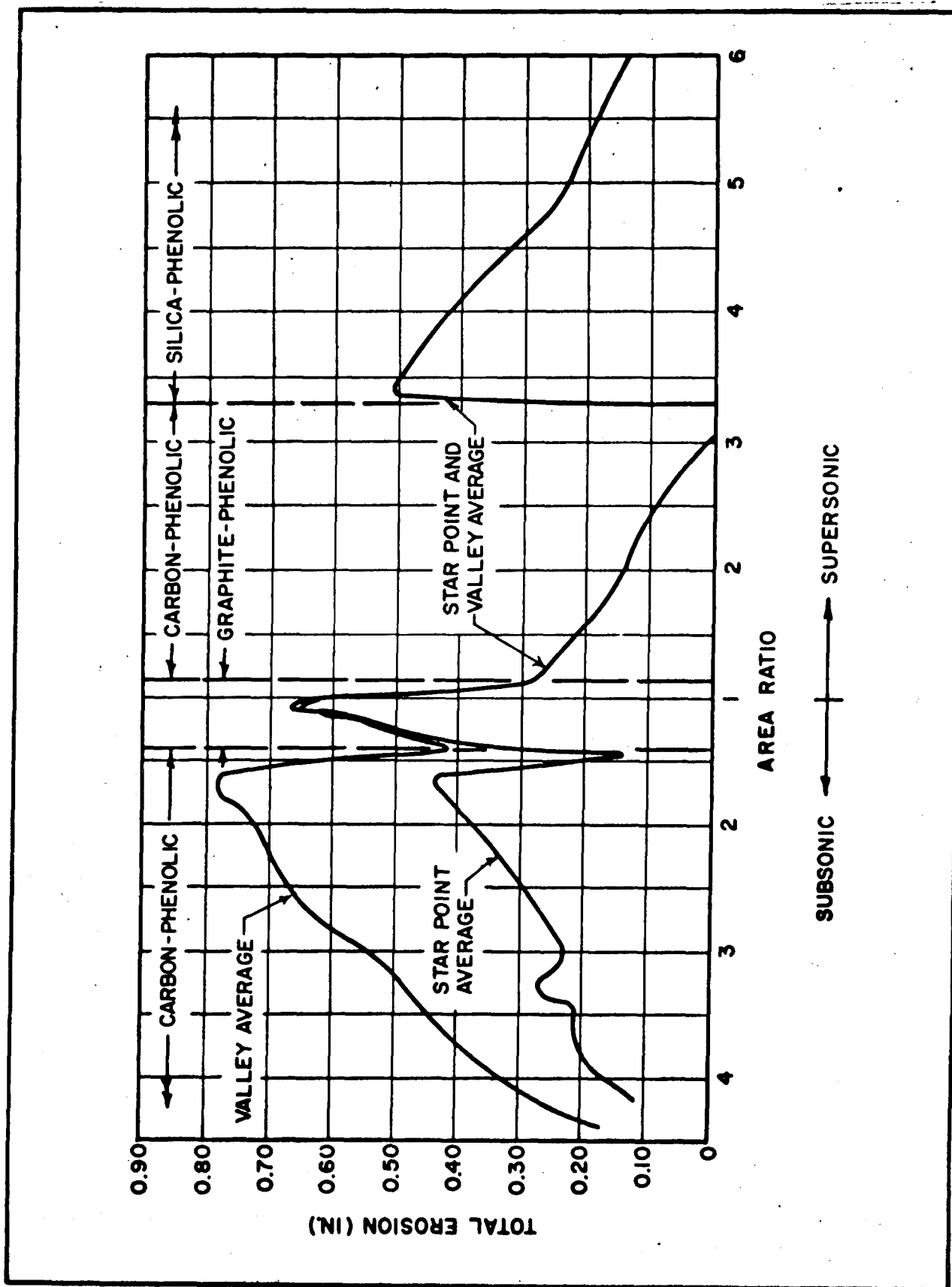
Figure 20 - Total Erosion Depths for 156-2C-1 Nozzle

TABLE XXIV

NOZZLE THROAT PRE- AND
POST-FIRING DIMENSIONS

Radial Location (deg)	Pre-Firing Diameter (in.)	Post-Firing Diameter (in.)
0	61.210	62.285
30	61.237	62.290
60	61.292	62.270
90	61.301	62.330
120	61.272	62.330
150	61.227	62.338

NOTE: The nozzle was conditioned for 24 hours at 73°F prior to taking of diametrical measurements.

TABLE XXV

PREDICTED VERSUS ACTUAL EROSION DEPTHS

Area Ratio	Predicted	Erosion Depth (in.) Actual		
		Average	Maximum	Minimum
-4.0	0.18	P=0.16 V=0.33	P=0.19 V=0.34	P=0.12 V=0.31
-3.0	0.19	P=0.23 V-0.56	P=0.26 V=0.57	P=0.20 V=0.54
-2.0	0.20	P-0.37 V=0.74	P=0.38 V=0.75	P=0.36 V=0.73
-1.5	0.21	P=0.20 V=0.55	P=0.22 V=0.62	P=0.19 V=0.50
-1.1	0.31	0.63	0.68	0.61
1.0	0.31	0.61	0.66	0.57
1.5	0.23	0.22	0.23	0.20
2.0	0.22	0.14	0.19	0.12
3.0	0.20	0.01	0.05	0.00
3.4	0.31	0.51	0.56	0.48
4.0	0.28	0.42	0.48	0.38
5.0	0.25	0.24	0.28	0.21
6.0	0.22	0.14	0.17	0.11
7.0	0.19	0.12	0.15	0.11

NOTE: P designates propellant star point and V designates propellant valley

TABLE XXVI

PREDICTED VERSUS ACTUAL CHAR DEPTHS

| Area Ratio | Char Depth (in.)* | | | |
| | | Actual | | |
	Predicted Average	Based on Average Erosion	Based on Maximum Erosion	Based on Minimum Erosion
-4.0	0.60	0.53	0.54	0.58
-3.0	0.58	0.49	0.53	0.51
-2.0	0.57	0.48	0.49	0.55
-1.5	0.55	0.46	0.47	0.50
-1.1	0.61	0.55	0.58	0.56
1.0	0.62	0.62	0.60	0.63
1.5	0.62	0.58	0.53	0.62
2.0	0.63	0.46	0.49	0.43
3.0	0.65	0.41	0.40	0.41
3.4	0.30	0.26	0.26	0.25
4.0	0.32	0.28	0.28	0.28
5.0	0.33	0.29	0.28	0.31
6.0	0.34	0.31	0.30	0.32
7.0	0.35	0.31	0.32	0.28

*Measured from the post-fire surface.

regions of the exit cone carbon and silica and the lower Mach number regions of the entrance cone carbon which were coplanar with the propellant star points.

B. ABLATIVE POST-TEST ANALYSIS

Following the static test, the nozzle portion of the exit cone outside the steel shell was removed and the nozzle shell and ablative returned to Rohr Corporation for disassembly. The bond lines between the ablative and steel shell were broken down by placing the assembly in an oven and heating to 350 to 400°F. In this temperature range the ablatives were free of the shell. Figure 21 shows the shell being removed from the forward ablative stack. Following removal of the ablatives a complete inspection of the adhesive pattern was conducted in order to determine the amount of air entrapment and the amount of pattern obliteration which had occurred. Figure 22 shows a section of the convergent stack and Figure 23 shows the mating section of the steel shell. The holes appearing in the ablative in Figure 22 were drilled to measure material erosion.

The divergent ablative bond line was free of any large void and contained very small amounts of air entrapment. In comparison, the entrance cone had the next best bond with the forward throat and mid throat being last and both showing approximately the same amount of pattern obliteration. Figure 24 shows the zinc chromate putty line between the entrance cone and forward throat after disassembly. The zinc chromate putty had lost its resilience and tacky qualities.

Following the disassembly inspection, the ablatives were sectioned and the erosion and char was determined. A program plan entitled "Post-Test Analyzation of the 156-2C-1 Nozzle Ablatives," dated 22 April, was initiated for the purpose of testing the expended 156-2C-1 nozzle ablatives. The first nine tasks of this plan were to be conducted by Rohr Corporation, Riverside, California, and the remaining tasks were put out for competitive bids. The last nine tasks were never started as a result of program termination.

The following is a summary of the test methods used and the results obtained from the first nine tasks up to the time of program termination.

Task 1

Test: Resin content

Method: 1)   Entrance cone and exit cone carbon - by vacuum
                 pyrolysis per Thiokol specification SB-SP-123

            2)   Forward, mid and aft throats - by vacuum pyrolysis
                 per Thiokol specification SB-SP-124

            3)   Exit cone silica - by pyrolysis per Thiokol spec-
                 ification SB-SP-125

Results: Table XXVII shows the results from these tests. The table
            indicates that resin content after static test compares favor-
            ably with the "as received" material with the exception of the
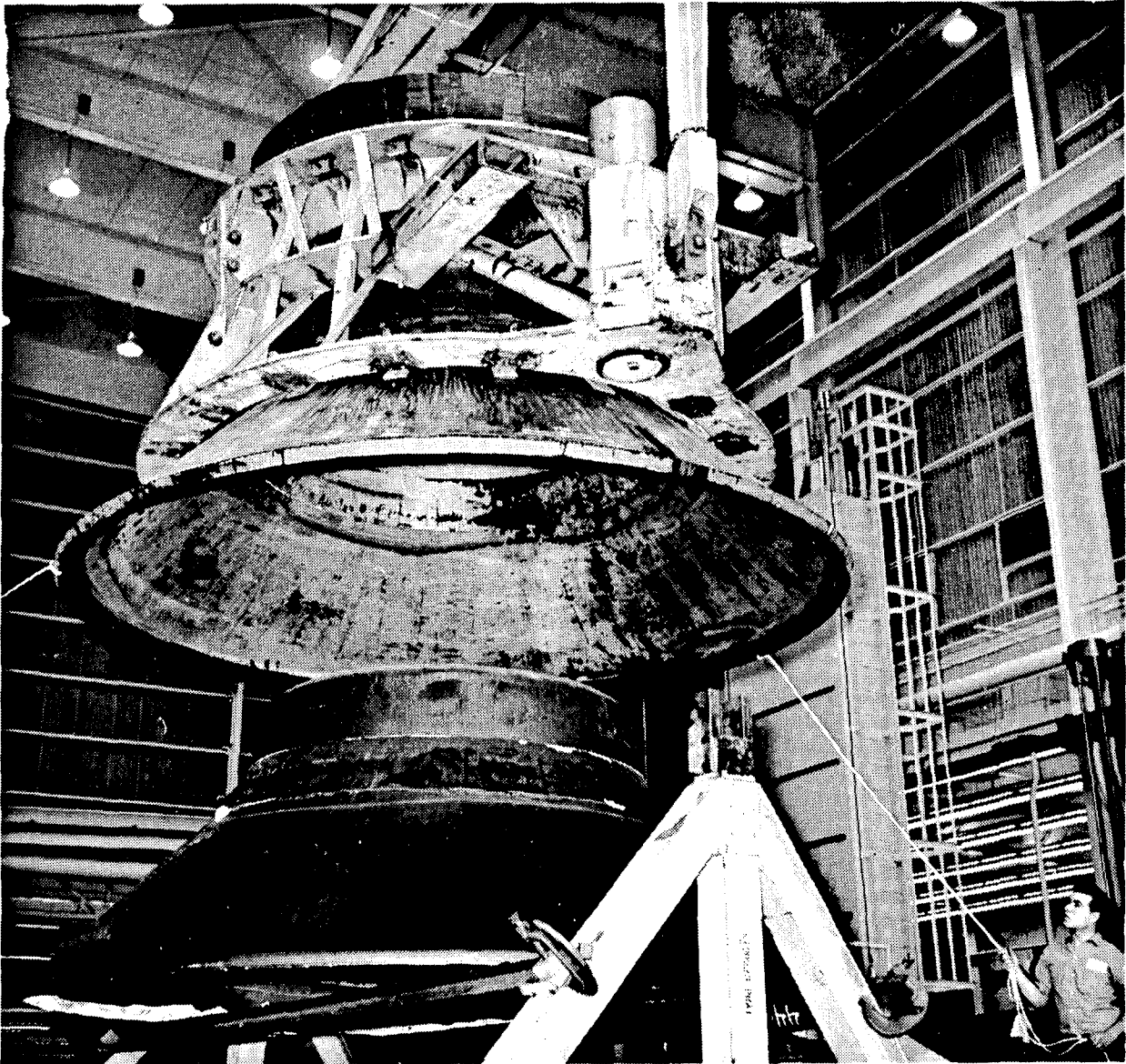
Figure 21 - Removal of Shell
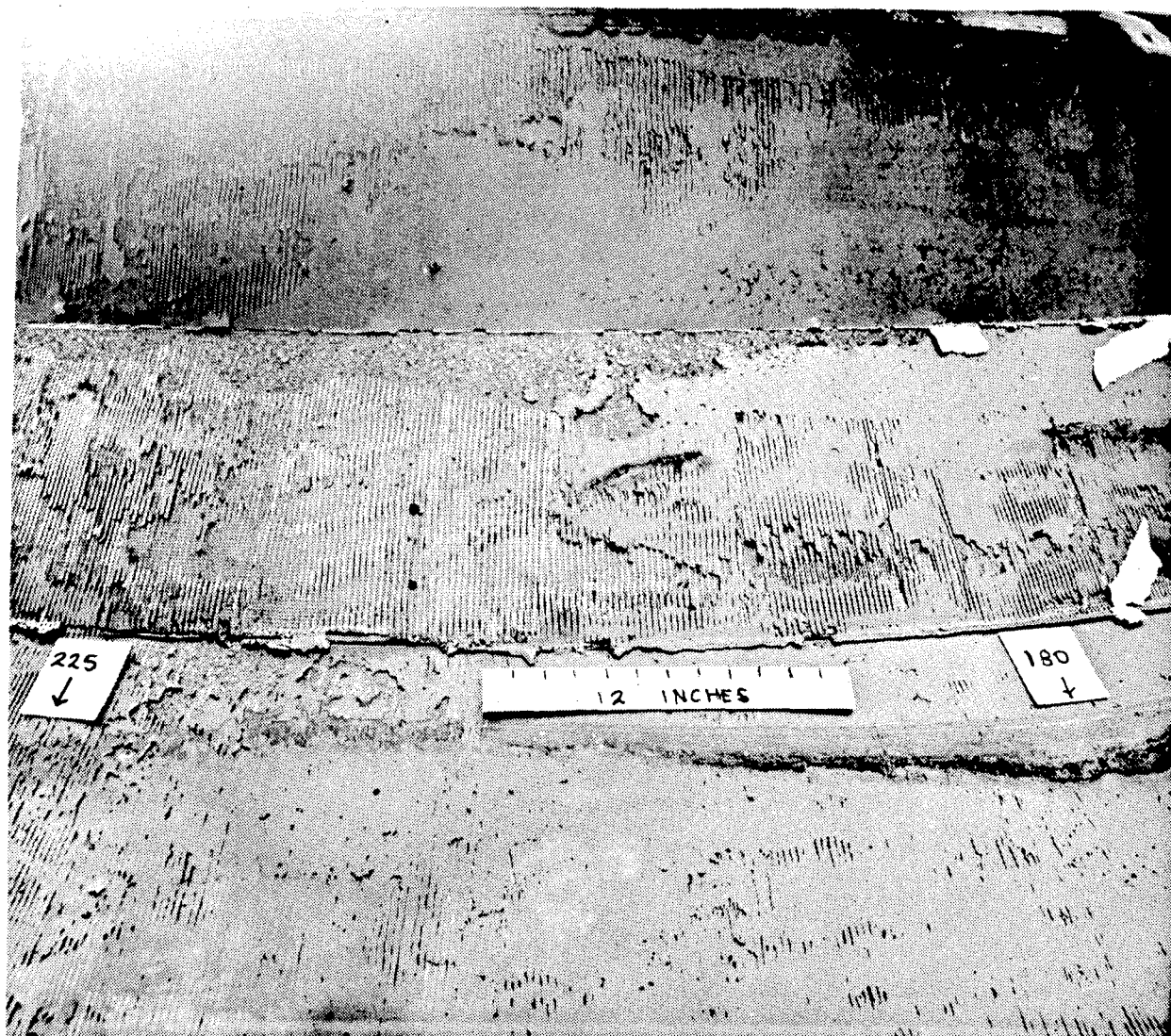
Figure 22 - Section of Convergent Stack

Figure 23 - Mating Section of Steel Shell

Figure 24 - Zinc Chromate Putty Line

TABLE XXVII

TASK I: RESIN CONTENT OF UNCHARRED ABLATIVE MATERIALS

Component 1) Name 2) Pin 3) Material	Pre-Fired Test Results of As-Received Raw Material		Sta. Location		Post Fired Test Results 156-2C-1	
	Test Method And/Or Procedure	Average %	Radial Degree	Longitudinal	Test Method And/Or Procedure	Average %
Exit Cone 1S11004-01-01 High-Silica	RMS-021 Para. 3.4.2	32.2	270 300 310	S5+20S S5+16S S5+28S	SB-SP-125 Para. 4.4.2	33.6 Notes
Exit Cone 1S11004-01-01 Carbon	RMS-020 Para. 3.4.2	33.6	30 120 0	S5+20 S5+20 S5+20	SB-SP-123A Para. 4.4.1.2 K Factor= 2.15	41.0 Notes
Aft Throat 1S11004-01-02 Graphite	RMS-019 Para. 3.4.2.1	36.2	0 30 120	S4-5 S4-5 S4-5	SB-SP-124 Para. 4.4.1.2	34.1 Notes
Mid Throat 1S11004-01-04 Graphite	RMS-019 Para. 3.4.2.1	34.0	0 30 120	S3-6 S3-3 S3-6	SB-SP-124 Para. 4.4.1.2	35.5 Notes
Forward Throat 1S11004-01-05 Graphite	RMS-019 Para. 3.4.2.1	35.1	0 30 120	S2-2 S2-6 S2-6	SB-SP-124 Para. 4.4.1.2	34.4 Notes
Entrance Cone 1S11004-01-06 Carbon	RMS-020 Para. 3.4.2	36.1	30 120 0	S1-6 S1-7 S1-7	SB-SP-123A Para. 4.4.1.2 K Factor= 1.84	34.1 Notes

NOTE 1: Resin content not required on as-cured components. Ref.: SB-SP-2.

NOTE 2: Raw materials cured on platen press, using vacuum pyrolysis method, per RMS-020 for carbon and RMS-019 for graphite.

NOTE 3: Carbon specimens from exit cone were retested after a 24 hour bake cycle at 300°F. Average % = 35.6

NOTE 4: Station locations for test specimens are graphically illustrated on Figures 25 and 26.

NOTE 5: Average based on three reported values, from locations shown.

exit cone carbon material. This material which had shown previous tendency to absorb moisture was subjected to a bake cycle at 300°F for 24 hours and retested. The resulting resin content was 35.6%.

Task 2 and Task 3

Test: Density of charred and uncharred ablative

Method: ASTM No. C493-62T

Results: Tests were not completed due to a delay in obtaining the test equipment and difficulty encountered in using this test for these materials.

Task 4

Test: Determine ply orientation

Method: The section removed for the erosion and char measurement was marked as to ply orientation with the aid of a magnifying glass and measurements were then taken.

Results: Table XXVIII shows the results of these measurements. The table indicates the maximum deviation of ply orientation from the nominal value was 4°40' on the aft end of the aft throat ablative. This deviation in this area would not adversly affect performance to any degree. Other deviations were so small or in such a direction that performance would not be adversely affected.

Task 5

Test: Flexure strength and modulus

Method: ASTM D790 and Thiokol specification SB-SP-2D

Results: Table XXIX shows the results of these tests and a comparison with values from the same test during the ablative processing. Figures 25 and 26 show the location of the specimen for each of these tests. The results show a slight decrease in the modulus of the material in most instances which may be explained by differences in specimen orientation in the two tests. Some variation in flexure strength can be noticed but none of the values in either case are outside the specification requirements.

Task 6

Test: Acetone extractables

Method: Federal Test Method No. 406, Method 7021

Results: Table XXX shows the results of these tests and a comparison with the in-process test for these ablatives. The results show both

TABLE XXVIII

TASK 4: TAPE ORIENTATION ANGLE OF NOZZLE
ABLATIVE COMPONENTS
156-2C-1

Component 1. Name 2. P/N 3. Material	Specification Requirement Angle Mandrel	Test Values	
		30° Radial Location	240° Radial Location
Exit Cone 1S11004-01-01 High-Silica and Carbon	0° ± 2°	2° 15' 3° 2° 3°	2° 40' 2° 15' 1° 10' 1° 15'
Aft Throat 1S11004-01-02 Graphite	30° ± 2°	25° 20' 31° 50'	26° 45' 30° 25'
Mid Throat 1S11004-01-04 Graphite	45° ± 2°	45° 15' 48° 27'	44° 40' 47° 55'
Forward Throat 1S11004-01-05 Graphite	60° ± 2°	58° 13' 60° 53'	57° 7' 59° 32'
Entrance Cone 1S11004-01-06 Carbon	60° ± 2°	62° 18' 61° 53' 60° 23' 59° 3' 58° 38' 59° 43' 60° 18'	63° 13' 61° 23' 60° 28' 58° 53' 58° 43' 59° 18' 59° 8'

NOTE 1: Tape orientation angle was measured at six (6) inch
intervals on the exit and entrance cone.

NOTE 2: Tape orientation angle was measured at each end
on the three throat components.

NOTE 3: Test values are listed in component aft end to forward
end order.

TABLE XXIX

TASK 5: FLEXURAL STRENGTH AND FLEXURAL MODULUS OF UNCHARRED ABLATIVE MATERIALS

Component 1.) Name 2.) P/N 3.) Material	In-Process Test Results 156-2C-1 Flexural Strength psi, avg.	Flexural Modulus psi x10^6, avg.	Station Location Radial	Long.	Post Fire Test Results 156-2C-1 Flexural Strength psi, avg.	Flexural Modulus psi x10^6, avg.
Exit Cone IS11004-01-01 High-Silica	20,449	2.515	300° 270° 310°	S5 + 16S S5 + 20S S5 + 28S	21,350	2.283
Exit Cone IS11004-01-01 Carbon	40,426	2.909	30° 120° 150°	S5 + 3 S5 + 15 S5 + 28	35,266	2.260
Aft Throat IS11004-01-02 Graphite	20,420	1.681	30° 120° 150°	S4 - 6 S4 - 4 S4 - 1	19,600	1.631
Mid Throat IS11004-01-04 Graphite	22,018	1.604	150° 120° 0°	S3 - 9 S3 - 6 S3 - 1	16,633	1.193
Forward Throat IS11004-01-05 Graphite	26,868	1.936	30° 120° 0°	S2 - 6 S2 - 6 S2 - 1	17,933	1.161
Entrance Cone IS11004-01-06 Carbon	31,042	2.362	0° 120° 150°	S1 - 35 S1 - 15 S1 - 5	36,133	2.241

NOTE 1: Flexural test specimens for in-process test results, were obtained from Q. C. excess material removed from part per stage drawings.

NOTE 2: Station locations for test specimens are graphically illustrated on Figures 25 and 26.

NOTE 3: In-process testing was performed per SB-SP-2. Post fire tests were performed per SB-SP-2D, paragraph 4.3.1.4.
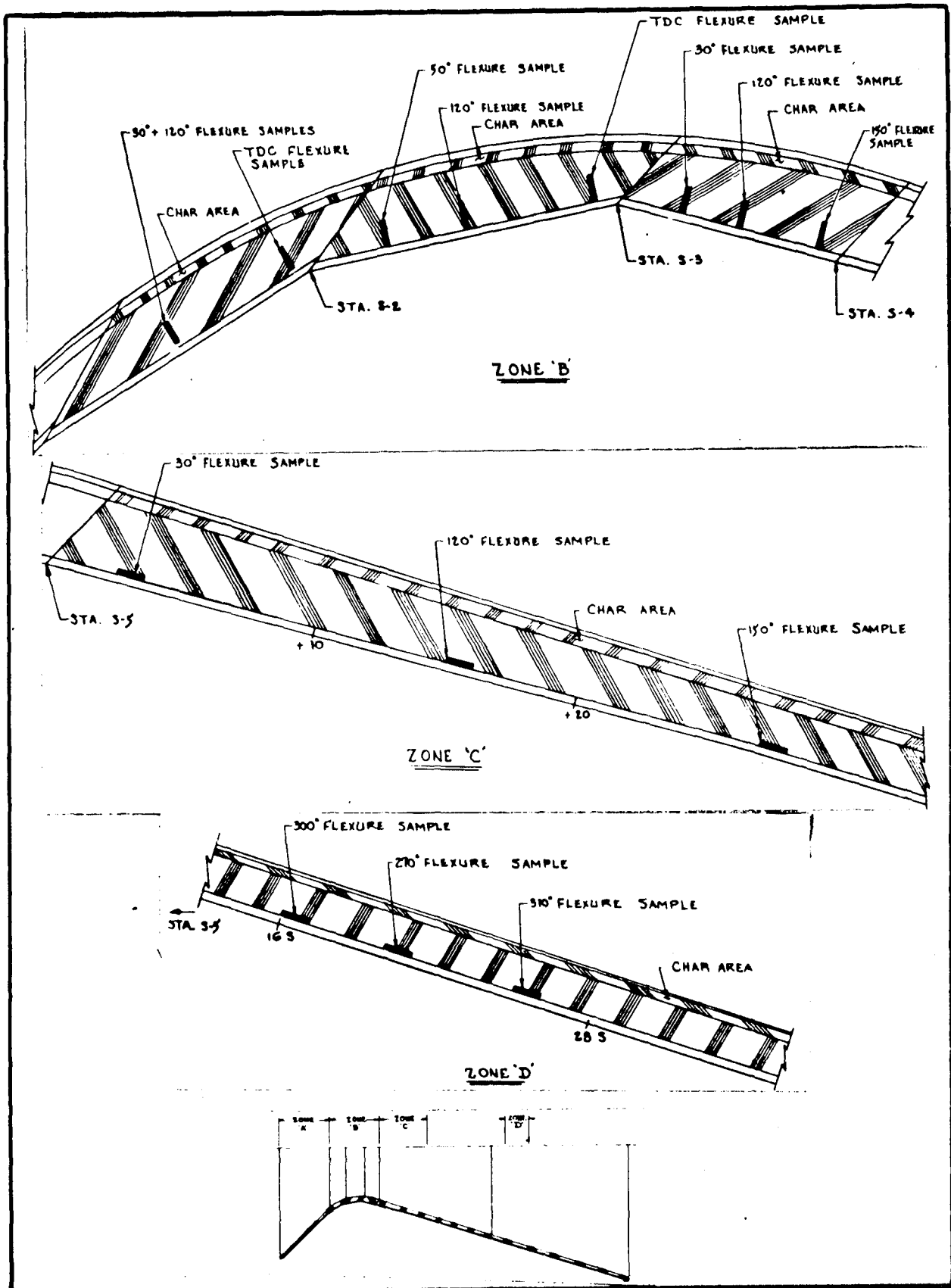
Figure 25 - Test Specimens Locations
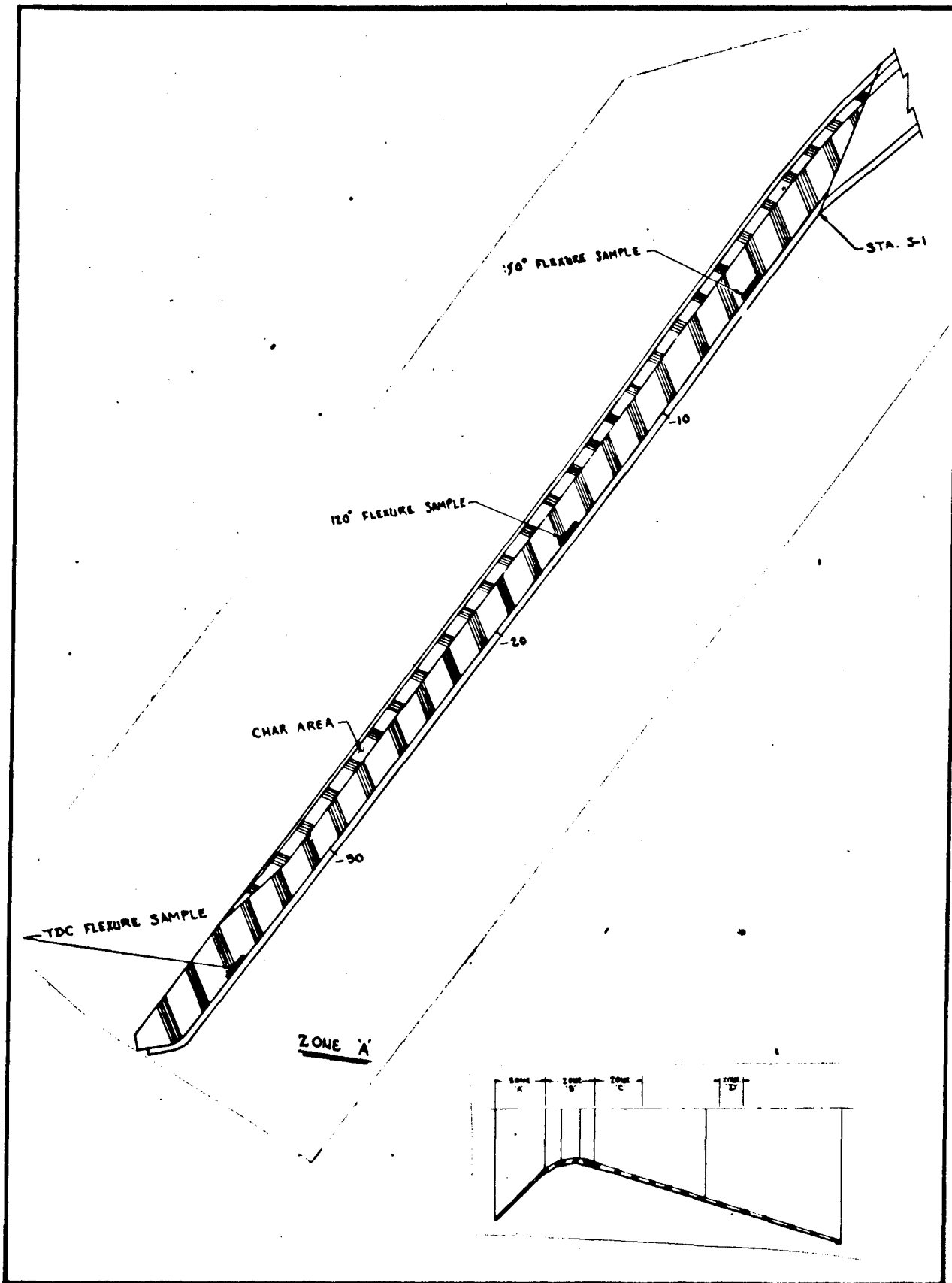
Figure 26 - Test Specimens Locations - Silica

TABLE XXX

TASK 6: ACETONE EXTRACTABLE VALUES OF UNCHARRED MATERIAL

Component 1.) Name 2.) P/N 3.) Material	In-Process Test Results 156-2C-1 Acetone Extractables % Average	Post-Fire Test Results 156-2C-1 Acetone Extractables % Average	Station Location
Exit Cone 1S11004-01-01 High-Silica	0.46	0.29	S5 + 18S (310°) S5 + 18S (330°)
Exit Cone 1S11004-01-01 Carbon	0.21	0.13	S5 + 2 (120°) S5 + 27 (150°)
Aft Throat 1S11004-01-02 Graphite	1.81	2.22	S4 - 7 (150°) S4 - 1 (150°)
Mid Throat 1S11004-01-04 Graphite	4.32	1.21	S3 - 7 (30°) S3 - 1 (30°)
Forward Throat 1S11004-01-05 Graphite	3.55	2.03	S2 - 7 (150°) S2 - 1 (150°)
Entrance Cone 1S11004-01-06 Carbon	4.49	1.73	S1 - 36 (120°) S1 - 2 (120°)

NOTE 1: Station locations for test specimens are graphically illustrated on Figures 25 and 26.

NOTE 2: In-process and post fire tests were conducted in accordance with SB-SP-2C and 2 D respectively, paragraph 4.3.1.5, and Federal Test Standard 406, Method 7021.

NOTE 3: In-process average values represent specimens from the O.D., I.D., and middle of Q.C. excess material.

NOTE 4: Post-fire average values based on three reported test values, representing specimens from O.D., I.D., and middle of component.

increases and decreases in the acetone extractable values after firing which depicts the inherent variability of this test.

Task 7

Test: Determination of hygroscopicity of FM-5064 ablative material

Method: An FM-5064 graphite component was selected which demonstrated acetone extractable values of approximately five (5) percent in the tests outlined under Task 6. Four samples were taken from the component. Two pieces were post-cured until the acetone extractables were reduced to approximately two (2) percent or less. All samples were then machined to provide equal surface areas. Each sample was weighed. All four samples were then subjected to a controlled temperature (room temperature) and 80 percent humidity conditions. Each of the four samples were weighed each day for a period covering seven consecutive working days.

Results: Results of these tests are shown in Table XXXI. The results indicate that this material with 2 percent acetone extractables will absorb 0.8 percent by weight moisture while a material with 5 percent extractable will absorb only 0.5 percent by weight moisture. Within the units of this test, the lower extractable content material will absorb more moisture than the higher extractable content material.

Task 8

Test: Determine weight loss of uncharred ablative material

Method: Samples of each ablative were obtained and tested as follows:

1. Place the samples in a closed container over desiccant for four hours.

2. Remove from desiccated container and weigh (record weight to four decimal places).

3. Place specimen in circulating oven which has been pre-heated to 300 ± 5°F and bake for 24 hours.

4. Remove specimen and immediately place in closed desiccated container for four hours.

5. Remove from container and weigh specimen. (Record weight to four decimal places).

6. Compute weight loss as follows:

$$\text{Weight Loss} = \frac{\text{Original Weight minus Final Weight}}{\text{Original Weight}} \times 100$$

Results: Table XXXII shows the results of the weight loss test and a comparison with some data, collected earlier in similar tests.

TABLE XXXI

TASK 7: HYGROSCOPICITY OF UNCHARRED ABLATIVE MATERIALS
AFT THROAT 1S 11004-01-02
156-2C-1

Pretest Requirements	Acetone Extraction Test			
	2% (Average) 2.2098		5% (Average) 5.3392	
	Weight of Specimens			
DATES	2%		5%	
	No. 1	No. 2	No. 1	No. 2
5-17-65 (initial)	14.0945	14.5190	14.8784	13.9576
5-18-65	14.1414	14.5601	14.9092	13.9868
5-19-65	14.1591	14.5785	14.9220	13.9987
5-20-65	14.1711	14.5922	14.9265	14.0125
5-21-65	14.1782	14.5980	14.9339	14.0173
5-24-65	14.1992	14.6254	14.9442	14.0278
5-25-65	14.2080	14.6291	14.9463	14.0315
5-26-65 (Final)	14.2109	14.6344	14.9509	14.0340

NOTE 1:   Constant humidity of 79.3 was maintained from a solution of NH_4Cl saturated salt solution. Temperature was ambient $75° \pm 5°F$.

NOTE 2:   Acetone extraction test average value based on three (3) reported values.

TABLE XXXII
TASK 8: WEIGHT LOSS OF UNCHARRED ABLATIVE MATERIAL

Component 1.) Name 2.) P/N 3.) Material 4.) Time @ Temperature	In-Process Test Results 156-2C-1 % Weight Loss Average	Post Fire Test Results 156-2C-1 % Weight Loss Average	Station Location
Exit Cone 1S11004-01-01 High Silica 24 hrs. @ 300°F	No tests performed	1.6983	S5 + 205 (270°) S5 + 165 (300°) S5 + 285 (330°)
Exit Cone 1S11004-01-01 Carbon 24 hrs. @ 300°F	3.8109 Note 1	3.3937	S5 + 20 (30°) S5 + 20 (120°) S5 + 20 (150°)
Aft Throat 1S11004-01-02 Graphite 24 hrs. @ 300°F	No tests performed	0.7859	S4 - 5 (0°) S4 - 5 (30°) S4 - 5 (120°)
Mid Throat 1S11004-01-04 Graphite 24 hrs. @ 300°F	No tests performed	0.3613	S3 - 6 (0°) S3 - 3 (30°) S3 - 6 (120°)
Forward Throat 1S11004-01-05 Graphite 24 hrs. @ 300°F	No tests performed	0.8255	S2 - 2 (0°) S2 - 2 (30°) S2 - 6 (120°)
Entrance Cone 1S11004-01-06 Carbon 24 hrs. @ 300°F	No tests performed	3.2453	S1 - 10 (30°) S1 - 6 (120°) S1 - 7 (150°)
Exit Cone 1S11004-01-01 Carbon 8 hrs @ 300°F	2.4634 Note 2	2.1038	S5 + 20 (30°) S5 + 20 (120°) S5 + 20 (150°)
Entrance Cone 1S11004-01-06 Carbon 8 hrs. @ 300°F	1.7398 Note 3	2.3826	S1 - 10 (30°) S1 - 6 (120°) S1 - 7 (150°)

NOTE 1: Per technical information request #15, 24 hours at 325° F 156-2C-1 Exit Cone.

NOTE 2: Per technical information report #15, 8 hours at 300° F 156-2C-1 Exit Cone.

NOTE 3: Per technical information report #5, 8 hours at 300° F 156-2C-1 Entrance Cone.

NOTE 4: Station Locations for test specimens are graphically illustrated on Figures 25 and 26.

These results serve to verify the fact that the carbon material will absorb more moisture than the other ablative materials.

Task 9

Test: Determine effect of epoxy Corlar coating on graphite material used to exclude moisture prior to motor test.

Method: A sample of FM-5064 from the 156-2C-1 ablatives was coated with the Corlar sealer used on the throat ablative for the nozzle. Acetone extractable content and hardness of the cone was measured before coating and after removal of the coating material from the coated surfaces.

Results: The results of the tests are shown in Table XXXIII. With the limited data, no definite conclusion could be drawn, however, there appears to be a slight effect on the surface as a result of the coating. How the surface change would affect ablative performance is not known.

TABLE XXXIII

TASK 9: CORLAR COATING OF GRAPHITE MATERIALS
THROAT 1S 11004-01-02
156-2C-1

Type of Test	Test Result (average)	Test Procedure and/or Method
Acetone extraction, % before Corlar coating	2.2498	SB-SP-2D Federal Test Standard 406 Method 7021
Acetone extraction, % after stripping Corlar coating	1.8560	SB-SP-2D Federal Test Standard 406 Method 7021
Barcol hardness before Corlar coating	54.0	
Barcol hardness after stripping Corlar coating	50.3	

NOTE 1: Enamel and primer were removed from the specimen with a putty knife. The surface was then sanded to remove all traces of primer prior to sampling for Barcol hardness and acetone extraction.

NOTE 2: Material for extractable tests removed from surface immediately below sanded area to a maximum depth of 0.300".

NOTE 3: Station locations for test specimens are graphically illustrated on Figures 25 and 26.

90

VIII. NOZZLE ADAPTER

A. DESIGN

The basic design premise for the adapter was to allow the use of a single
large nozzle design for the 156-2C-1 and 260-SL motors. Overall nozzle
design was such that the nozzle could be attached directly to the aft end
of the 156-2C-1 motor case or could be used with the adapter for attach-
ment to the 260-SL motor case.

The adapter was made of 250 ksi grade maraging steel. The interior was to
be covered with a mastic insulation to protect it from high temperature gases
during motor operation. Table II summarized the materials used in design.

Table XXXIV summarizes the geometric design and weights of the adapter.
Thiokol drawing 1S 11005 shows the detail of the adapter design.

B. MATERIAL

The requirements for composition and mechanical properties of the shell
steel are shown in Tables III and IV, respectively.

It had also been intended to use a tape wrapped component as an insulation in
the adapter. Due to the subscale work and concurrent large case insulation
work, an alternate approach was chosen. At first, a vulcanized Buna-N in-
sulation was favored. As the result of subscale motor testing the mastic in-
sulation-Thiokol's TI-H704B was selected. This material offered a saving of
time and money. Although the program termination negated the mastic's use
in the adapter, this same material performed satisfactorily as the case insulation in
the 156-2C-1 motor and in the nozzle entrance of the 65-SS subscale motors.

C. STRUCTURAL ANALYSIS

The structural analysis conducted on the adapter has been reported in Section
V. After this analysis, the flange portion of the steel nozzle shell and adapter
shell were reanalyzed from a structural standpoint based on an improved
design. The second structural analysis of the redesigned nozzle flange area
and the adapter shell is presented in a Huntsville Division report entitled,
"Structural and Dynamic Analysis of the Half-Length 260-SL-1 Inch Diameter
Space Booster Motor Case," dated March 9, 1964.

Figures 27 and 28 show margins of safety of the adapter related to the inter-
face with other components and under hydro and static conditions.

D. FABRICATION

1. 260-SL-1 Adapter Fabrication

For nozzle adapter fabrication, the conical section and both attachment flange
forgings were stacked, welded on the outside, reverted, prepared for welding

TABLE XXXIV

ADAPTER GEOMETRY AND WEIGHT

Ref. Drawing 1S 11005

Dimensions	
Length, (in.)	26.5
Large attach flange outside dia., (in.)	191.5
Small attach flange inside dia., (in.)	136.5
Adapter Calculated Weights	
Steel housing, (lb)	6828
Mastic insulation (TI-H704B), (lb)	5650
Total	12,478
Actual steel component shipping wt., (lb)	7490*

*Component was machined to clean-up only

90.0R

Adapter Flange at
Shear Lip
M.S. = 0.394
M.S. = 0.533

Adapter Membrane
M.S. = 1.900 (Hydro)
M.S. = 2.190 (Static Firing)

Inner Bolts
M.S. = 0.532 (Hydro)
M.S. = 0.685 (Static Firing)

Adapter Flange at Bolt Circle
M.S. = 2.728 (Hydro)
M.S. = 3.100 (Static Firing)

Outer Bolts
M.S. = 0.469 (Hydro)
M.S. = 0.615 (Static Firing)

Case Membrane
M.S. = 1.620 (Hydro)
M.S. = 1.890 (Static Firing)
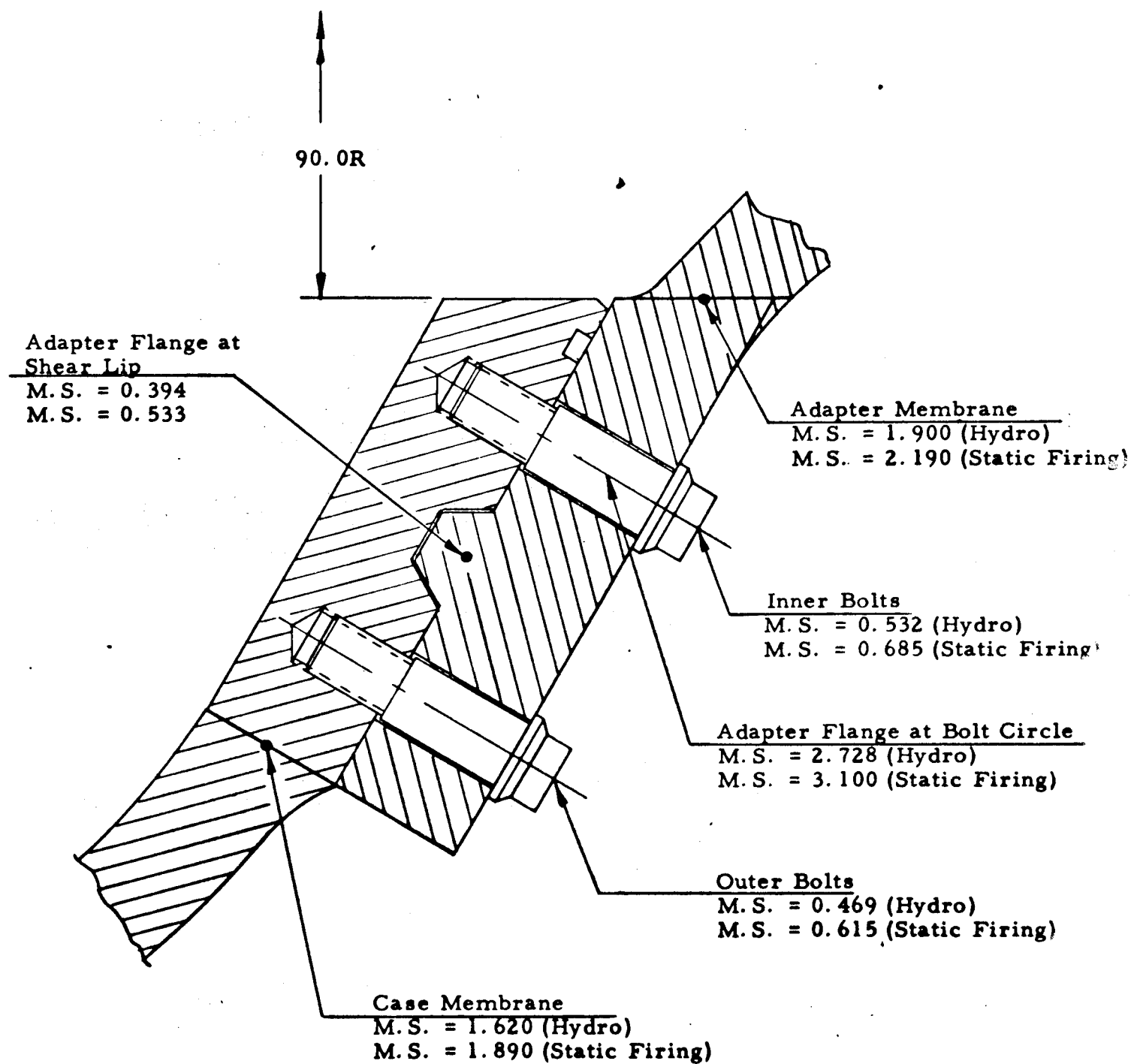
Figure 27 - 260 Case to Adapter Margins of Safety

Nozzle or Fixture Membrane
M.S. = 0.513 (Hydro)
M.S. = 0.663 (Static)

68.28 R

Shear Lip
M.S. = 2.41
          (Hydro)
M.S. = 2.75 (Static)

Adapter Membrane
M.S. = 1.117 (Hydro)
M.S. = 1.328 (Static)

Flange at Bolt Circle
M.S. = 0.701 (Hydro)
M.S. = 0.870 (Static)

Inner Bolts
M.S. = 1.04 (Hydro)
M.S. = 1.24 (Static)

Outer Bolts
M.S. = 3.935 (Hydro)
M.S. = 4.427 (Static)

Nozzle and Hydro Fixture
Flange
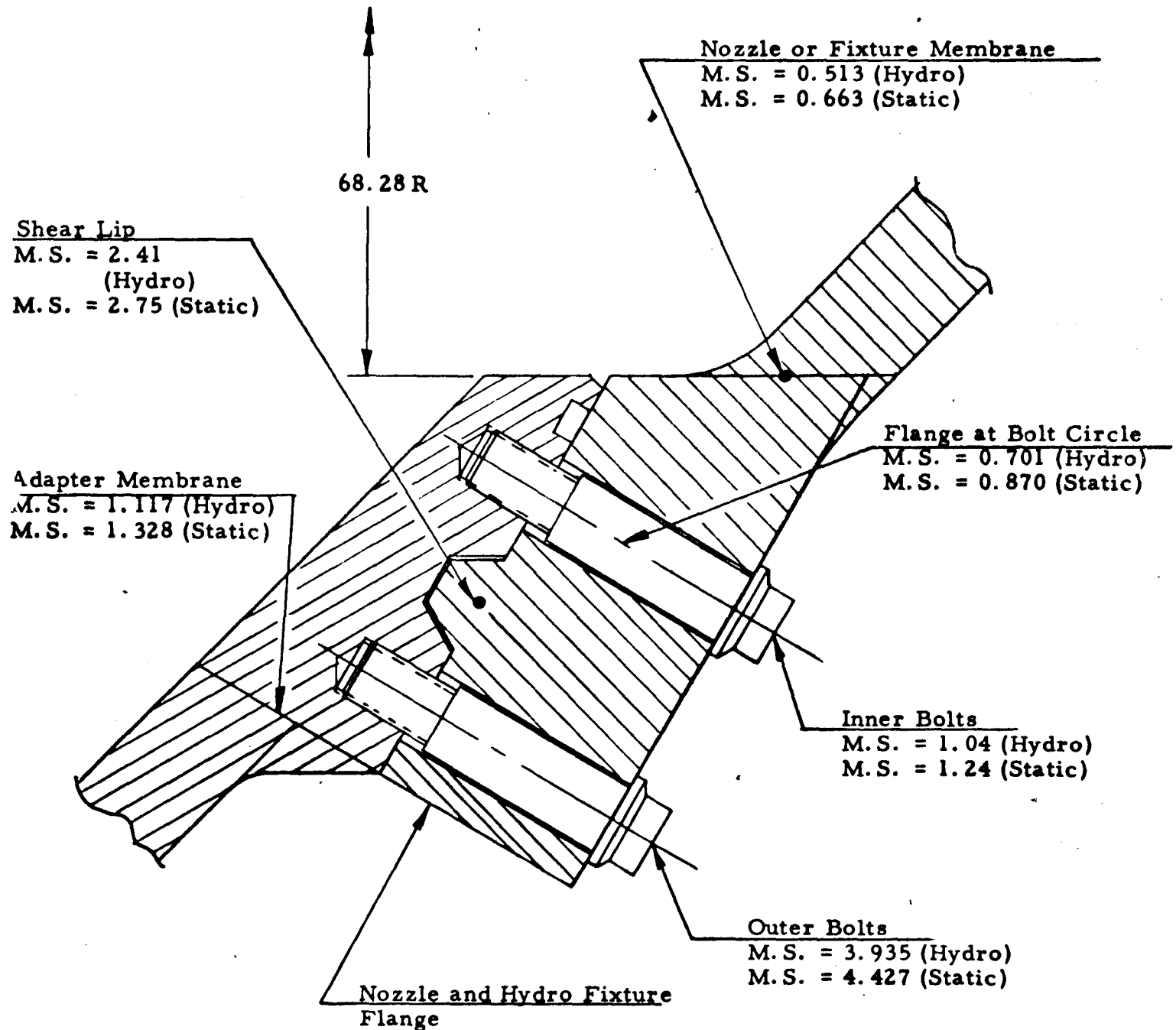
NOTE: Margins shown for hydro condition apply for the adapter to hydro fixture analysis, and margins shown for static condition apply for adapter to nozzle analysis.

Figure 28 - 260 Adapter to Nozzle and Hydro Fixture Margins of Safety

and then welded on the inside. Figure 29 shows adapter segments and weld locations.

Following the completion of sub-arc welding and a long series of numerous repairs, the Unit No. 1 nozzle adapter was subjected to two anneal and size cycles for dimensional control and then aged. The first attempt to age the unit was aborted when the temperature reached 600°F after an error in the method of attaching thermocouples was discovered. The thermocouples had mistakenly been buried inside blocks rather than attached to the surface.

A second attempt at aging the component was successful. Figure 30 shows the location of the thermocouples and the location of the part in the furnace. Tables XXXV, XXXVI, and XXXVII show the results of the test specimens which accompanied the part through the furnace.

2. 260-SL-2 Adapter Fabrication

Fabrication of the 260-SL-2 adapter was analogous to fabrication of Unit No. 2 nozzle shell. The frequency of weld repair dropped sharply. There were only nine weld defects in this part. Two were short cracks and the rest were inclusions.

At program termination, the adapter had one weld repair remaining. Only aging, machining, drilling and tapping were required for completion of the component.
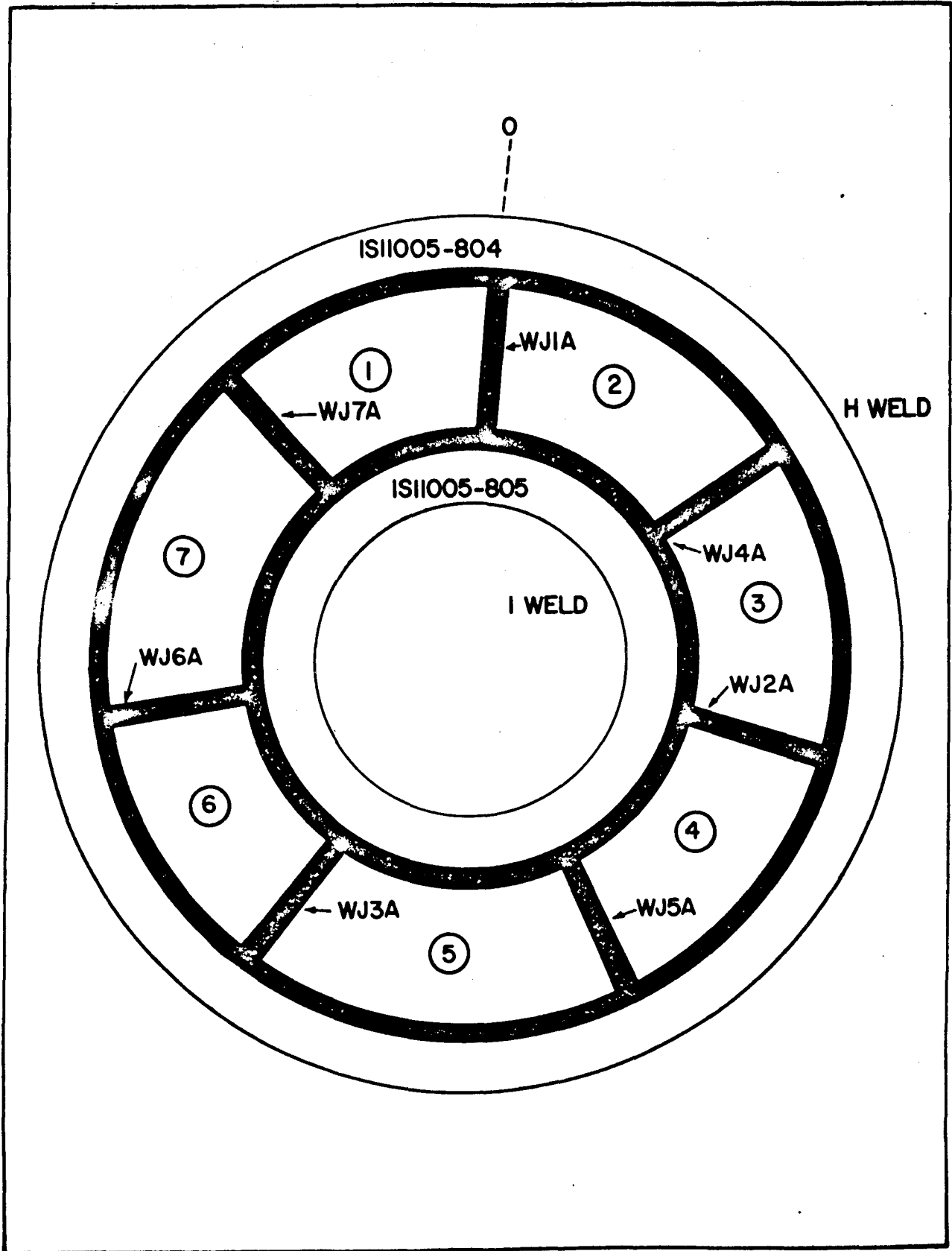
Figure 29 - 260-SL-1 Adapter Segments and Weld Locations
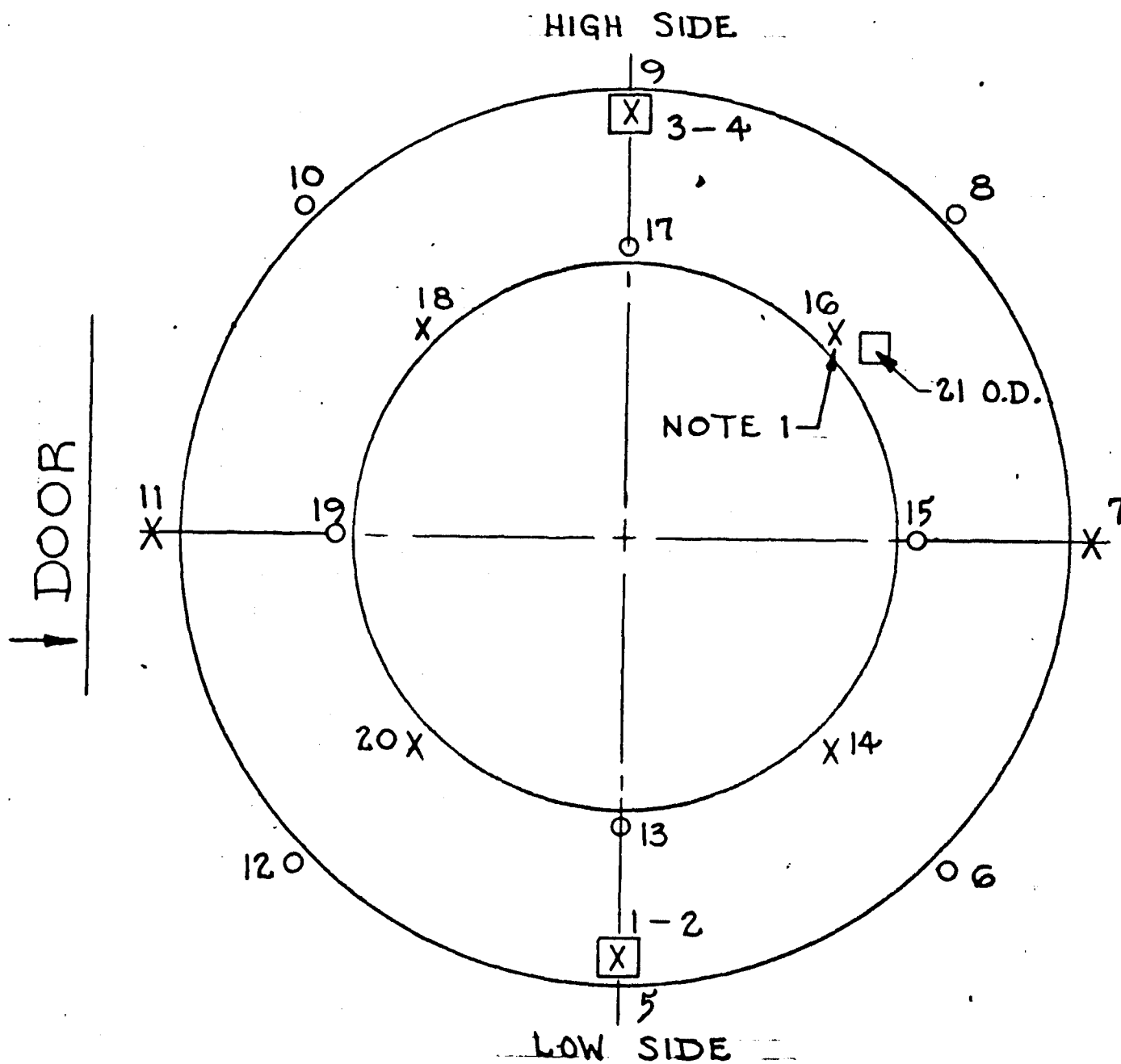
Figure 30 - Thermocouple Location for 260-SL-1 Adapter Aging

TABLE XXXV

PRODUCTION TEST OF 260-SL-1 ADAPTER LONGITUDINAL TEST BAR WELDS

TENSILE DATA

Longitudinal Welds	Weld Pass	Yield Strength (ksi)	Ultimate Tensile Strength (ksi)	Elongation (%)	Reduction of Area (%)	Fracture Location
Weld 7A	OD	227.5	251.0	6.2	22.8	Weld
0.252 in.	OD	227.0	251.0	9.8	30.9	Weld
dia. test	ID	242.4	251.0	9.2	31.4	Weld
bars	ID	228.1	250.5	10.0	45.2	Weld
Weld 6A	--	221.0	236.9	4.0	11.0	Weld
0.505 in.	--	222.7	237.6	10.2	39.7	Weld
dia. test	--	217.2	234.1	8.6	36.3	Weld
bars						

FRACTURE TOUGHNESS DATA

Longitudinal Welds	Weld Pass	Fracture Toughness W/A (in. lb/in.^{2})[*]	Average
Weld 7A	OD	215	--
	ID	250, 266, 265	257
Weld 5A[**]	OD	245, 247, 273, 218, 223	241
	ID	314, 277, 305, 291	296

[*]Bars cracked in aged condition; normal practice is to crack the bars prior to aging.

[**]Supplemental longitudinal weld specimens from weld 5A, aged in a laboratory furnace and tested for W/A values only.

TABLE XXXVI

PRODUCTION TESTS OF 260-SL-1 ADAPTER

CIRCUMFERENTIAL TEST BAR WELDS

TENSILE DATA

Forging	Weld Pass	Yield Strength (ksi)	Ultimate Yield Strength (ksi)	Elongation (%)	Reduction of Area (%)	Fracture Location
804 to cone						
0.505 in.	--	225.8	236.7	9.5	41.0	Weld
dia. test bars	--	223.5	236.5	8.2	25.5	Weld
	--	224.1	238.1	5.0	14.5	Weld
0.252 in.	OD	231.4	243.6	2.6	5.6	Weld
dia. test bars	OD	232.3	244.4	8.0	27.8	Weld
	ID	235.4	241.4	1.5	1.2	Weld
805 to cone						
0.505 in.	--	231.5	244.1	5.0	20.3	Weld
dia. test bars	--	229.8	242.4	7.1	32.2	Weld
	--	232.3	244.8	4.5	16.6	Weld
0.252 in.	OD	235.1	245.5	4.0	12.2	Weld
dia. test bars						
	ID	232.6	244.0	*	*	HAZ
	ID	233.4	245.0	8.7	36.8	Weld

FRACTURE TOUGHNESS DATA

Forging	Weld Pass	Fracture Toughness W/A (in. lb/in.^{2})	Avg.
804 to cone			
	OD	287, 269, 318	291
	ID	266, 288, 281	278
805 to cone			
	OD	254, 386	320
	ID	216	216
Supplemental welds**	OD	277, 317, 319, 269, 274	291
	ID	280, 253, 269, 319, 315	287

NOTES: 1. Test bars were aged at 825 F for 3-1/2 hours.
*Bar broke in fillet; unable to calculate percent elongation or percent reduction of area.
**Supplemental circumferential weld specimens aged in laboratory furnace and tested for W/A values only.

TABLE XXXVII

PRODUCTION TESTS OF 260-SL-1 ADAPTER
PARENT MATERIAL PROPERTIES

Parent Material	Yield Strength (ksi)	Ult Tensile Strength (ksi)	Elongation (%)	Reduction of Area (%)
Cone	227.1	239.6	9.0	36.3
(plate 41705,	226.8	238.1	9.2	38.4
heat 53471	234.2	242.2	9.4	39.0
Forging 804	238.8	241.3	10.5	47.0
	242.6	255.3	10.8	47.8
	242.6	255.5	10.2	46.2
Forging 805	235.8	247.6	9.7	40.2
	231.9	246.8	10.4	43.6
	234.7	247.1	10.8	47.0

NOTE: Test bars were aged at 835 F for 3-1/2 hours.

IX. DEVELOPMENT AND INVESTIGATIONS

A. NOZZLE MATERIAL INVESTIGATION

1. Ablatives

a. Tape Splices Development

During the initial phases of tape wrapping for the 156-2C-1 nozzle components, problems were encountered with tape splices. Tape splices, necessary to join adjacent pieces of prepreg tape into a large roll of continuous type wrapping, pulled apart when subjected to the wrapping conditions of tension and heat.

Several splicing techniques were investigated. One of these, developed by the Fiberite Corporation, was the hot dimpled splice. This approach involved pressing the sections to be joined in a heated tool resembling a waffle iron, but having protruding balls which mated with cavities of the same shape. Failure of these splices occurred, however, and appeared to be caused by poor flexibility of the splices which were required to follow a circuitous route around the rollers of the tape wrapping head. As an immediate replacement, straight and zig-zag stitched nylon splices were investigated. The straight stitch weakened the parent material because of damage to the tape yarns caused by close spacing of the needle holes. Zig-zag stitch wrapping tests made with carbon warp tape showed that a half-tape-width overlap with three transverse zig-zag stitches provided marginal reliability for production wrapping temperatures and tape tensions. This type of splice was the most reliable and available, so tape stocks were reworked to replace all dimpled splices with sewn joints.

Subsequently, Fiberite modified its dimple splicing techniques by increasing the number of dimples per square inch of area (high density dimples). These splices are compared with the overlap zig-zag splices in Tables XXXVIII and XXXIX. The high density dimple splices exhibited better high temperature breaking strengths than the sewn splices, but no improvement in flexibility was noted.

A longitudinally sewn zig-zag stitch was investigated. Test results with this splice and the 7.3-inch-wide MX-2600 silica warp tape are shown in Table XL. Several test splices, sewn in the pattern sketched in Figure 31 were run through the production wrapping equipment under actual wrapping conditions. All splices were satisfactory and passed through the equipment with a minimum of tape distortion at 240°F and 14 pounds per inch-width tension. Material received for wrapping of the exit cone was spliced by this method. No reductions in tape tensions or temperature were necessary.

b. Silica Tape Breaking Strength Tests

An unexpected materials problem arose when tape wrapping of the silica portion of the exit cone started. With adequate or even very low tape tension, repeated breakage of the tape occurred during the wrapping process. The frequency of breakage made it impossible to perform the wrapping operation.

Tests of room temperature breaking strength, which was a normal part of

TABLE XXXVIII

DATA FROM TESTING SPLICES IN TWO-INCH-WIDE CARBON
WARP TAPE RUN AT TEN FEET PER MINUTE

Material	Type of Splice	Test Temp (F)[1]	Breaking Strength (lb)	Type of Failure
MX 4926	1.1-in. overlap high density dimple	Ambient	33	Splice
		150	28	Tape
		155	21	Tape
		240	18	Splice
		260	23	Splice
MX 4926	4-in. overlap, zig-zag Stitch, 4 rows, nylon thread	Ambient	74	At last stitching
		Ambient	56	At last stitching
		130	20	Tape
		240	11	Splice
		240	5	Splice
		250	8	Splice

NOTE 1:   Specimens heated by heat gun; temperature measured with
            T/C junction in contact with tape surface.

TABLE XXXIX

DATA FROM TESTING SPLICES IN TWO-INCH-WIDE SILICA
WARP TAPE RUN AT TEN FEET PER MINUTE

Material	Type of Splice	Test Temp (F)[1]	Breaking Strength (lb)	Type of Failure
MX 2600	1. 1-in. overlap high density dimple	Ambient	77	Splice
		Ambient	84	Splice
		130	72	Splice
		140	88	Tape
		250	35	Splice
		260	31	Splice
MX 2600	4-in. overlap zig-zag stitch, 4 rows, nylon thread	Ambient	140	At last stitching
		Ambient	170	At last stitching
		130	36	At last stitching
		130	23	At last stitching
		140	22	At last stitching
		250	12. 5	At last stitching
		260	12. 5	At last stitching

NOTE: 1. Specimens heated with heat gun; temperature measured with T/C junction in contact with tape surface

TABLE XL

DATA FROM TESTING LONGITUDINAL-STITCH SPLICES IN SILICA
WARP TAPE RUN AT TEN FEET PER MINUTE

Splice Type	Test Temp (F)[1]	Tape Test Width (in.)	Breaking Strength (lb/in. width)	Type of Failure
	Ambient	1.0	126	Tape
	Ambient	1.0	128	Tape
	250	0.8	24	Tape
Longitudinal, zig-zag stitch	Ambient	1.0	50	One stitch, thread tore
	160	0.65	37	One stitch
	275	0.75	21	One stitch
	255	2.0	15	Two stitches

NOTES: 1. MX 2600 tape

2. Specimens heated by heat gun; temperature measured
with T/C junction in contact with tape surface

DIRECTION OF PAY-OFF FROM SPOOL

0.4 IN.
0.6 IN.
(TYP)
2 PLACES

OVERLAP

STITCHES 1.5 INCHES APART
BETWEEN EDGE STITCHES
(1 1/4 IN. MINIMUM, 5/8 IN.
MAXIMUM)

℄ STITCH

ZIG-ZAG
STITCH (TYP)

0.5 IN.
1.5 IN.
(TYP)

PATTERN FACES OUTSIDE OF TAPE ROLL
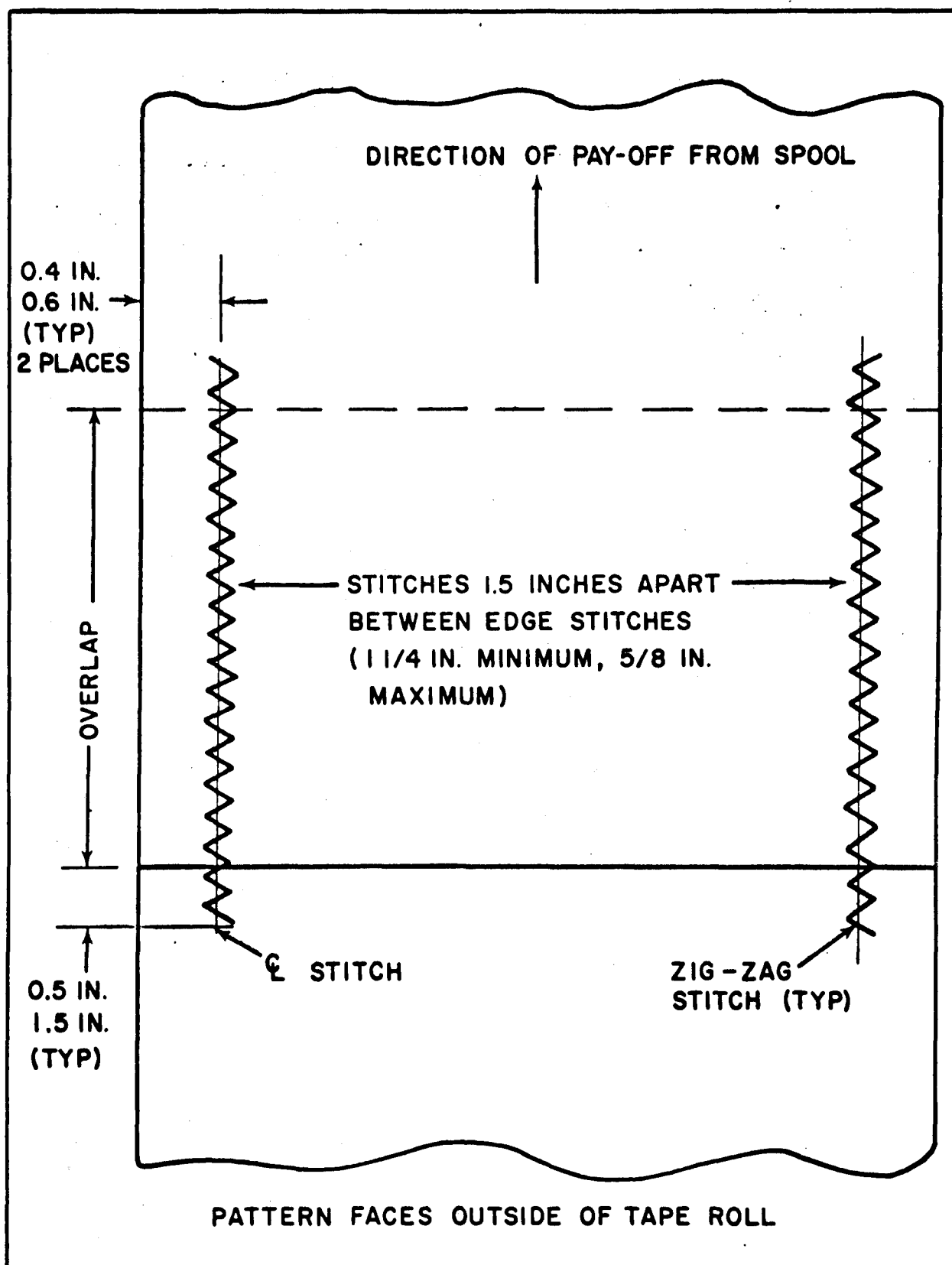
Figure 31 - Sketch of Satisfactory Zig-Zag Pattern, 7.3-Inch-Wide MX 2600
Silica Warp Tape

received-material inspection, did not provide any correlation with production wrapping experiences. Also, an examination of the tape wrapping head, to determine if any misalignment existed that might cause unequal tensioning across the tape width, revealed no discrepancies.

A careful re-examination of the tape failures during wrapping showed that the tape always broke while in the heating zone of the heat lamps. Temperature checks verified that the tape temperature in the region of the heaters was at the intended 250°F level. Since no progress was made by room temperature testing of materials, laboratory testing at an elevated temperature (250°F) was begun. Laboratory testing revealed that material which displayed adequate room temperature breaking strengths of from 80 to 120 pounds per inch of width broke at significantly lower values when heated to 250°F. These tests resulted in hot breaking strengths from as high as 60 pounds per inch of width to as low as 2 pounds per inch of width. Material having different levels of hot breaking strength was selected for test wrapping using full-scale tooling. This procedure resulted in an excellent correlation between hot breaking strength and the wrapping of the tape. Material displaying hot breaking strengths of 20 to 30 pounds per inch of width provided marginal results while material with strengths of more than 30 pounds per inch performed adequately. Material with strength less than 20 pounds per inch of width was virtually unwrappable because of repeated breakage. The results of the tests indicated that damaged fibers existed in the silica fabric which could transmit tensile loads into adjacent, undamaged fibers and back across the break by means of shear between the fibers and the resin (at room temperature). When the tape was heated (causing a sharp decrease in resin viscosity) this load transferral could not be accomplished; therefore, a rapid loading of the undamaged fibers occurred causing tape failure.

To obtain a better definition of this problem, hot breaking strength values for the warp and fill directions were compared. The warp-direction tests, instead of producing higher breaking strength values than the fill-direction tests, as should have occurred, did just the opposite and produced lower values. This suggested warp fiber damage caused by flexing during processing by the material supplier. Subsequent investigations confirmed this to be the cause of the MX-2600 silica tape breakage, and corrective action was taken. Table XLI shows warp versus fill data.

As a result of these investigations, a 250°F breaking strength test was incorporated into the material specification, and the minimum, warp-direction breaking strength at 250°F was set at 35 pounds per inch of width.

2. Adhesive Investigations

Analyses of adhesive bonding cycles involving heating revealed that complications would be encountered with adhesive bond lines as a result of differential thermal expansions between plastic and steel. The difference in the coefficients of expansion between plastic and steel is enough to cause a significant gap between components during heating cycles because of the large nozzle diameters. The gap resulting from differential expansion would prevent attainment of a good bond when using an elevated-temperature curing adhesive.

The adhesive system selected was Shell Chemical Company's Epon 913

TABLE XLI

FIBERITE MX-2600 SILICA TAPE BREAKING STRENGTHS

Test Direction	Test Temperature	Breaking Strength (lb/in. width)	Average Breaking Strength (lb/in. width)
Warp	Room temperature	48.5	60.0
		48.0	
		67.5	
		87.0	
		49.0	
	250 F	5.0	9.8
		8.0	
		14.0	
		15.0	
		7.0	
Fill	Room temperature	64.0	74.4
		59.0	
		76.0	
		91.0	
		82.3	
	250 F	21.0	28.6
		32.0	
		27.0	
		29.0	
		34.0	

NOTE: Elevated temperature tests performed by heating specimens with a heat gun and measuring temperature by thermocouple junction in contact with back side of tape surface

which can be cured at 75°F and has an eight-to-nine hour potlife. The Epon 913 is a two-part epoxy-resin-base adhesive. Its selection was based upon the following factors:

1. Ambient curing adhesive system

2. Long potlife (8 hours minimum anticipated to be required)

3. Successful use by Thiokol in previous programs

The following areas were then investigated in order to obtain data pertinent to the assembly of the 156-2C-1 nozzle.

a. Flow Test

Unbonded areas under the forward throat ablative of 65-SS nozzles indicated that the 156-2C-1 nozzle would require careful definition of bonding conditions to prevent a reoccurrence of this problem. Since the time required to apply adhesive and assemble each ablative would be much longer for the large nozzle, the flow and potlife characteristic of the adhesive were important contributors to the success of the assembly operation. Tests were initiated to determine load requirements to obtain flow of the selected epoxy adhesive system (Shell Chemical Company's Epon 913). These tests were planned to provide a basis for establishing the method and minimum loading conditions for bonding the ablative components into the steel shell and for setting restrictions on adhesive working or pot life.

To determine adhesive flow under load, two 10 x 10 inch steel surfaces were coated with the Epon 913 adhesive. The coated faces were brought into contact with each other, and a uniformly distributed compressive load was applied to the panels. Compressive loads of 3, 6, and 9 psi were studied since these loads represented the practical limits of the mechanical forces that could be applied in seating the ablative components into the steel housing. Flow characteristics were determined by measurement of panel movement during loading and by measurement of the final glue line thickness after removal of the compressive load. To further simulate production practices, various lapse times (from one to eight hours) between adhesive mixing and adhesive loading were incorporated to study the effects of adhesive flow and viscosity with time. Also, flow characteristics were substantiated visually by using a saw-tooth adhesive coating pattern applied to each of the mating surfaces. Complete obliteration of this pattern during pressurization was considered essential for proper adherend mating. A saw-tooth pattern was selected for the actual production part since a pattern of this type results in a uniform distribution of adhesive and aids in eliminating air entrapment For the flow tests, the applied adhesive thickness did not exceed one-eighth inch per facing surface. Mating saw-tooth pattern coatings were evaluated at right angles to one another with the grooves running parallel. Results of tests are tabulated in Table XLII.

Flow tests indicated a minimum seating or bonding pressure of 6 psi would be required and that component seating should commence within six hours from the time of mixing of the adhesive system.

TABLE XLII

ROOM TEMPERATURE ADHESIVE FLOW CHARACTERISTICS - EPON 913

LOAD PRESSURE	3 psi			6 psi				9 psi		
LAPSE TIME***	1	4	8	1	4	6	8	1	4	8
Time under compressive load, minutes	15	14	2.1*	15	15	15	15	15	15	15
Glueline thickness after unloading, inches	0.092	0.100	0.102	0.087	0.097	0.105	0.106	0.079	0.096	0.092
% Void-free bondline area**	90	90	50	100	100	100	50	100	100	50

*   No further movement under load.

**   As determined from residual adhesive saw-tooth pattern visual after separating mating faces.

*** Time between adhesive mixing and application of load (hrs).

b. Application Pattern

In order to determine the optimum adhesive pattern and the applicator con-
figuration necessary to achieve that pattern, an investigation was conducted
to determine the following:

1. The advantages and/or disadvantages of cross-
pattern application (adhesive applied on the
ablatives at 90° to that applied on the steel shell)
versus a parallel-pattern application (adhesive
applied in the same direction as the ablatives
and steel shell).

2. The advantages of a wide saw-tooth adhesive
pattern versus a close saw tooth pattern.

3. The amount of compensation required on the
applicator tooth shape for surface tension of the
adhesive.

The tests consisted of applying selected adhesive patterns to 1/4-inch x 10-
inch x 10-inch panels of acrylic Plexiglass. In all cases, Epon 913 adhesive
was used as the adhesive. The panels were pressed together with a prede-
termined load to determine the glue line thickness, percentage of coverage,
and flow characteristics for each pattern and applicator used. The trans-
parent acrylic panels were visually examined and the best condition selected.

Figure 32 shows a typical cross-pattern panel which was found to create
excessive air entrapment, which in turn prevented a complete bond. Note
the air had forced the adhesive aside as it collected in the large void area.
Figure 33 shows two (2) typical parallel-patterns which were applied with
applicators which each had a different tooth spacing. The parallel-pattern
application was selected as the approach to be used on the first nozzle. The
configuration of the applicator tooth required to give a specific size of ad-
hesive head was determined by applying adhesive to an aluminum panel with
varying sizes of applicator teeth and allowing the adhesive to cure in an oven.
The patterns were then measured on an optical comparator and the measure-
ments were used to calculate the volume of adhesives applied and the amount
of decrease in bead that occurred because of surface tension between the
applicator and adhesive. Results of these tests are shown in Figure 34. The
depth of the applicator tooth was selected to provide an adhesive bead high
enough to contact the surface of the mating part under the maximum anticipa-
ted gap condition. The pitch or spacing of the teeth was selected to give the
desired volume of adhesive.

The desired volume of adhesive was derived from the gap existing between the
ablative and the steel shell at the time of the dry fit. Different applicators
were chosen for the different conical sections based on the average gap exist-
ing in the section. The applicators were designed to minimize the distortion
of the adhesive bead when the applicators were pressed against the curved
surfaces of the steel and ablatives.

The test resulted in the selection of a parallel pattern for adhesive application
with an adhesive bead height equal to the maximum gap allowable between the
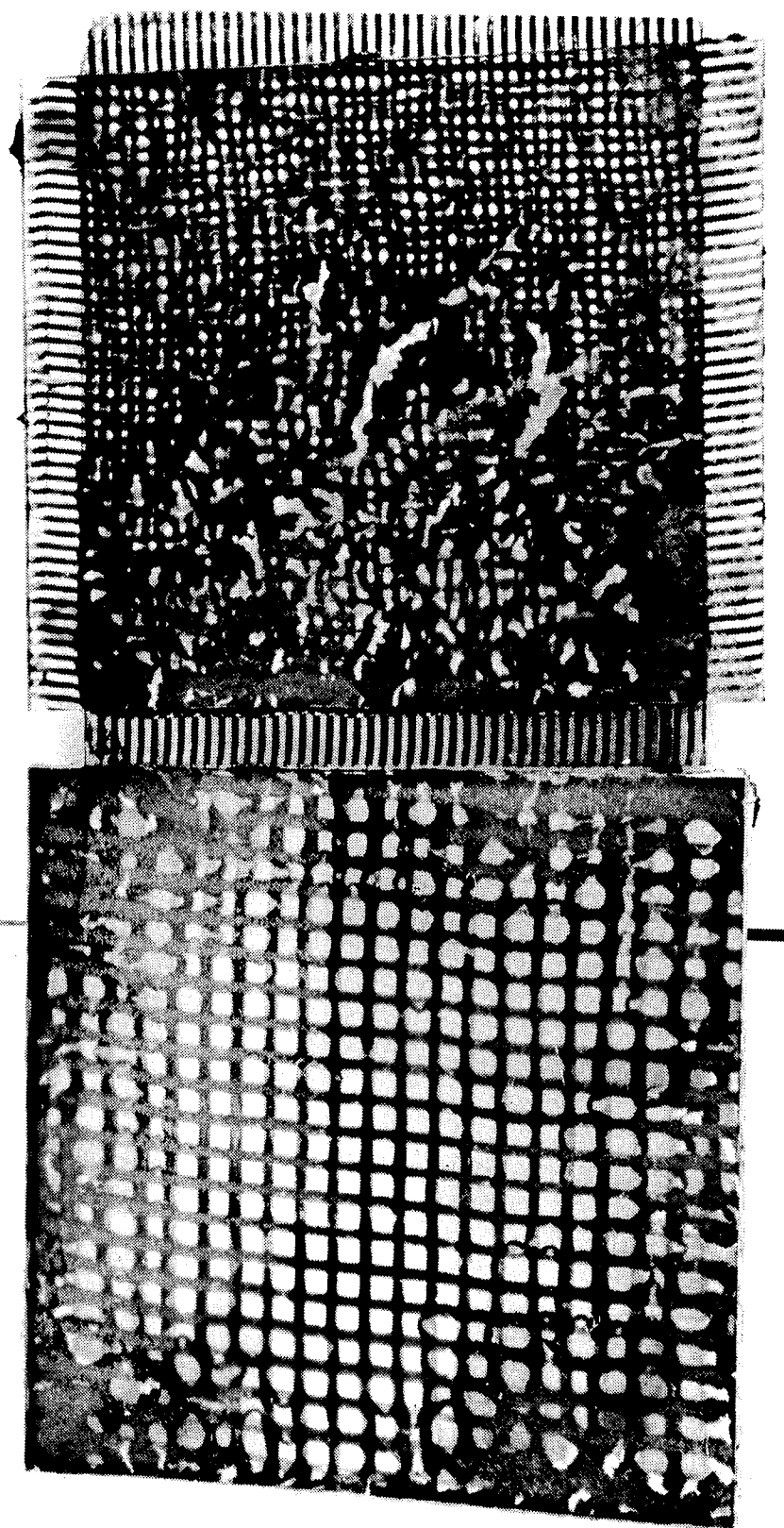
Figure 32 - Photo Cross Adhesive Pattern

Figure 33 - Photo Parallel Adhesive Pattern
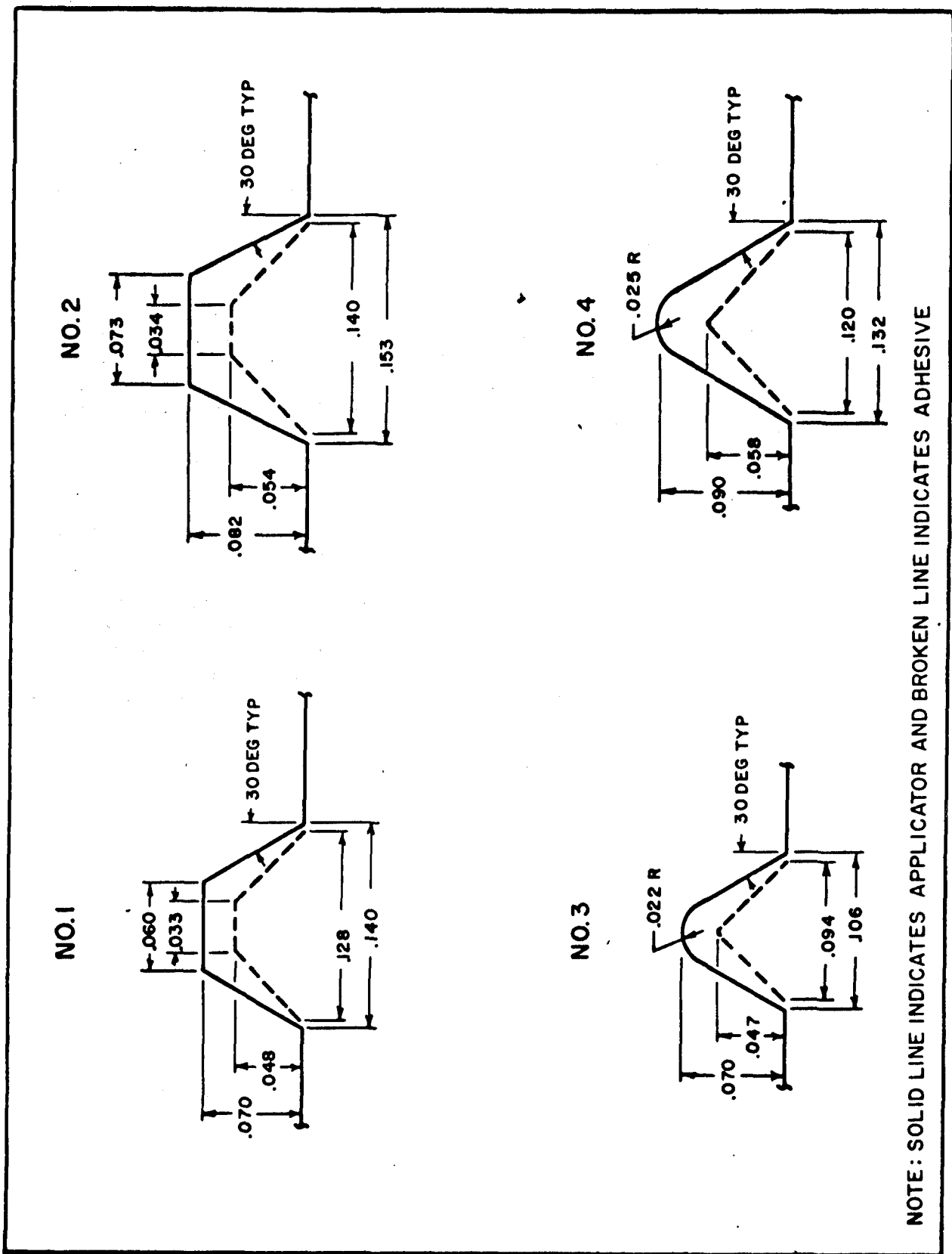
Figure 34 - Adhesive Applicator Teeth

NOTE: SOLID LINE INDICATES APPLICATOR AND BROKEN LINE INDICATES ADHESIVE

ablative and the steel shell. The number of adhesive beads per inch of sur-
face was varied to give a sufficient volume of adhesive to fill gaps of 0.030,
0.040, and 0.050 inch. The proper applicator was chosen according to the
volume required for any given cone.

Additional adhesive application tests were conducted to determine speed and
actual method of applying the adhesive. It was found necessary to trowel the
adhesive on the surface in a thin, even coat with a smooth surface trowel, and
then the adhesive was re-trowelled with a sawtooth blade to form the adhesive
beads.

c. Thickness Versus Strength

The investigation of the problems associated with a one step assembly bonding
operation pointed out that control of bond line thickness would be one of the
major difficulties. Studies were conducted to determine the effect of thick-
ness on tensile·shear strength and flatwise tensile properties. Glue line
thickness studies were performed by bonding two 1-1/2-inch diameter stain-
less steel facing blocks with the Epon 913 adhesive. The steel blocks were
sandblasted and wiped prior to adhesive application. Bond line thickness of
0.031 to 0.375 inch was attained through the use of small spacer blocks. An
excessive amount of adhesive was applied to each face block and the blocks
allowed to settle together, forcing the excess resin out until contact with the
spacers was made. The specimens were then cured 72 hours at room tem-
perature before flatwise tensile testing. Results of this study are listed in
Table XLIII. The face tension results indicated an approximately 50-percent
loss of flatwise tensile strength increasing from a bond line thickness of 0.031
up to 0.375 inch. A minimum average strength of 1072 psi was obtained at a
bond line thickness of 0.125 inch. Earlier tests on thinner bonds have yielded
pure tensile strength capabilities in excess of 4000 psi for this material.

In addition to the flatwise tensile strength tests, a similar study was com-
pleted to determine the effect of thickness on tensile shear strength proper-
ties. Double-lap, shear-type specimens were used to eliminate bending
stresses that would have been encountered had the standard overlap shear
specimens been used with these heavy glue line thicknesses. Cured glue line
thicknesses of 1/32, 1/16, 1/8, 1/4, and 3/8 inch were examined.

Stainless steel adherends, 0.250 x 1 x 4 inches, were prepared for bonding by
light sandblasting with a number 36 garnet abrasive grit and wiped just prior
to coating with the Epon 913 paste. A small jig was employed for shimming
of the adherends to maintain the desired bond line thickness during curing.
A one-inch overlap was used. Enough adhesive was applied to result in ex-
cess flow during mating of the adherends, eliminating possible entrapment
of air. The specimens were cured for 72 hours at ambient temperature, under
contact pressure, before removal from the holding fixture for testing. Three
specimens for each bond line thickness were prepared.

The data from the tensile shear tests were statistically analyzed. Tensile
shear strength was found to be related to bond line thickness by a log-log
function. Regression analysis of the fifteen data points yielded the prediction
equation

$$\log y = 3.5784 - 2.854 \log (100x)$$

TABLE XLIII

ADHESIVE BOND LINE THICKNESS VS
FLATWISE TENSILE STRENGTH

Bond Line Thickness (in.)	Flatwise Tensile Strength (psi)	Average Flatwise Tensile Strength (psi)	% Cohesive Failure
0.031	2497	2545	90
	2593		80
0.063	1778	1940	80
	1744		70
	2299		95
0.125	1314	1072	70
	1149		70
	753		50
0.250	1087	1253	80
	1631		90
	1042		60
0.375	1418	1320	80
	1772		80
	770		60

NOTE: Epon 913 was cured 72 hours at room temperature under contact pressure.

where

y = tensile shear strength (psi)

x = bond line thickness, (in.)

The standard error estimate was 0.0717, from which a 90 percent confidence lower boundary was calculated. Figure 35 shows the regression line and confidence limit. Various thicknesses of the adhesive and the corresponding expected minimum strengths at the 90 percent confidence level are tabulated as follows:

Bond Line Thickness (in.)	90% Confidence Minimum Tensile Shear Strength (psi)
0.03	2493
0.04	2332
0.05	2210
0.06	2114
0.07	1978
0.08	1966
0.09	1905
0.10	1852

The above data may be used to estimate the minimum strength of the bond, when the thickness of the Epon 913 is known.

3. Tie Laminate Material Selection

Bi-directional glass fabric was selected as the reinforcement for the tie laminate. Since a 300°F oven large enough to enclose the entire nozzle assembly would be required if phenolic resin were used and because of problems of different coefficient of thermal expansion for the steel and ablative, it was not feasible to use a temperature cured resin system. Investigations were conducted to select a structural resin capable of curing at ambient temperature.

Three resins that might satisfy the requirements for an ambient curing system were investigated. These resins were:

1. Selectron 5003 polyester resin marketed by Pittsburg Plate Company

2. ERL-2772 epoxy resin marketed by the Bakelite Corporation

3. E-782 epoxy resin marketed by U. S. Polymeric Corporation

The first two resins were suitable for wet-dip impregnation of glass fabric whereas the third resin could be pre-impregnated on the fabric and stored under refrigeration until use. Potlife of all systems was six hours or more, but the Selectron 5003 resin was considered superior because ultraviolet light

EQUATION OF LINE = LOG y = 3.5784 - 0.2854 LOG (100 X)

STANDARD ERROR = 0.0717
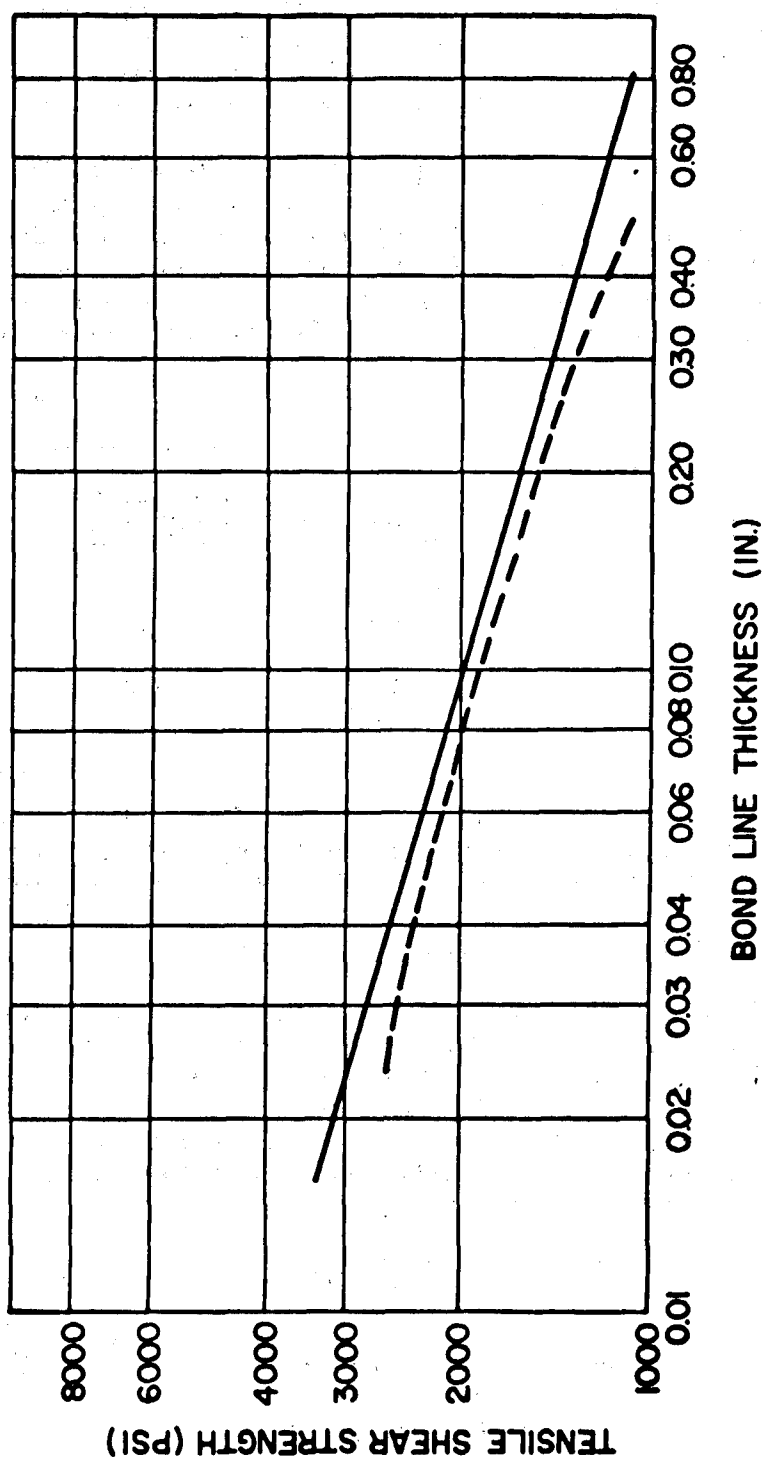
Figure 35 - Regression Line and Lower 90-Percent Confidence Boundary
for Tensile Shear Strength versus Bond Line Thickness

was required to trigger the cure cycle. Resin gellation occurred within four hours when the Selectron 5003 resin was exposed to ultraviolet light.

A series of laboratory tests were performed to determine physical properties attainable with each resin when impregnated on bidirectional glass fabric. The averages of the values obtained are presented in Table XLIV and may be compared with design values which would be used if a phenolic resin were used.

The Selectron system required use of Selectron 5236 polyester primer for satisfactory adhesion to steel or reinforced plastic laminates. Tests of adhesion (tensile shear strength) to steel and phenolic laminates were conducted for the Selectron and the other two systems. Selectron 5003 exhibited adequate adhesive shear strength to both steel and phenolic laminate materials but less than epoxy systems. The results are as follows:

		Adhesion (psi)		
Material	Cure Conditions	Selectron 5003/5236	Bakelite ERL-2772	U. S. Polymeric E-782
Steel	Ambient	723	3,228	3,089
	120 F	1,978	3,752	3,245
Phenolic laminate	Ambient	1,646	2,365	1,404
	120 F	2,030	2,510	2,495

The combination of mechanical and physical properties, potlife, and curing characteristics of the Selectron 5003 polyester resin system was the most desirable. Further verification testing of this system involved a mock wet lay-up on a small mandrel surface. Tack and drape were good in the critical throat area. No difficulties were encountered.

Because radiant heating from the plume at an unknown heat flux level was anticipated, flammability tests of cured laminate panels were conducted. Kindling temperature or scorch tests were performed on Selectron 5003/181 glass fabric laminates in accordance with ASTM specification D 635-56T. Specimens, 0.125 inch by 0.5 inch, were ignited as specified. All three specimens burned out within the self-extinguishing range. The results of these tests are as follows:

Flammability Property	Specimen		
	1	2	3
Burning time, in/sec	120	135	130
Extent of burning, in	4	3.75	2.75
Burning rate, in/min	0.5	0.44	0.46

Because physical strength of the laminate degraded rapidly with elevated temperature exposure, it was concluded that a thermal protective coating would be needed even though the laminate was classed as self-extinguishing.

TABLE XLIV

EVALUATION OF CANDIDATE MATERIAL PROPERTIES FOR NOZZLE TIE LAMINATES

Properties	Design Value (Phenolic Laminate)	Materials*		
		5003 Selectron	ERL-2772	E-782
Tensile Strength (psi)	40,000	53,000	52,000	43,200
Tensile Modulus (psi)	3.4×10^6	3.3×10^6	3.1×10^6	2.9×10^6
Tensile Strength after 500 F Air Blast for 2 min. (psi)	34,000	35,700	16,800	16,900
Interlaminar Shear (psi)	1,800	2,740	3,640	1,700
Shear to Steel (psi)	1,450	1,980	3,750	3,250
Shear to Phenolic (psi)	1,600	2,030	2,510	2,500
Flexure Strength (psi)	80,000	76,500	79,800	60,800
Flexure Modulus (psi)	4.0×10^6	3.9×10^6	3.5×10^6	3.5×10^6

* Bidirectional (181) Glass Fabric Reinforcement

Section IV of this report details the thermal protection of the tie laminates.

Tests were also conducted on the bidirectional glass cloth - Selectron 5003 resin system to determine the point in processing after which it would be safe to move the nozzle assembly without damage; tests were conducted to obtain shear strength versus cure time characteristics of the polyester resin in the tie laminate (i.e., the laminate which locks the nozzle exit cone ablative into the steel shell). The criteria established was that 80-percent of ultimate cure strength would be developed prior to moving the nozzle.

Lap shear specimens were made by coating cured MX-4600 glass-phenolic laminates with Selectron 5236 primer and applying a set layup of 181 glass cloth and Selectron 5003 polyester resin. Control lap shear specimens were also made, using a grit-blasted 301 stainless steel panel instead of the MX-4600 laminate. The samples were cured for two hours by heat lamps followed by exposure to room temperature.

Results of testing are shown in Table XLV. After being cured for 24 hours, 80-percent of ultimate strength was developed. This was, therefore, the minimum cure time allowed before further processing involving handling was permitted.

4. Glass Laminate Processing

The bi-directional-phenolic impregnated glass laminates were designed to serve the dual function of providing strength to the ablative components during handling and to seal circumferential delaminations against possible gas leaks. In order to provide maximum strength, the cure for these laminates was planned to be a hydroclave cure at 1000 psi. As tooling designs and fabrication planning advanced, it became apparent that loads imposed during handling would be significantly lower than originally anticipated. Accordingly, it was concluded that a reduced structural capability, such as that attained by an autoclave or vacuum-bag-curing technique would be satisfactory. Experimental results from 200 psi autoclaved components indicate a problem with wrinkling unless intermediate debulks were used. Since vacuum-bag curing would not require intermediate debulking operations and since it was less costly than autoclave curing, an investigation of this approach was performed. Test panels of MX-4600 were laid-up in the laboratory, vacuum-bag cured, and tested for mechanical properties. With the exception of tensile modulus, results compared favorably with data from the supplier. Table XLVI contains the tabulated results from these tests. For comparison the mean flexural strength obtained during in-process testing on the 156-2C-1 nozzle was 58,100 psi.

B. ABLATIVE TAPE WRAPPING

The tape wrapping heads designed for the 156- and 260-inch bias tape components were not adequate to provide the required guidance of bias tape.

TABLE XLV

SHEAR STRENGTH VERSUS CURE TIME OF
SELECTRON 5003 RESIN AND 5236 PRIMER

Time (hr)	Shear Strength (psi)	
	MX-4600 Laminate	301 Steel
8	398	738
16	503	955
24	515	970
36	530	992
48	540	1011
Full Cure	646	1182

NOTE: All specimens were 100-percent adhesive failures.

TABLE XLVI

MECHANICAL PROPERTIES OF VACUUM CURED MX-4600 GLASS LAMINATES

Cure	Tensile Strength (psi)	Tensile Modulus X 10^6(psi)	Flexural Strength (psi)	Flexural Modulus X 10^6(psi)	Density (g/cc)
1000 psi, minimum values[1]	60,000	4.5	90,000	3.5	2.03
Vacuum pressure, typical[1]	50,000	4.0	60,000	3.0	1.67
Laboratory, vacuum pressure	48,800	3.1	63,300	3.6	1.73
	50,200	3.1	62,700	3.4	1.72
	48,200	3.1	61,900	3.4	1.74
	48,000	3.1	62,900	3.3	1.73
	48,000	3.3	61,400	3.4	--

[1]Fiberite data sheet

Several different types of guide rollers, trough-type guides, edge guide de-
vices, and edge trimming devices were tried without any appreciable amount
of success. The location of the quartz lamps on these wrapping heads was
such that the heat was not applied to the tape at the correct point in the wrap-
ping process. The heat was positioned such that the tape was heated prior to
the forming rolls. While some heat was required for forming, if enough heat
were applied to make the tape tack, the resin would soften to the point where
the forming rolls would become coated and stop functioning. To solve these
problems, numerous modifications were made to the wrapping heads. The
following is a summation of the changes and results:

1. The bias tape forming rolls were moved back
   about 8 to 12 inches from the compression
   roller and down to a point closer to the sur-
   face of the tape which had already been applied
   to the mandrel. This permitted manual lineup
   of the edge of the tape as it crossed the last
   forming and adjustment of its location by hand
   to make it feed inside of the inner edge of the
   compression roll.

2. With this overhang of tape on the inner edge of
   the roller, excess tape was manually knife
   trimmed as it passed beneath the compression
   roller. Manual trimming replaced the desired
   guidance of the inner-most edge of the tape.

3. The quartz lamps used for heating of tape were
   moved to the area provided when the form rol-
   lers were moved back. Tack temperature was
   thereby applied to the tape just before it passed
   under the compression roll and after passing
   through the form rolls. A small amount of heat
   was applied to the outer edge of the tape ahead
   of the form rolls to allow it to form readily.

To provide assurance that the inside surface of the component was free of
voids or pockets caused by improper tracking or trimming of the tape edge
against the mandrel surface, the throat area mandrels were re-machined so
that the throats would not be wrapped to net ID. The throat ablatives were
machined to obtain the net dimension.

While the modification to the bias tape wrapping heads was still in process,
the test wrapping development program was started on the aft throat mandrel.
The aft throat trials consisted of wrapping two quarter-inch-thick rings fol-
lowed by one-inch-thick ring to be hydroclave cured. The quarter-inch rings
were wrapped at tape speeds of five and ten feet per minute. Acceptance of
wrapping parameters was based on measured as-wrapped ply thickness and
as-wrapped laminate specific gravity tests. After approval of the five feet
per minute trial, a one-inch-thick hydroclave test ring was wrapped by the
same procedure. Parameters used in fabricating these three wraps are tab-
ulated in Table XLVII. As-wrapped percent of theoretical density and specific

TABLE XLVII

DATA FROM TRIAL WRAPPING OF GRAPHITE BIAS TAPE TO FORM AFT THROAT TEST RINGS

No. of Plies	As-Received Tape Thickness (in.)	Wrapped Laminate Thickness (in.)	Average Ply Thickness (in.)	Wrapped Tape Width (in.)	Tape Angle (deg)	Tape Temp 4-In. before Roll (F)	Laminate Temp after Roll (F)	Pressure Roll Temp (F)	Mandrel Temp (F)	Air Temp (F)
Trial 1: Wrapping Speed of 5 ft/min onto One-Quarter-Inch Ring										
4	0.024	0.085	0.021	4.75	60	215	90	100	--	--
8	--	0.160	0.020	4.6	60	210	95	110	--	--
12	--	0.210	0.018	5.1	60	200	100	105	--	--
14	0.024	0.240	0.017	4.6	60	200	95	105	--	--
Trial 2: Wrapping Speed of 10 ft/min onto One-Quarter-Inch Ring										
4	0.023	--	--	5.4	60	180	--	100	--	--
8	--	--	--	5.2	60	160	--	105	--	--
12	--	--	--	6.0	60	175	--	115	--	--
14	0.023	--	0.0184	4.9	60	175	--	120	--	62
Trial 3: Wrapping Speed of 5 ft/min onto One-Inch Ring										
5	0.021	0.095	0.0190	4.7	60	210	90	105	55	63
10	--	0.175	0.0175	4.5	60	200	90	115	65	64
13	--	0.235	0.0180	4.9	60.5	190	90	115	62	64
20	--	0.350	0.0175	5.0	60.5	205	95	110	65	65
25	0.021	0.415	0.0166	4.4	60.5	200	90	110	55	66
30	--	0.540	0.0180	4.5	60.5	185	90	105	60	68
35	--	0.630	0.0180	4.5	60.5	190	105	120	65	68
40	0.025	0.730	0.0183	4.5	60.5	200	105	115	65	70
45	--	0.820	0.0182	4.6	60.5	195	100	105	70	68
50	--	0.950	0.0190	4.6	60.5	200	105	115	70	68
53	0.025	1.020	0.0192	4.6	60.5	210	105	115	70	68

NOTES:
1. U. S. Polymeric 6.8-inch FM 5064 tape was used; Betts mill
2. Roll pressure was 681 pounds for each wrapping
3. Resin build-up was removed from Teflon forming rolls after 13th wrap

gravity are shown in Table XLVIII. The one-inch-thick, trial 3, aft throat
test ring was cured in the hydroclave with standard heat-up and cool-down
rates but was held at 350°F for two hours (instead of the usual four) to expe-
dite scheduling. The test ring cured wrinkle-free, and final specific gravities
were satisfactory. Ply thickness, density, and acetone extraction data on the
cured ring are presented in Table XLIX. With the experience gained in this
trial wrap and with improved guidance techniques, bias wrapping of the for-
ward and mid-throat test rings was accomplished at a tape wrapping speed of
ten feet per minute. The entrance cone trial wraps were made with speeds of
6 and 13 feet per minute. Parameters from these trial wraps are shown in
Table L. Results of the trial wraps for the carbon and silica warp tape are
shown in Table LI. As-wrapped densities for each of the entrance cone, for-
ward throat, mid throat and exit cone trial wraps are shown in Table LII.
Establishment of warp tape or parallel-to-centerline wrapping parameters
was complicated by heat flux problems with the two different tapes caused by
positioning of heater and color of tape. Uneven, and incorrect amounts of
heat caused excessive resin pickup on the pressure rolls, and poor tacking of
the tapes. Tape speeds and heater location were adjusted until a workable
combination was found which would give a satisfactory degree of debulk.

A wrapping speed of 20 feet per minute was established and approved for car-
bon tape. The higher reflectivity and bulk of silica tape shifted emphasis to
tape heating mechanisms in an attempt to heat the tape to wrapping tempera-
tures without an extreme temperature drop through the tape thickness. This
consideration, along with splice failures, limited the maximum wrapping
speed of silica tape to 13 feet per minute.

A two-inch-thick composite (carbon/silica) test ring was wrapped as a final
demonstration of laminate integrity by vertically tracking tape down the coni-
cally-shaped mandrel. The wrapping consisted of 66 plies of MX 4926 8.5-
inch-wide carbon tape under 36 plies of MX 2600 7.3-inch-wide silica tape.
Wrapping data are shown in Table LIII and the resulting as-wrapped density
is shown in Table LIV. The results obtained on this program were used to
establish controls for fabrication of the 156-2C-1 and 260-SL-1 ablatives.

C. HYDROCLAVE BAG DEVELOPMENT

An investigation of rubber materials was conducted to select one suitable for
use in hydroclave bags. A critical phase in processing ablative materials is
the hydroclave operation because high temperatures, high pressures, and
movement of the ablative as it debulks cause degradation of the hydroclave
bag material and introduce stresses into the bag. If water reaches uncured
ablative material through ruptures in the bag prior to resin cure large quan-
tities of the expensive hygroscopic material may be contaminated.

Four candidate materials were selected and evaluated:

Material	Type
Stoner SMR-14	Buna-N
Stoner SMR81-6	Butyl
Kirkhill 265B612E	Neoprene
Kirkhill 665C1187A	Butyl

TABLE XLVIII

AS-WRAPPED DENSITY OF GRAPHITE BIAS TAPE
FORMING AFT THROAT TEST RINGS

Trial	Quadrant	Specimen Location	Specific Gravity	As-Wrapped Density (% of Theoretical)[1]
1	1	OD	1.270	87.6
			1.265	87.2
		ID	1.190	82.0
			1.195	82.4
	2	OD	1.223	84.3
			1.211	83.5
		ID	1.225	84.5
	3	OD	1.205	83.1
		ID	1.208	83.3
			1.209	83.4
	4	OD	1.287	88.8
			1.279	88.2
		ID	1.200	82.8
			1.210	83.4
2	1	OD	1.235	85.2
			1.237	85.3
	2	OD	1.212	83.6
			1.215	83.8
		ID	1.185	81.7
			1.205	83.1
	3	OD	1.219	84.1
		ID	1.185	81.7
	4	OD	1.215	83.8
			1.200	82.8
		ID	1.185	81.7
			1.225	84.5
3	--	ID	1.405	96.9
		OD	1.308	90.2

NOTE: 1. Percentage based on a cured specific gravity
of 1.45 (FM 5064 graphite)

TABLE XLIX

DATA FROM CURED GRAPHITE-TAPE-WRAPPED ONE-INCH-THICK AFT THROAT TEST RING

Ring Quadrant	Specimen Location	Specific Gravity	Ply Thickness (in.)[1]	Extractable Acetone (%)[2]
1	ID	1.459	0.0160	4.21
	Center		0.0163	4.12
	OD	1.462	0.0167	2.75
2	ID	1.460	0.0159	4.25
	Center		0.0162	3.88
	OD	1.450	0.0163	4.88
3	ID	1.462	0.0175	3.02
	Center		0.0180	4.59
	OD	1.460	0.0183	3.45
4	ID	1.458	0.0176	3.34
	Center		0.0179	4.74
	OD	1.455	0.0182	1.57

NOTES: 1. Based on a reported 53-ply wrap

2. Average of two tests

TABLE L

TRIAL WRAPPING OF BIAS TAPE TEST RINGS

Test Ring & Material	No. of Plies	As-Received Tape Thickness (in.)	Wrapped Laminate Thickness (in.)	Avg Ply Thickness (in.)	As-Wrapped Tape Width (in.)	Tape Temp 4-In. before Roll (FP)	Laminate Temp 180-Deg from Roll (F)	Pressure Roll Temp (F)	Roll Pressure (lb/in. width)	Tape Speed (ft/min)
Mid Throat Graphite Tape FM-5064 9.2" wide	14	0.0215	0.240	0.0172	6.3/6.5	170/220	80	105	210	10
Fwd Throat Graphite Tape FM-5064 10.2" wide	22	0.025/0.027	0.420	0.0191	7.2/8.0	200/250	90/95	90/120	300	10
Entr Cone Carbon Tape FM-5063 13.5" wide First Trial	15	0.024	0.280	0.019	8.9/9.3	210/235	---	85/90	150/175	6
Entr Cone Carbon Tape FM-5063 13.5" wide Second Trial	11	0.0245	0.215	0.0195	8.8/10.5	200/260	---	75/90	150	12/19

128

TABLE LI

DATA FROM TRIAL WRAPPING OF WARP TAPE TO FORM EXIT CONE TEST RING

Test Ring and Material	No. of Plies	As-Received Tape Thickness (in.)	Wrapped Laminate Thickness (in.)	Avg Ply Thickness (in.)	Tape Temp 3-in before Roll (F)	Laminate Temp 3-In. before Roll (F)	Pressure Roll Temp (F)	Laminate Temp before Heater (F)	Total Tape Tension (lb)	Roll Pressure (lb/in. width)	Tape Speed (ft/min)
First Trial Wrap Carbon Tape MX-4926	16	0.0237 to .0255	0.275	0.0172	255/270	160/230	150/180	90	30/60	160	13
Second Trial Wrap Carbon Tape MX-4926	12	0.0244 to .0255	0.1875	0.0156	295/325	175/195	105/160	90	60	300	5
Third Trial Wrap Carbon Tape MX-4926	17	0.0244 to .0250	0.272	0.0160	300/310	220/290	175/185	100	60	300	13
Fourth Trial Wrap Carbon Tape MX-4926	18	0.0245 to .0250	0.276	0.0153	260/300	240/280	120/150	90/100	60	300	20
Fifth Trial Wrap Carbon Tape MX-4926	15	0.0247 to .0255	0.2165	0.0145	290/300	110	90/115	90	80	240	20
First Silica MX-2600	10	0.0350 to .0365	.261	0.0261	285/295	140/170	90/100	90	100	300	5
Second Silica MX-2600	10	.0355 to .0360	.269	0.0269	280/290	145/150	100	90	55	300	13

NOTES: 1. Carbon Material 8.5-inch wide MX-4926

2. Silica Material 7.3-inch wide MX-2600

TABLE LII

AS-WRAPPED DENSITY TESTS

Component	Trial	Material	Density g/cc		As-Wrapped Density % Theoretical	
			Range	Average	Range	Average
Entrance Cone	1	Carbon FM-5063	1.181 - 1.307	1.262	84.4 - 93.3	90.1
	2		1.230 - 1.338	1.284	87.9 - 95.6	91.7
Forward Throat	1	Graphite FM 5064	1.250 - 1.395	1.327	86.2 - 96.2	91.6
Mid-Throat	1	Graphite FM 5064	1.210 - 1.380	1.300	83.4 - 95.2	89.7
Exit Cone	1 Note 3	Carbon MX-4926	1.189 - 1.228	1.208	85.7 - 87.7	86.3
	2 Note 4		1.200 - 1.288	1.251	85.7 - 91.8	89.4
	3 Note 4		1.220 - 1.275	1.246	87.2 - 91.1	89.0
	4 Note 4		1.215 - 1.255	1.230	86.8 - 89.6	87.8
	5 Note 4		1.309 - 1.347	1.326	93.5 - 96.2	94.7
	1 Note 4	High-Silica MX-2600	1.600 - 1.625	1.615	92.0 - 93.4	92.8
	2 Note 4		1.560 - 1.600	1.578	89.7 - 92.0	90.8

Note 1: Percentage based on a cured density of:
    a. 1.45 for forward and mid-throat graphite
    b. 1.40 for exit and entrance cone carbon
    c. 1.74 for exit cone high-silica

Note 2: Averages shown here are on eight (8) reported values.

Note 3: Specimens were taken at mid-point and lower edge of as-wrapped laminate.

Note 4: Specimens were taken at upper and lower edges of as-wrapped laminate.

TABLE LIII

DATA FROM TRIAL WRAPPING OF CARBON AND SILICA WARP TAPES TO FORM TWO-INCH-THICK COMPOSITE TEST RING

No. of Plies	Wrapped Laminate Thickness (in.)	Avg Ply Thickness (in.)	Tape Temp 3-In. before Roll (F)	Laminate Temp 3-In. before Roll (F)	Pressure Roll Temp	Laminate Temp before Heater (F)	Total Tape Tension (lb)	Roll Pressure (lb/in. width)	Tape Speed (ft/min)
Carbon Tape									
3	--	--	290	105	95	100	80	260	20
14	--	--	250	115	90	120	80	260	20
21	--	--	250	120	90	95	80	260	20
30	--	--	280	120	90	120	80	260	20
33	--	--	260	115	90	115	80	260	20
45	--	--	280	140	90	100	80	260	20
50	--	--	260	--	--	--	80	260	20
54	--	--	250	140	90	100	80	260	20
60	--	--	240	--	--	--		260	20
65.5	0.983	0.0150	--	--	--	--			
Silica Tape									
3	--	--	280	145	90	100	100	300	13
10	--	--	300	170	100	--	100	300	13
21	--	--	300	155	90	--	100	300	13
30	--	--	300	170	95	--	100	300	13
36	0.940	0.0261	--	--	--	--	100	300	13

NOTES: 8.5-In. MX 4926 Carbon Warp Tape

1. All dimpled splices failed. Several splices failed before reaching heat lamp area.
2. Good tack; good compaction

7.3-In. MX 2600 Silica Warp Tape

1. All dimpled splices failed
2. Good tack; good compaction obtained
3. Temperature drop of 15 to 20 F through tape thickness three inches before pressure roll

TABLE LIV

AS-WRAPPED DENSITY OF CARBON AND SILICA WARP TAPES
FORMING TWO-INCH-THICK COMPOSITE TEST RING

Laminate	Quadrant	Specimen Location[1]	Specific Gravity	As-Wrapped Density (% of Theoretical)[2]
Carbon	1	Top	1.269	90.6
		Bottom	1.270	90.7
	2	Top	1.223	87.4
		Bottom	1.274	91.0
	3	Top	1.302	93.0
		Bottom	1.304	93.1
	4	Top	1.301	92.9
		Bottom	1.288	92.0
Silica	1	Top	1.636	94.0
		Bottom	1.692	97.2
	2	Top	1.669	95.9
		Bottom	1.670	96.0
	3.	Top	1.667	95.8
		Bottom	1.664	95.6
	4.	Top	1.677	96.4
		Bottom	1.654	95.1

NOTES: 1. Specimens were taken at top and bottom portions
of as-wrapped laminate

2. Percentage based on a cured specific gravity of
1.40, MX 4926 carbon, and 1.74, MX 2600 silica

All test samples of these materials were cured at a pressure of 200 psi and at temperatures of 310° to 315°F. Candidates were compared for strength retention at 300°F, retention of elongation capability at 300°F, and resistance to deterioration when folded over or wrinkled and subjected to a high temperature and pressure environment.

Criteria for selection of a material included retention of a minimum tensile strength of 1,000 psi after exposure for 60 hours to temperatures of 300° to 350°F. The period selected corresponded to projected requirements for hydroclave bag usage. Figure 36 shows the relationship of tensile strength and period of exposure to a 325°F silicone oil bath for each of the candidate materials. As shown by this figure, Kirkhill 665C1187A butyl was the only material satisfying the requirement for tensile strength retention. Also shown on this figure is the relationship of tensile strength and exposure time for the selected material when exposed to the hydroclave conditions.

It was found that samples of the selected butyl material, when exposed to hydroclave conditions for more than 60 hours, began to deteriorate. Tensile strength went below 1,000 psi, elongation went below 300 percent, and surface degradation occurred which resulted in crazing and cracking of about 50 percent of the membrane thickness. By limiting the use period to 60 hours or less, none of the ablative components for the 156-2C-1 or 260-SL-1 were subjected to water contamination because of hydroclave bag rupture.

D. NONDESTRUCTIVE TESTING

1. Ablative NDT

Nondestructive testing of ablative components for the large nozzles was limited to radiographic inspection of the cured ablative components and ultrasonic inspection of all secondary bond lines between ablatives and the reinforcement glass laminates. All ablative components were radiographed radially parallel to the ply orientation. Thickness of the ablatives along plies varied from approximately two inches to as much as 11 to 12 inches. The ablative assemblies were generally radiographed after the glass reinforcement laminate had been applied. Radiographic techniques used on the ablatives produced a 2 percent sensitivity level. The radiographic film of the silica materials in the exit cone clearly shows the orientation of each ply as well as any deviations. The carbon and graphite materials do not give the same sharpness on the film; however, the sensitivity and contrast of the film for these materials were such that defects were readily detectable. The wrinkle conditions in the glass reinforcement laminate were visible on the radiographic film. The ablative components used on the 156-2C-1 motor were subjected to a 100 percent radiographic inspection.

The ablative components for the forward, mid and aft throats of Unit #2 nozzle were 100 percent radiographically inspected, but the entrance cone and exit cone ablative for this nozzle were radiographed on a sampling plan which covered approximately 45 percent of the entrance cone and 25 percent of the exit cone. The glass-to-ablative bond lines on these ablative components were 100 percent ultrasonically inspected.

The tangential radiographic technique which was used on the bond lines of the
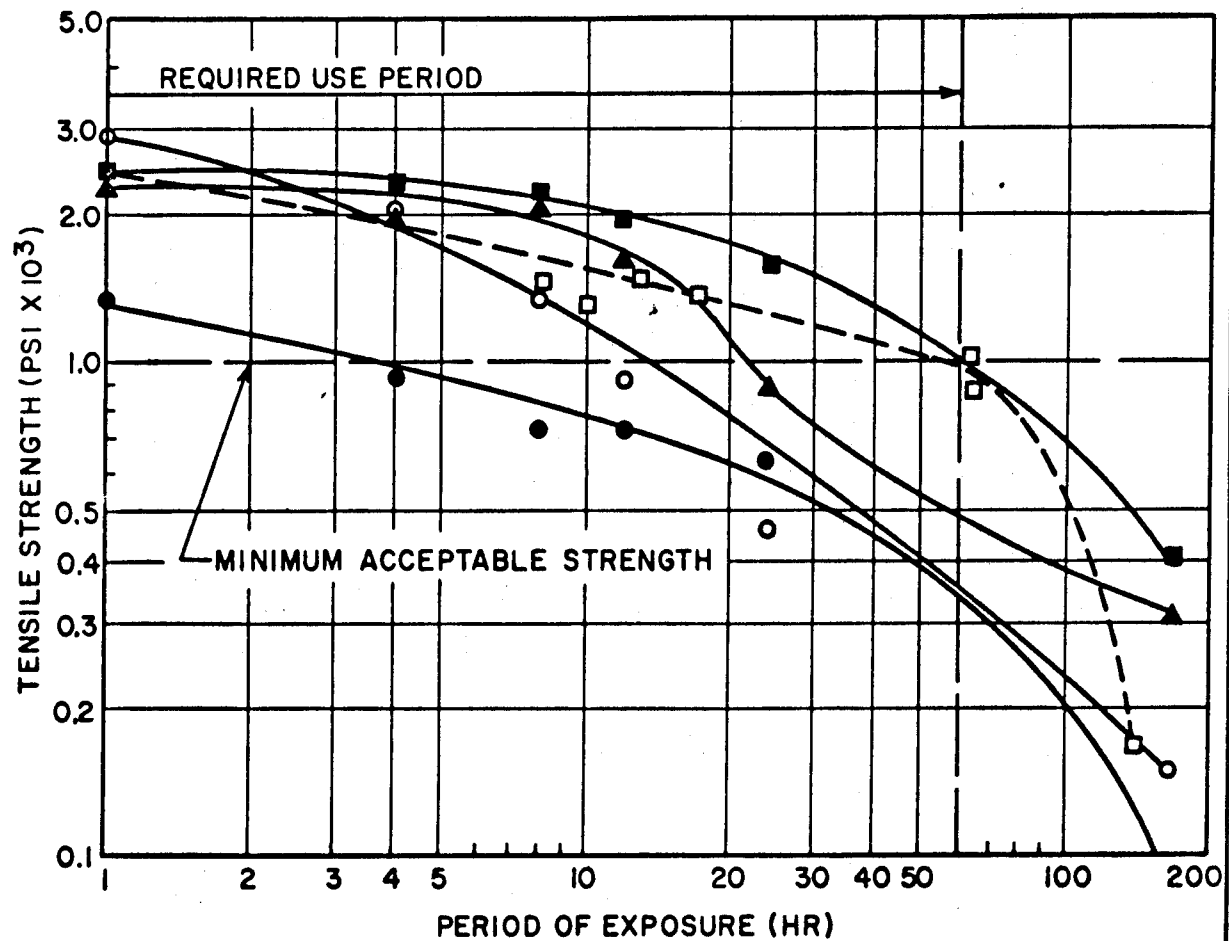
Figure 36 - Period of Hydroclave Exposure vs Tensile Strength for Hydro-
clave Bags

subscale were not used on the large nozzle components since the thickness which would have to be penetrated exceeded the limits of the portable equipment available for this work.

The bond lines between the glass and ablative on these components were subjected to a 100 percent ultrasonic inspection. The standard for the ultrasonic inspection of these bonds was a composite panel of steel and glass with known defects in the bond line.

No delaminations or cracks were found in any of the Unit #1 or #2 nozzle ablatives with the exception of the mid throat for the Unit #1 nozzle. This component was cracked in a mishap while undergoing final machining. Minor unbond conditions were detected between the glass and the ablative near the exit plane rovings on the Unit #1 exit cone.

2. Steel NDT

Original plans for nondestructive testing of the steel nozzle shell and nozzle adapter required radiographic, ultrasonic, and dye penetrant inspection of all welds after welding with only ultrasonic inspection of welds after aging and final machining.

Early in the program, difficulty was encountered in interpreting some of the ultrasonic defects; and on at least two occasions, areas were excavated which apparently did not contain any defects. This, coupled with the fact that the geometry in the area of the circumferential welds was not easily accessible with a commercially available crystal and also that the surface condition of the weld after grinding in these areas was poor, led to the deletion of the ultrasonic inspection prior to aging and machining.

After the Unit #1, 156-2C-1 nozzle shell had been aged and machined, one defect was located by ultrasonic inspection, confirmed by radiographic inspection, and repaired. Following grit blast of this same unit, some surface imperfections led to the discovery of additional dye penetrant indications in the weld and, eventually, to a complete radiographic inspection of the weld. This inspection revealed additional indications which had been missed by the previous ultrasonic inspection. In some cases, the defect could not be picked up by ultrasonics, even after its location was known. The geometry of the component in combination with the commercially available crystals, which do not contain curved wedge blocks to match the contour of the part, contributed to the lack of ability to find the defects.

To avoid future problems of this type, the process was changed to require a radiographic, ultrasonic, and dye penetrant inspection prior to aging and after final machining. This process was used on the 260-SL-1 adapter. Numerous defects were found in the part after aging and machining even though the part was radiographically acceptable after all weld repair had been completed prior to the anneal-size and age cycles. These problems of failure to find defects led to additional modifications in the NDT procedure.

The procedures now required a complete radiographic, ultrasonic, and dye penetrant inspection after all anneal and size operations had been completed and again after aging and finish machining.

A 300 KV x-ray head and Dupont 506 film were used in the radiographic inspection of the 156-2C-1 nozzle shell and the 260-SL-1 adapter. The penetrameters used were made of maraging steel and met the requirements of MIL-STD-453. A 1.4 percent sensitivity was maintained on the film for the steel components. The ultrasonic standard for the welds was a 0.200-inch-long by 0.070-inch-deep fingernail notch. Eighty percent amplitude on this notch was the acceptable limit for ultrasonic defects. All dye penetrant inspection was completed in accordance with the requirements of MIL-I-6866.

3. Assembly NDT

A 100 percent ultrasonic inspection was conducted on the adhesive bonds of the 156-2C-1 nozzle assembly in the following areas:

1. The bond line between the ablative component and the steel shell.

2. The bond between the tie laminate and the nozzle shell and the tie laminate and exit cone structural laminate.

3. The bond between the filament wound glass and the tie laminates.

The defect standard for this inspection of the assembly was a composite sample made of maraging steel, bi-directional glass, ablative materials, and Epon 913 adhesive. The standard was fabricated as shown in Figure 37. The different areas shown as the standard are as follows:

1. Total lack of bond between steel and adhesive (for a section with parallel surfaces).

2. Bonded area which has had pressure applied (for a section with parallel surfaces).

3. Bonded area simulating production application (for a section with parallel surfaces).

4. Bond between steel and adhesive, but no bond between adhesive and ablative.

5. Bonded area which has had pressure applied (for a tapered section).

6. Total lack of bond between steel and adhesive (for a tapered section).

7. Bonded area simulating production application (for a tapered section).

8. Bond between steel and glass (for the tie laminate to steel section).
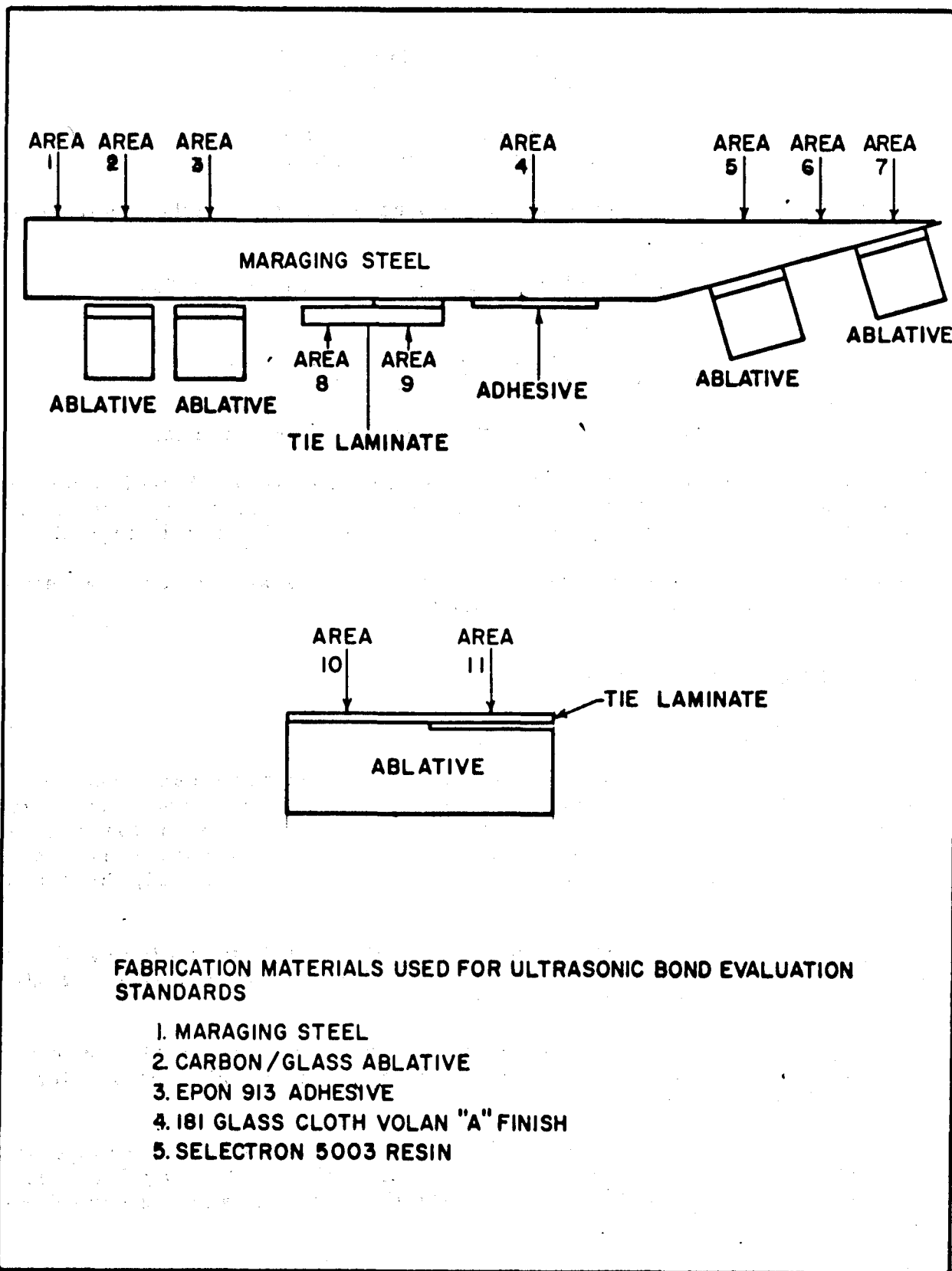
Figure 37 - Ultrasonic Standard for Bond Line

FABRICATION MATERIALS USED FOR ULTRASONIC BOND EVALUATION STANDARDS

1. MARAGING STEEL
2. CARBON/GLASS ABLATIVE
3. EPON 913 ADHESIVE
4. 181 GLASS CLOTH VOLAN "A" FINISH
5. SELECTRON 5003 RESIN

9. Unbond between steel and glass (for the tie laminate to steel section).

10. Bond between glass and glass (for the tie laminate to glass/ablative section).

11. Unbond between glass and glass (for the tie laminate to glass/ablative section).

The equipment used in evaluation of the bond line in the nozzle assembly was as follows:

1. Magnaflux 810B Pulse-echo type ultrasonic flaw detection instrument.

2. Magnaflux Z1H-C 3/4" Diameter, 2.25 mc straight beam ultrasonic transducer.

3. SAE 10 oil or glycerine/water mix for couplant.

Less than five percent of the ablative-to-steel bond areas showed an unbonded condition. This check was proven to be reasonably accurate by a visual inspection after disassembly of the nozzle (see Section VII of this report).

No unbonded conditions were detected in the tie laminate-to-nozzle assembly bonds or the roving-to-tie laminate bonds.

E. NOZZLE METALLURGY

1. General

Metallurgy of the large nozzle and the 260-inch case was closely related since materials and welding processes were the same for both components. Case program information and data were used extensively throughout the large nozzle program. Welding problems were more acute for the nozzle than the case since higher energy weld input was needed to cope with generally thicker sections used for the nozzle.

Another nozzle problem area given considerable attention was the establishing of proper aging cycles because of furnace limitations coupled with strength and toughness requirements for the part.

TIG repair welding problems caused some difficulty. The problem was mainly attributable to the mechanics of repair site preparation rather than actual repair welding technique.

A major problem in nozzle shell fabrication was shrinkage and warpage which resulted from numerous reversion and anneal cycles. These cycles were required to overcome weld cracking of the first weld pass by the second weld pass.

Major problems encountered in fabrication of the adapter and nozzle steel shell are discussed below.

2. Problem Areas

a. Reforming Maraging Steel

Distortion during welding of longitudinal passes in the nozzle section sub-assemblies necessitated a reforming operation prior to assembly welding. The first attempt at reforming resulted in failure of the longitudinal weld for its full length. The reforming operation was done with the section in the as-welded condition. Investigation into cause of failure produced the following recommended procedure for future work of this nature: grind weld reinforcement flush; anneal section prior to reforming operation; and apply reforming loads in a gradual controllable manner over a wider span. These steps were followed in the next attempt which also resulted in weld failure. The component was overformed in the first reforming operation and failed when corrective reforming was attempted. Examination of this section showed cracks in the parent metal HAZ running parallel to the weld as well as the massive weld centerline crack. Micros taken from the parent material cracks showed an oxide film or scale on all parent material crack surfaces indicating that the parent metal cracking took place before the reforming operation and were not attributable to the reforming operation. No attempt had been made to control or record the maximum press load; therefore, it was impossible to determine whether the weld's annealed strength had been exceeded in the reforming operation. In order to evaluate this possibility two studies were conducted; one to determine the load-strain cure for annealed maraging steel; and two to determine the load required for reforming maraging steel. Table LV has the results of tensile tests of annealed maraging steel and Figure 38 is the load-strain curve from test No. 7, which is typical for annealed maraging steel. These values were used in the second study for determination of the forming load limits for annealed maraging steel. This study also established the forming requirements for the heavier 1.55 inch thick section of the redesigned shell.

The study consisted of forming a bar in a jig, with a 300,000 pound Tinius-Olsen tensile testing machine (see Figure 39). Properties for the proportional limit, yield point and ultimate tensile strength were obtained from the previous study and used to calculate the load required to attain extreme fiber stress at the three aforementioned conditions. At each of the determined loads, deflection under load and permanent set after removal of load were recorded, see Table LVI.

From this data it was determined that the maximum plastic bending factor, K, to be used for forming would be set at 1.70. However, the preferred range of K would be 1.4 to 1.6 which would incorporate a reasonable safety factor. Using a press brake with a die span of 13'0" the forming loads for the various plate thicknesses were tabulated as shown in Table LVII. The strain rate differential was not accommodated as maraging steel in previous tests had not shown any strain rate sensitivity within the ranges used with the testing machine and the capabilities of the press brake.

Another specimen, 1.926" x 1.628", was loaded in the same test fixturing to approximately 1.7 x F_{tu}, 81,200 lbs. The set was recorded and the bar subjected to reverse bending using the same 81,200 lbs. load and the set recorded again. The load was increased to obtain initial drop-off and failure as obtained for the previous tests. The results and comparison to the previous results

TABLE LV

MECHANICAL PROPERTIES OF ANNEALED MARAGING STEEL

Test No.	F_{tu} (ksi)	F_{ty} (0.2%) (ksi)	EL% (1")	RA%
1	141.2	115.0	15.2	66.4
2	140.8	110.3	15.0	68.0
3	141.8	113.0	13.6	61.4
4	139.8	108.8	14.5	62.5
5	140.0	110.7	15.6	68.2
6	142.0	131.0	N/A	N/A*
7	140.7	133.3	15.0	N/A*

*Instron no Extensometer

F_{tu} = Ultimate tensile strength

F_{ty} = Yield strength
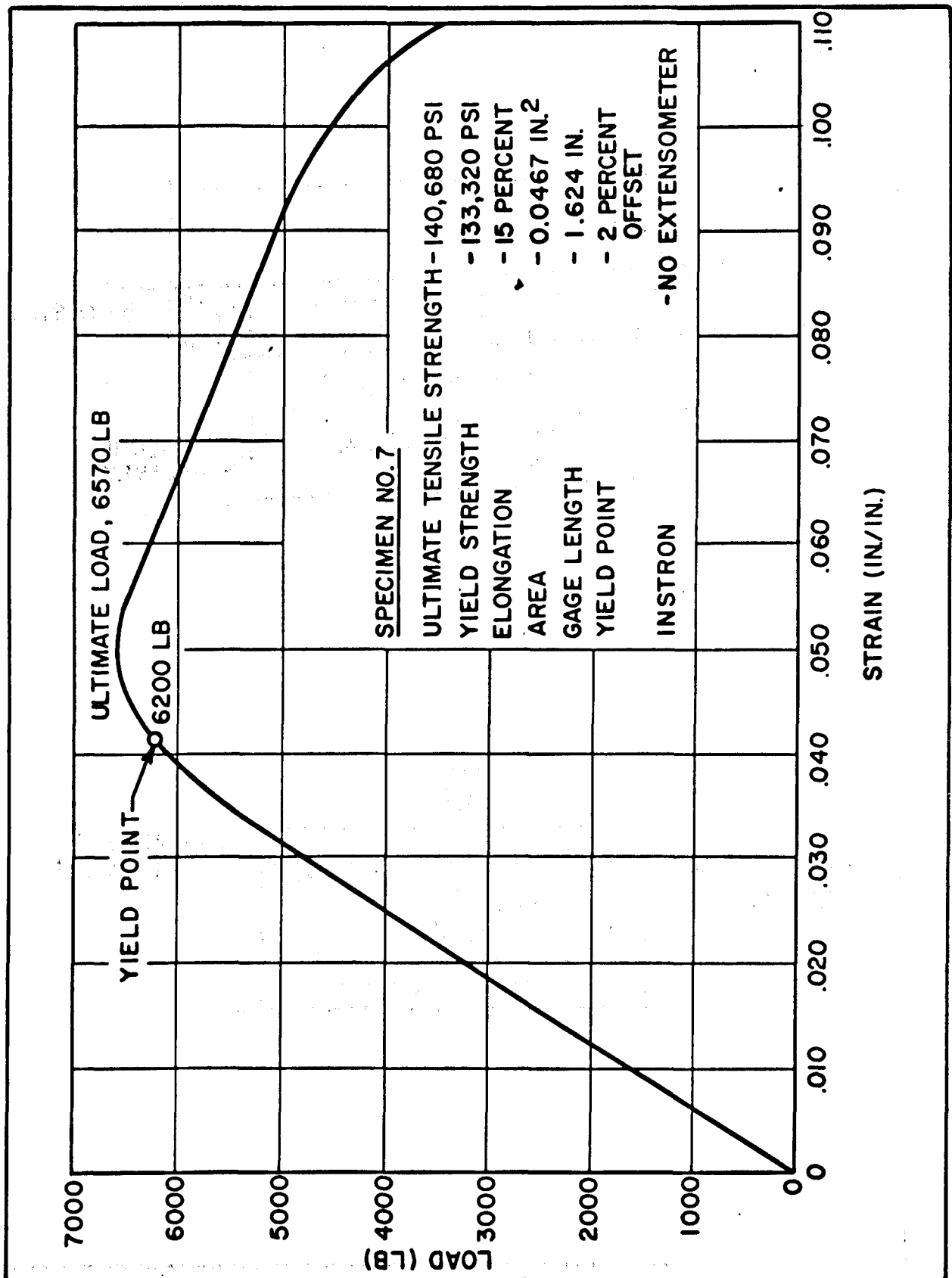
Figure 38 - Stress Strain Curve of Annealed Maraging Steel
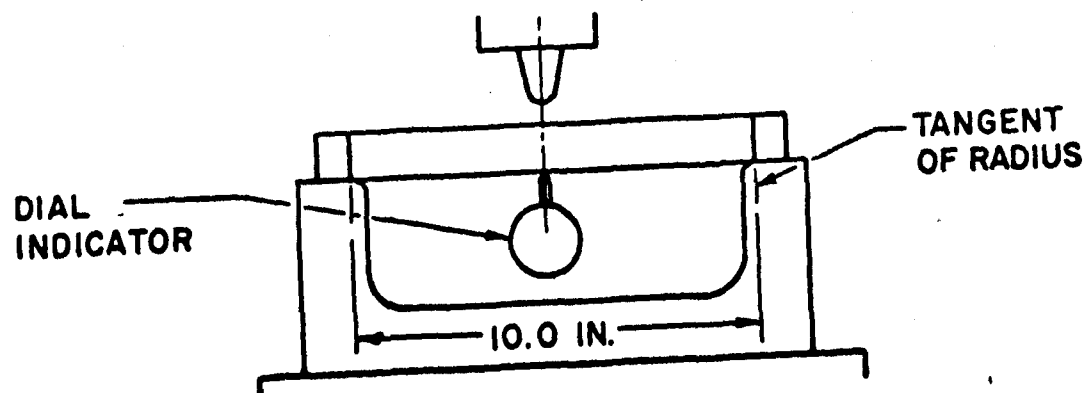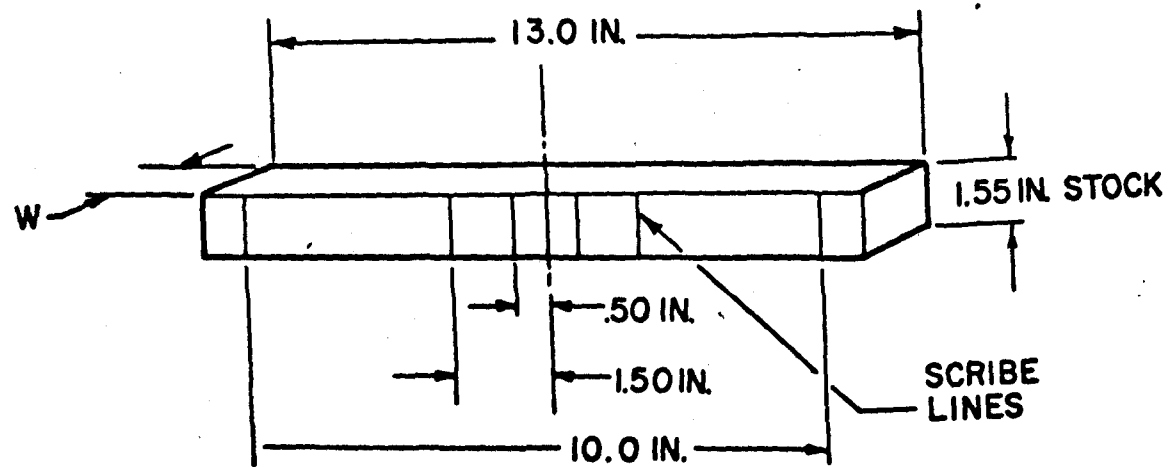
Figure 39 - Test Bar and Set Up

TABLE LVI

LOAD-DEFLECTION-SET DATA

Specimen Load (lbs)	1 (1.627 x 1.954) Deflection	Set	2 (1.626 x 1.954) Deflection	Set	3 (1.627 x 1.953) Deflection	Set
13,000	0.019	0.0015	0.020	0.0013	0.018	0.0005
34,600	0.053	0.009	0.055	0.0095	0.053	0.007
48,800	0.0805	0.019	0.083	0.0195	0.080	0.0163
58,600	0.1045	0.031	0.107	0.0320	0.104	0.028
68,400	0.137	0.052	0.142	0.0545	0.135	0.048
73,300	0.159	0.069	0.162	0.072	0.1585	0.0673
81,200	0.220	0.136	0.225	0.143	0.218	0.1215
Initial Pt. of Load Drop-Off	87,500#		87,000#		85,000#	
Failure	89,250#		89,000#		89,000#	
K*	1.79		1.78		1.74	

NOTES: 1. K* = Max. Load/Ult. Load (based on initial point of load drop-off)
2. The initial point of load drop-off is the point at which the load-deflection curve changes significantly and is similar to a conventional yield point.
3. The term "failure", as applied to these tests, is the point at which the specimen can no longer sustain the maximum applied load. There is no rupturing or cracking evidenced and the specimens were bent to approximately 90 degrees. It is felt that this bending could be increased further with no cracking.

TABLE LVII

FORMING LOADS - 13' SPAN PRESS BRAKE

Stock (in.)	Actual Thickness (in.)	Plate Width (in.)	Preferred Load Range (tons)	Maximum Load (tons)
1.125	1.17	36.25	251-287	305
1.250	1.32	14.00	124-141	150
1.550	1.63	38.50	518-591	630

are in Table LVIII.

The conclusions which can be drawn from this series of tests are that the failed sections had been overloaded and that in the annealed condition reforming of welded maraging sections can be accomplished provided material limits are not exceeded. The forming of the sections was extended further to the conical ring subassemblies and to the final nozzle shell and adapter assemblies in that all completed cone and final assemblies required anneal and size operation. These size cycles were required to provide a steel shell contour with clean up stock in the proper location.

Size cycles consisted of placing the part in a furnace, heating to $1650^{\circ}F$, and maintaining it at that temperature for one hour per inch of thickness. At the completion of this cycle, the part was removed from the furnace and, as rapidly as possible, put in place on a tool which had been fabricated to the correct contour. The hot conical section or subassembly was then restrained to prevent movement up the cone during cooldown. Figure 40 shows a typical tool for sizing of the nozzle adapter. In most instances the tool served to round the component but cones with a half-angle of 30 degrees or less were forced down on the tool which caused increase in diameter. Two or more cycles were generally required to obtain the correct contour.

b. Properties of Thick Plate

The thick plate problem for the nozzle was the same as for the case. For this reason the flange concept was changed from thick plate formed and welded to ring rolled forgings. The majority of the plate for nozzle fabrication was approximately 1-1/2" thick. This thickness plate fell in the same category as the 1-7/8 inch thick plate for the Y-rings and typically had the same mechanical properties. The properties of the plate and forgings used are included in the Material Properties section of this report.

c. Submerged-Arc Welding

All of the welds in the nozzle shell parts were made by the two pass sub-arc technique. The Rohr welding effort was concerned primarily with adapting 260" case welding technology to the thicker sections required for the nozzle. Due to the increase in section size, the welding energy and filler wire diameter had to be increased. Several welds were made and tested using various weld parameters. These welds were tested for response to aging, fracture toughness, chemistry, and the effects of energy input on bare material. The optimum conditions were then used to make a 56" long qualification weld using the following parameters and obtaining the results as shown below:

1. Joint Configuration

    Type - Double "U"
    Unchamfered Level - 5/8"
    Radius - 5/16"
    Chamfer Angle - none required
    Root Opening - none

2. Welding Parameters

144

TABLE LVIII

TEST RESULTS - FORMING STUDY

| Specimen 4 | | Average Load |
Load (lbs.)	Set (in.)	of Specimens 1, 2, & 3 (lbs.)
81,200	.155	
specimen reversed		
81,200	+.040	
83,000	Initial drop-off	86,500
87,750	Failure	89,000

NOTE: The specimen for this test is slightly narrower in width, but the decrease in moment of inertia is insignificant relative to correlation of results to specimen 1, 2, and 3.
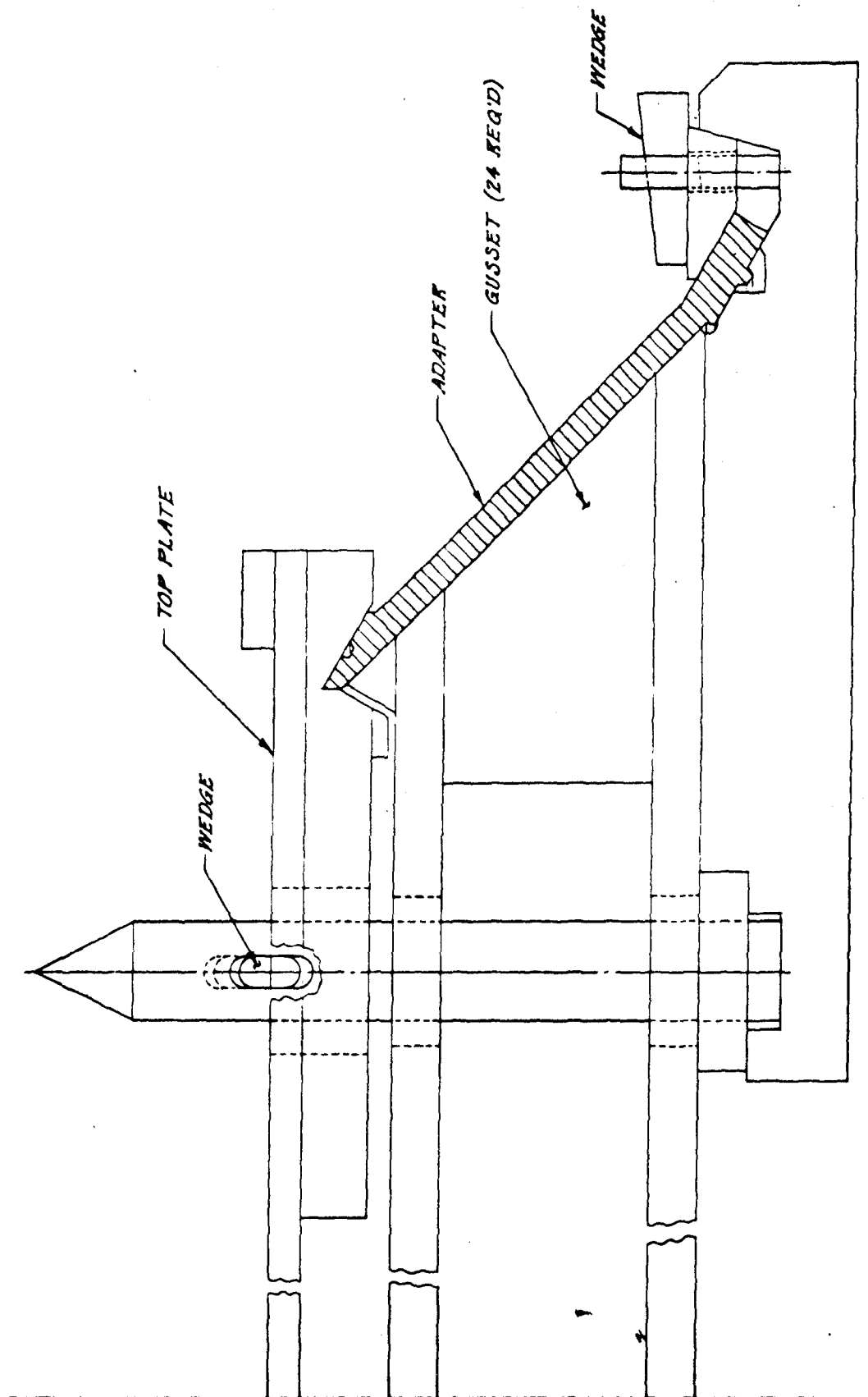
Figure 40 - Tool for Sizing Adapter

Volts - 33
Amps - 650 first pass
       - 725 second pass
Speed - 8 inches per minute
Wire diameter - 5/32"
Energy input - first pass - 148,700 joules per inch
               - second pass - 179,500 joules per inch

3. Properties

Tensile Properties Average of 15 Tests Each
Location (aged 3 hours at 900°F)

	YS Ksi	UTS, Ksi	%EL (2")	RA
First weld pass	216.7	232.9	3.4	26.5
	231.6	243.4	3.8	30.0
Second weld pass	225.8	234.7	4.9	41.2

Fracture Toughness W/A

Notch on Surface

First pass - 451.4 (average 23 tests)

Second pass - 374.2 (average 19 tests)

Notch Through Thickness

First pass - 427.1 (average 20 tests)

Second pass - 382.6 (average 20 tests)

In addition, the normal type of start-stop, "T" intersections, and repair qualification panels were made with comparable results. Repair welding as such is covered in the next section of this report. The difference in strength between the first and second pass is due to the partial reversion of the first pass by the heat input of the second pass. The reversion cycle which was added to the welding process to prevent the cracking in the first weld pass also created a need for a subsequent anneal cycle after depositing the second pass. The anneal cycle eliminated the reverted zone in the first pass thereby eliminating the variations in strength level between the passes. These changes in thermal treatment did not require requalification of the welding process.

d. Repair Welding

Repair welding for the nozzle parts was accomplished by both TIG and subarc methods. Subarc repair was used only when a major portion of a weld had to be removed. TIG was used for the major portion of the repairs in both the nozzle and adapter shells.

(1) TIG Repairing

The major problem with TIG repairing was not the mechanics of the repair welding technique, but rather the technique for repair site excavation. Initially, the excavations were made just large enough to remove the defect; therefore, deep, straight sided excavations resulted. In effect, the excavation configuration resulted in a situation similar to plug welding. Under any circumstances, plug welding is subject to difficulty: generally cracking or porosity. In welding this type of excavation the welder "traps" his arc against the steep sides which results in cold shuts and porosity. After changing to a sloping side wall elongated type of excavation, this problem was alleviated. The parameters used for the TIG repair followed very closely those for case TIG repair within equipment limitations. For this reason, TIG repair qualification consisted mainly of evaluation for soundness and mechanical properties. Typical evaluations were (1) properties of TIG repairs after the change was made in excavation configuration, and (2) aged versus unaged TIG repairs in an aged part. The excavations for the first evaluation were made in standard two pass subarc welds in 1-1/4 inch thick material and repairs were 5 inches long by 1/2 inch deep by 3/16 inch root with sloped sides. One excavation was made at the subarc fusion line, another in the subarc weld centerline. After welding, the repaired panel was reverted at 1250 F for 1-3/4 hours, annealed and aged at 840 F for 3-1/2 hours. X-ray evaluation revealed no rejectable defects in the repair zones. The results of the tensile test bars and the fracture toughness (W/A) test are in Table LIX, which indicate this procedure was adequate for nozzle shell use.

The excavations for the aged versus unaged TIG repair properties evaluation were both in the subarc centerline one 1/4 inch deep, the other 3/4 inch deep. Both excavations were five inches long with sloped sides and approximately 3/16" wide at the root. These excavations were made in an aged subarc weld with no reversion or annealing after TIG repair; however, the aged repair results are from bars that had been aged at 840 F for 3-1/2 hours. The results of the tensile tests are in Table LX. Using the stress levels anticipated at motor maximum operating pressure in the nozzle and adapter welds as a guide, these results indicated that in many cases repairs made after component aging need not be reaged.

(2) Sub-Arc Repairing

Although the majority of the weld repairing was accomplished by TIG, four panels of sub-arc welded repairs were made and tested. The location and configuration of repair zones are shown in Figure 41. The repair type and thermal treatment sequence is as shown in Table LXI. The repair welding parameters used are in Table LXII. The mechanical and fracture toughness properties obtained from these welds are in Table LXIII.

This data indicates the repair by sub-arc is an acceptable practice; however, the same type of thermal treatment should be used with sub-arc repair that is used in original sub-arc welding, namely reversion prior to repair and anneal and annealing after repair.

e. Thermal Treatment

Thermal treatments employed with the nozzle parts were identical in nature to those used for the case; however, the number of reversion and anneal cycles

148

TABLE LIX

TIG REPAIR OF SUB-ARC WELD -
NEW REPAIR EXCAVATION CONFIGURATION

Location of Repair	YS (0.2%) (ksi).	UTS (ksi)	El % (1 in)**	R/A %	W/A in-lbs/in^2
Centerline	212.0	218.5	7.6	30.0	727
Fusion Line	213.1	219.1	6.1	23.2	656

NOTE: Tensile results average of three tests and W/A results of five tests

TABLE LX

TIG REPAIR OF SUB-ARC WELD* -
AS REPAIR AND AS REPAIRED AND AGED

	YS (0.2%) (ksi)	UTS (ksi)	El %	R/A %
First Sub-Arc Pass prior to Repair				
	197.0	220.5	6.0	18.0
	192.0	219.5	10.0	30.4
Second Sub-Arc Pass prior to Repair				
	210.0	230.5	8.0	31.4
	212.5	232.5	3.0	5.0
One-fourth-inch deep Repair Tested in As-repaired Condition				
	121.0	153.5	12.0	49.0
	121.0	153.5	15.0	59.4
	121.0	153.5	12.0	45.8
Three-fourth-inch deep Repair Tested in As-repaired Condition				
	116.0	149.5	7.0	26.2
	121.0	152.0	10.0	43.2
	115.0	150.0	10.0	44.4

TABLE LX
(continued)

	YS (0.2%) (ksi)	UTS (ksi)	El %	R/A %
One-fourth-inch deep Repair Aged 840°F for three and one-half hours				
	212.5	228.0	3.3	7.1
	207.5	225.0	10.0	39.3
	205.5	222.0	5.0	16.3
Three-fourth-inch deep Repair Aged 840°F for three and one-half hours				
	197.0	210.0	10.0	45.2
	195.0	210.0	11.0	48.5
	192.0	209.0	10.0	35.0

* No reversion after first sub-arc pass prior to second pass; therefore, aged strength of welds shown is lower than average for actual nozzle and adapter parts.

** R-3 (0.252-in. dia.) bars; therefore, one-inch gage length is 4-D.
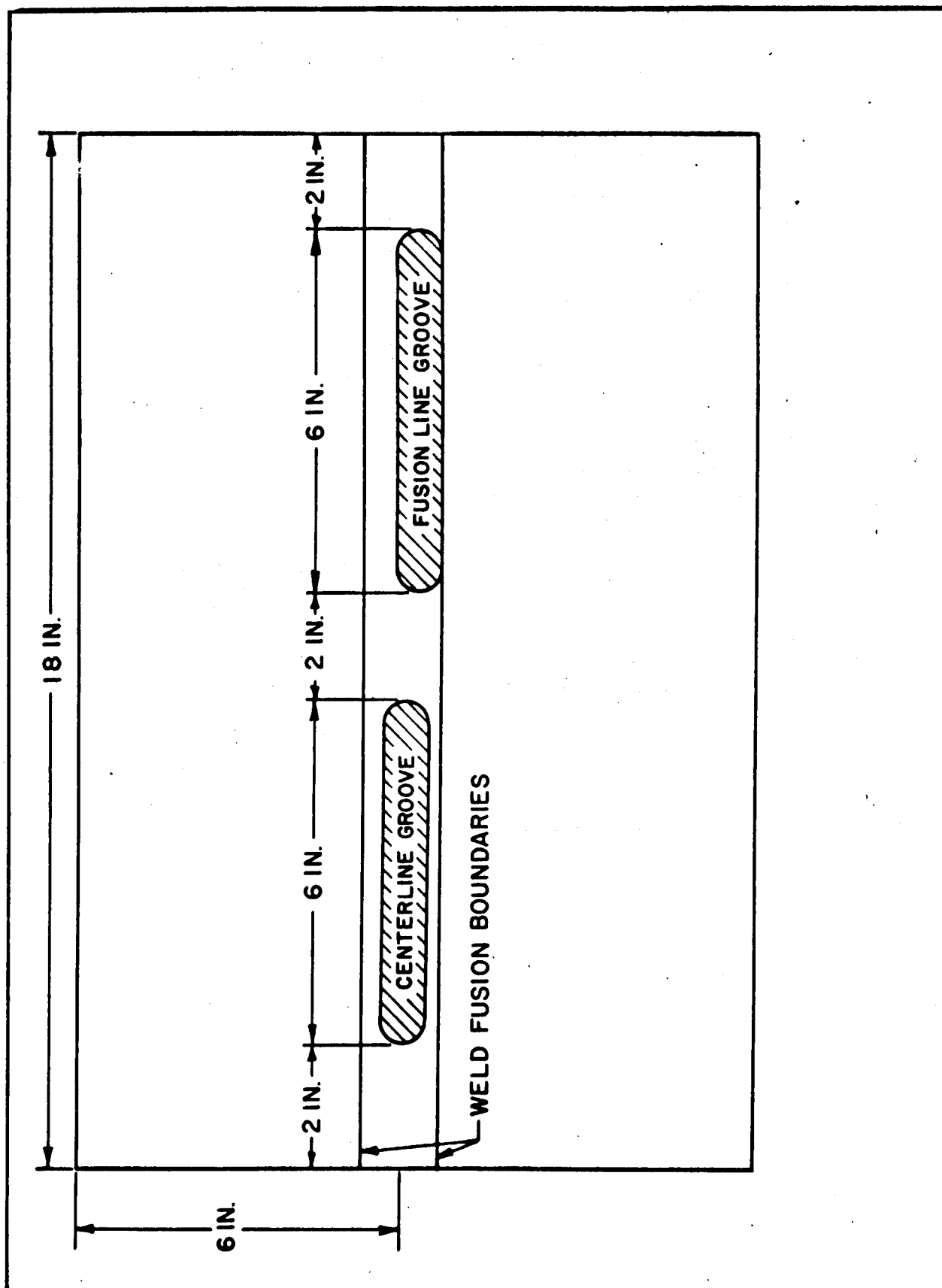
Figure 41 - Location and Shape of Grooves, Top View and Side View

TABLE LXI

SUB-ARC REPAIR TYPE AND THERMAL TREATMENTS

Panel No.	Repair Type	Thermal Cycles
1	Center and fusion line, one side only	Weld - repair - age $900^{\circ}F$, 3 hrs
2	Center and fusion line, one side only	Weld - revert - $1250^{\circ}F$, 2-1/2 hrs Repair - anneal $1550^{\circ}F$, 1-1/3 hrs - age - $900^{\circ}F$, 3 hrs
3	Center and fusion line, both sides, bac to back	Weld - anneal - $1550^{\circ}F$, 1-1/3 hrs Repair (1st side) - anneal $1550^{\circ}F$ - 1-1/3 hrs Repair (2nd side) - age $900^{\circ}F$ - 3 hrs
4	Center and fusion line, both sides, back to back	Weld - revert - $1250^{\circ}F$ - 3-1/3 hrs Repair (1st side) - revert $1250^{\circ}F$ - 1-1/3 hrs Repair (2nd side) - anneal $1550^{\circ}F$ - 1-1/3 hrs - age $900^{\circ}F$ - 3 hrs

TABLE LXII

WELD PARAMETERS FOR SUB-ARC WELD REPAIR

Plate	Repair Identification	Initial Weld Repair			Second Weld Repair (Reverse Side of Plate)		
		Voltage	Amperage	Travel (ipm)	Voltage	Amperage	Travel (ipm)
1	Centerline	40	780	6	--	--	--
	Fusion Line	40	800	6	--	--	--
2	Both	40	700	6	--	--	--
3	Both	40	880	6	39	780	6
4	Both	40	880	6	40	825	6

TABLE LXIII

TENSILE AND FRACTURE TOUGHNESS (W/A) SUB-ARC REPAIRS

	YS (0.2%) (ksi)	UTS (ksi)	El % (2 in)	R/A %	W/A In-Lbs/in^2
Panel No. 1					
Centerline rep. avg. (3)	216.2	224.4	3.6	30.5	490
Fusion line rep. avg. (2)	226.5	241.5	3.5	27.9	350
Control avg. (3)	234.8	244.2	5.4	46.3	---
Panel No. 2					
Centerline rep. avg. (3)	233.1	241.9	4.5	37.1	340
Fusion line repair-1 test	223.8	230.0	3.3	27.0	388
Control avg. (2)	235.7	244.9	4.9	42.3	---
Panel No. 3					
Centerline rep. avg. (6)	222.7	236.3	3.5	28.2	334(avg. 14)
Fusion line rep. avg. (6)	213.6	228.1	2.4	15.1	---
Control avg. (3)	234.8	244.2	5.4	46.3	---
Panel No. 4					
Centerline rep. avg. (5)	229.4	239.9	4.2	35.9	308(avg. 4)
Fusion line rep. avg. (6)	229.0	240.0	3.7	26.7	299(avg. 4)
Control avg. (4)	251.3	244.1	5.5	16.2	323(avg. 6)

and equipment used were not the same. For local aging a different method for heating was used: resistance strip heaters in place of the Quartz lamps used for local aging of case components.

Major difficulties encountered were shrinkage associated with numerous anneal and revert cycles which resulted in dimensional control difficulties, and temperature control with equipment used for aging.

(1) Furnace Atmosphere

The furnace used for the nozzle parts was gas fired. Since the products of combustion were different than those encountered in the oil fired furnace used in case aging, the effect on mechanical properties was investigated.

The results in Table LXIV show the mechanical properties of bars machined after annealing were slightly higher than the properties of bars machined and then annealed in the gas fired furnace. The control bar annealed in an electric furnace had properties approximately the same as bars machined after annealing. Fracture toughness tests indicated no significant difference whether machined prior to or after annealing in the gas fired furnace.

Due to tolerance limitations machining of the nozzle and adapter shells after annealing was required; therefore, annealing in the gas fired furnace posed no problem.

(2) Reversion and Annealing

Properties of the parent material were obtained after one through six anneal cycles and properties of welds after six revert and fifteen anneal cycles.

The parent material bars were treated as shown in Table LXV, with results as shown in Table LXVI. The first series of welded specimens were treated similar to parent material bars, Table LXVII, with results shown in Table LXVIII. The second series of welded specimens were exposed to a combination of revert and anneal cycles, Table LXIX, with tensile and fracture toughness properties (W/A) obtained shown in Table LXX.

In addition to the above, welded samples and parent material samples were measured after various revert and anneal cycles to obtain shrinkage data. Welded bars were subjected to the cycles in Table LXXI, and measured for length shrinkage only; whereas, the parent material sample was subjected to cycles as shown in Table LXXII and measured in all three directions.

The following conclusions were derived from the studies:

1. A 155°F anneal following a 1650°F anneal increased aged strength.

2. Multiple anneals do not adversely affect aged properties.

3. Welded material responds to annealing cycles in much the same manner as parent material.

155

TABLE LXIV

MECHANICAL PROPERTIES OF MARAGING STEEL
ANNEALED IN GAS-FIRED FURNACE

Test No.	YS (ksi)	UTS (ksi)	El % (1 -in. -4D)	RA %	W/A in.-lbs/in.^{2}
Specimens machined prior to annealing					
1	231.0	241.5	10.8	48.5	1098
2	231.6	242.2	10.3	45.3	1195
3	226.5	242.3	10.5	47.0	1879*
4	226.5	241.3	10.5	45.8	1344
5	228.5	242.2	10.0	41.6	1110
6	232.0	245.8	11.0	50.0	1335
Avg.	229.3	242.6	10.5	46.5	1216
Specimens machined after annealing					
1	238.0	248.5	10.0	47.2	1196
2	236.2	246.5	10.5	47.8	1286
3	239.0	249.5	10.2	47.0	1333
4	239.2	249.7	9.3	39.3	1355
5	239.0	249.5	9.3	44.0	1194
6	-----	-----	----	----	2026*
Avg.	238.3	248.7	9.8	45.1	1273
Control specimen - annealed in electric furnace					
Avg.	237.0	245.5	10.4	46.5	----

*Not included in average

156

TABLE LXV

ANNEAL CYCLES FOR PARENT MATERIAL BARS

Group I		Group II		Group III		Group IV		Group V	
Degs F	Hrs	Degs F	Hrs	Degs F	Hrs	Degs F	Hrs	Degs F	Hrs
1650	1	1650	1	1650	1	1650	1	1650	1
		1500	1	1650	1	1650	1	1650	1
900	3			1500	1	1650	1	1650	1
		900	3					1650	1
				900	3	900	3	1650	1
								900	3

TABLE LXVI

TENSILE RESULTS - PARENT MATERIAL ANNEAL CYCLES

Group	YS (0.2 %) (ksi)	UTS (ksi)	El % (1-in-4D)	RA %
Control	229.7	243.2	8.0	34.5
I	231.0	243.2	8.0	39.9
	229.0	242.0	8.5	42.2
	227.5	242.5	8.5	45.0
II	242.0	251.5	7.5	37.4
	241.7	253.0	7.0	30.3
	243.3	254.0	7.0	36.3
III	241.0	252.2	7.5	45.2
	242.2	254.0	7.5	41.7
	243.5	253.0	8.0	45.0
IV	230.0	244.0	8.0	44.6
	231.0	244.7	8.7	47.8
V	235.0	244.5	8.3	48.0
	233.0	243.5	8.6	47.0
	237.0	248.0	8.2	44.6

NOTE: Control specimens, mill annealed and aged, at 900°F for 3 hours.

TABLE LXVII

TREATMENT OF WELDED TEST SPECIMENS .

Group VI		Group VII		Group VIII	
Degs F	Hrs	Degs F	Hrs	Degs F	Hrs
1650	1	1650	1	1650	1
1650	1	1650	1	1650	1
		1650	1	1650	1
900	3	⁄		1650	1
		900	3		
				900	3

TABLE LXVIII

TENSILE RESULTS OF WELDED SPECIMENS ANNEAL CYCLES

Group	YS (0.2 %) (ksi)	UTS (ksi)	El % (1-in-4D)	RA %
VI	236.2	246.8	5.5	25.1
	232.7	246.6	6.3	25.4
VII	236.2	249.1	6.7	30.4
	235.6	247.7	2.0	7.4
VIII	235.6	249.0	7.1	35.7
	234.0	248.6	6.0	26.1

TABLE LXIX

REVERT AND ANNEAL CYCLES - WELDED SAMPLES

1 - Revert - 1250°F	1-3/4 hrs.		12 - Anneal - 1650°F	1-3/4 hrs.
2 - Anneal - 1650°F	1-3/4 hrs.		13 - Anneal - 1650°F	1-3/4 hrs.
3 - Revert - 1250°F	1-3/4 hrs.		14 - Anneal - 1650°F	1-3/4 hrs.
4 - Revert - 1250°F	1-3/4 hrs.		15 - Anneal - 1650°F	1-3/4 hrs.
5 - Revert - 1250°F	1-3/4 hrs.		16 - Anneal - 1650°F	1-3/4 hrs.
6 - Anneal - 1650°F	1-3/4 hrs.		17 - Anneal - 1650°F	1-3/4 hrs.
7 - Anneal - 1650°F	1-3/4 hrs.		18 - Anneal - 1650°F	1-3/4 hrs.
8 - Revert - 1250°F	1-3/4 hrs.		19 - Anneal - 1650°F	1-3/4 hrs.
9 - Revert - 1250°F	1-3/4 hrs.		20 - Anneal - 1650°F	1-3/4 hrs.
10 - Anneal - 1650°F	1-3/4 hrs.		21 - Anneal - 1650°F	1-3/4 hrs.
11 - Anneal - 1650°F	1-3/4 hrs.		22 - Aged - 840°F	3-1/2 hrs.

TABLE LXX

MECHANICAL AND FRACTURE TOUGHNESS vs. REVERT AND ANNEAL

Location	YS (0.2%) (ksi)	UTS (ksi)	El % (1"-4D)	% RA	W/A (in.-lbs/in.^{2})
1st Weld Pass	210.0	224.0	8.0	32.0	349
	208.0	223.0	9.0	33.0	338
	207.0	223.0	9.0	37.0	343
2nd Weld Pass	212.0	227.5	10.0	46.0	402
	212.0	228.0	11.0	47.0	401
Average	209.8	225.1	9.4	39.0	372

TABLE LXXI

REVERT AND ANNEAL SHRINKAGE - WELDED MATERIAL

	Condition	Length
1.	As Welded	7.865"
2.	Annealed - 1650°F	7.860"
3.	Reverted - 1250°F	7.823"
4.	Anneal - 1650°F	7.851"
5.	Reverted - 1250°F	7.819"
6.	Anneal - 1650°F	7.849"
7.	Reverted - 1250°F	7.807"
8.	Anneal - 1650°F	7.841" = 0.024 shrinkage = 0.00305 in./in.
9.	Aged - 900°F	7.828" = 0.037 shrinkage = 0.0047 in./in.

$$\frac{7.841 - 7.828}{7.841} = 0.00165 \text{ in./in.}$$

TABLE LXXII

UNWELDED MARAGING STEEL SHRINKAGE DATA

Specimen Condition	Width (in.)	Length (in.)	Thickness (in.)
As-received-mill annealed	5.0402	9.9365	1.5971
Annealed condition	5.0300	9.9260	1.6091
1650°F-1-3/4 hrs	0.0102S	0.0105S	0.0048E
Reverted-1250°F-1-3/4 hrs	5.0130	9.8795	1.5938
	0.0170S	0.465S	0.0081S
Annealed-1650°F-1-3/4 hrs	5.0252	9.9105	1.6066
	0.0122E	0.0310E	0.0128E
Reverted-1250°F-1-3/4 hrs	5.0007	9.8652	1.5966
	0.0245S	0.0453S	0.0070S
Annealed-1650°F-1-3/4 hrs	5.0155	9.8855	1.6124
	0.0148E	0.0203E	0.0128E
Reverted-1250°F-1-3/4 hrs	4.9947	9.8430	1.6043
	0.0208S	0.0425S	0.0081S
Annealed-1650°F-1-3/4 hrs	5.0075	9.8702	1.6154
	0.0128E	0.0272E	0.0111E
Reverted-1250°F-1-3/4 hrs	4.9755	9.8080	1.6133
	0.0320S	0.0622S	0.0021S
Annealed-1650°F-1-3/4 hrs	4.9980	9.8535	1.6211
	0.0225E	0.0455E	0.0078E
Reverted-1250°F-1-3/4 hrs	4.9717	9.8032	1.6129
	0.0263S	0.0502S	0.00825S
Annealed-1650°F-1-3/4 hrs	4.9875	9.8362	1.6259
	0.0158E	0.0330E	0.0120E
Aged-900°F-3 hrs	4.9870	9.8322	1.6247
	0.0005S	0.0040S	0.0012S
Total Change	0.0532S	0.1043S	0.0276E

NOTES:
1. S = Shrinkage
2. E = Expansion
3. Original volume = 79.9858 cu. in.
4. Final volume = 78.0475 cu. in.
5. Total volumetric change(s) = 1.9383 cu. in.
6. Percent volumetric change(s) = 2.42 percent
7. $\dfrac{9.9260-9.8322}{9.9260}$ = 0.00945 in./in.
8. $\dfrac{9.8362-9.8322}{9.8362}$ = 0.000406 in./in.
9. $\dfrac{9.9365-9.8322}{9.9365}$ = 0.0105 in./in.

4. Reversion followed by anneal, even for an extended number of cycles, does not adversely affect either mechanical or fracture toughness properties.

5. The shrinkage of maraging steel continues throughout thermal cycling even to the extent of 12 such cycles.

6. The aging shrinkage of 0.00165 in./in. for a welded specimen bar, after reversion and anneal was four times greater than for unwelded material.

f. Aging

The effects of various furnace heating rates and temperature control ranges on the properties of the nozzle parts were studied by aging specimens according to the schedule in Table LXXIII. The samples were tested for mechanical properties only with the results shown in Table LXXIV.

The results indicate that control of the furnace heat up time is required to preclude overaging of the part.

The 156-2C-1 nozzle shell was the first production part aged. The results shown in Section VI.A., Table XVIII, of this report indicated that the furnace control was not adequate and the part dwelled too long in the range 600 F to 835 F; therefore, it was slightly overaged. This confirms previous work in this area.

The 260-SL-1 adapter was aged employing tighter control and shorter heating times; however, tests (see Section VIII. D. of this report) indicated some degree of over-aging. Due to a difference in cross section size, test bars and actual welds were tested for hardness to establish if there was a mass effect with the results as shown in Table LXXV.

These results indicate that the aged component is not as hard as the test bar for the most part; however, the Rc results from the adapter welds do indicate sufficient hardness.

After aging, defects were discovered in the adapter which required repair and re-aging. Rather than re-age the entire part, it was decided to locally age the repaired welds to determine the mechanical properties of TIG repairs in aged welds which were subsequently locally aged, several repair welds were aged for varying times as shown in Table LXXVI. The properties obtained are in Table LXXVII. For this local aging, it was determined that Inconel electric resistance strip heaters would be used. Test panels were set up and heated to determine time and temperature control obtainable by this method. The optimum set up, Figure 42, and cycle was then applied to the adapter welds and a time temperature profile similar to the one shown in Figure 43 was employed. The local aging cycle seen by the adapter is shown in Table LXXVIII. This cycle was then employed to age adapter test

TABLE LXXIII

AGING SCHEDULES, CHARGING & HEATING

Group I

Charge into R. T. furnace and heat at rate of 100°F per hour.

Group II

Charge when furnace reaches 350°F - continue heating at 100°F per hour.

Group III

Charge when furnace reaches 600°F - continue heating at 50°F per hour.

Group IV

Charge when furnace reaches 750°F - continue heating at 50° per hour.

Group V

Charge when furnace reaches 900°F - after furnace recovers 900° hold 3 hours - remove and air cool all samples.

TABLE LXXIV

MECHANICAL PROPERTIES - AGING VARIATIONS

Group	Y.S. (0.2%) (ksi)	UTS (ksi)	El % (1"-4D)	RA%
I	242.4	254.7	9.0	40.1
	243.4	256.8	9.0	42.6
II	240.4	254.7	8.8	38.0
	239.4	253.8	8.8	42.6
III	240.2	253.8	8.2	40.9
	240.2	254.7	8.8	41.4
IV	238.3	252.8	8.3	36.7
	243.3	253.8	8.4	37.6
V	229.7	242.3	9.0	39.6
	226.0	240.3	10.0	45.4

TABLE LXXV

COMPARISON OF HARDNESS OF WELDED TEST BAR
AND ADAPTER WELDS

| Weld | Weld Pass | Hardness R_c* | |
		Adapter	Test Bar
Longitudinal	ID	47.7	49.2
	OD	47.0	48.6
Circumferential	ID	47.4	49.5
	OD	59.6	48.9
Circumferential	ID	46.8	47.7
	OD	48.5	48.3

* Average of a minimum of 18 readings taken with a portable Brinell hammer.

TABLE LXXVI

TIME TEMPERATURE CYCLES, TIG REPAIRS IN AGED SUB-ARC WELDS

Group I	Group II	Group III
TIG Repaired No Post TIG Repair Aging	Post TIG Repair Heat to 800 F Air Cool	Post TIG Repair Heat to 835 F Air Cool
Group IV	Group V	Group VI
Post TIG Repair Heat to 825-850 F Hold 30 Minutes	Post TIG Repair Heat to 825-850 F Hold 105 Minutes	Post TIG Repair Heat to 825-850 F Hold 165 Minutes

NOTE: Heating cycle; Change R. T. heat to 500 F and stabilize; 500 F to 800 F in 1 hour; 800 F to 825-850 F range in 15 minutes

TABLE LXXVII

PHASE I - TENSILE TESTING OF SPECIMENS SUBJECTED TO VARIOUS TIME-TEMPERATURE CYCLES

Group	UTS (ksi)	YS (ksi)	Elongation 1 in. (%)	Elongation 2 in. (%)	R of A (%)
I	150.5	124.0	15.0	8.0	63.0
	150.5	117.0	15.0	8.0	59.0
	148.5	113.0	16.0	9.0	66.0
Average	149.8	118.0	15.3	8.3	62.7
II	176.0	157.0	14.0	8.0	56 0
	178.0	160.0	13.0	7.0	46.0☆
	178.0	164.0	15.0	9 0	60.0
Average	177.3	160.3	14.0	8 0	54.0
III	184.0	169.0	13.0	7.0	52.0
	184.0	169.0	13.0	7.0	55.0
	183.5	168.0	13.0	7.0	52.0
Average	183.8	168.7	13.0	7.0	53.0
IV	198.5	185.0	13 0	7.0	53.0
	198.5	185.0	13.0	7.0	53.0
	199.0	189.0	13.0	7.0	50.0
Average	198.7	186.3	13.0	7 0	52.0
V	212.0	201.5	12 0	6.0	50.0
	217.0	205.0	12.0	7.0	51.0
	211.0	202.0	12.0	7.0	51.0
Average	213.3	202.8	12.0	6.7	50.7
VI	220.5	207.0	11 0	6.0	44.0
	219.5	209.0	12.0	6.0	50.0
	221.0	210 0	12.0	6.0	50.0
Average	220.3	208.7	11.7	6.0	48.0

☆Tensile specimen failed along fusion lines. All other tensile specimens failed in the TIG weld.

165
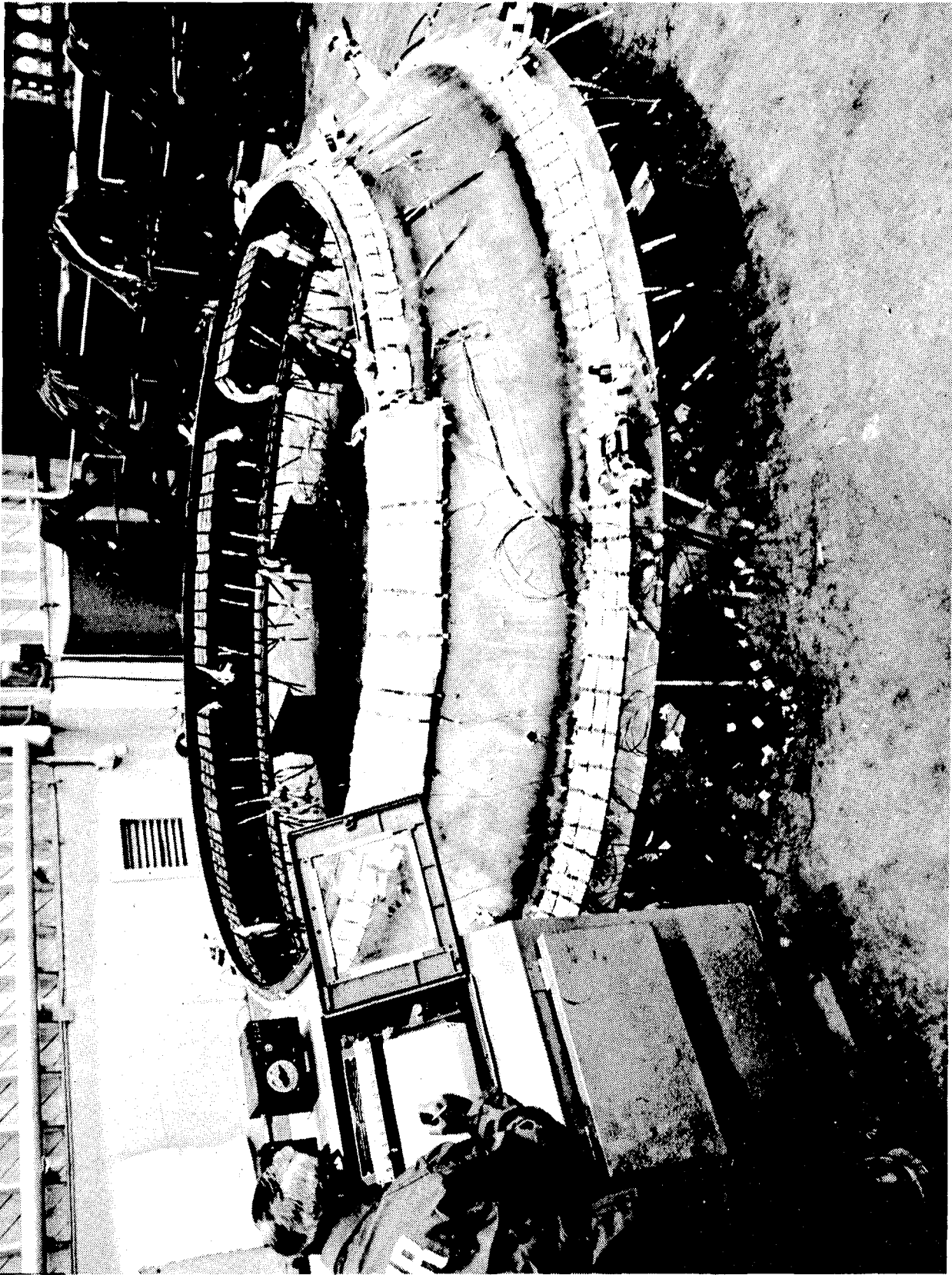
Figure 42 - Production Setup for Local Aging 260-SL-1 Adapter Repairs
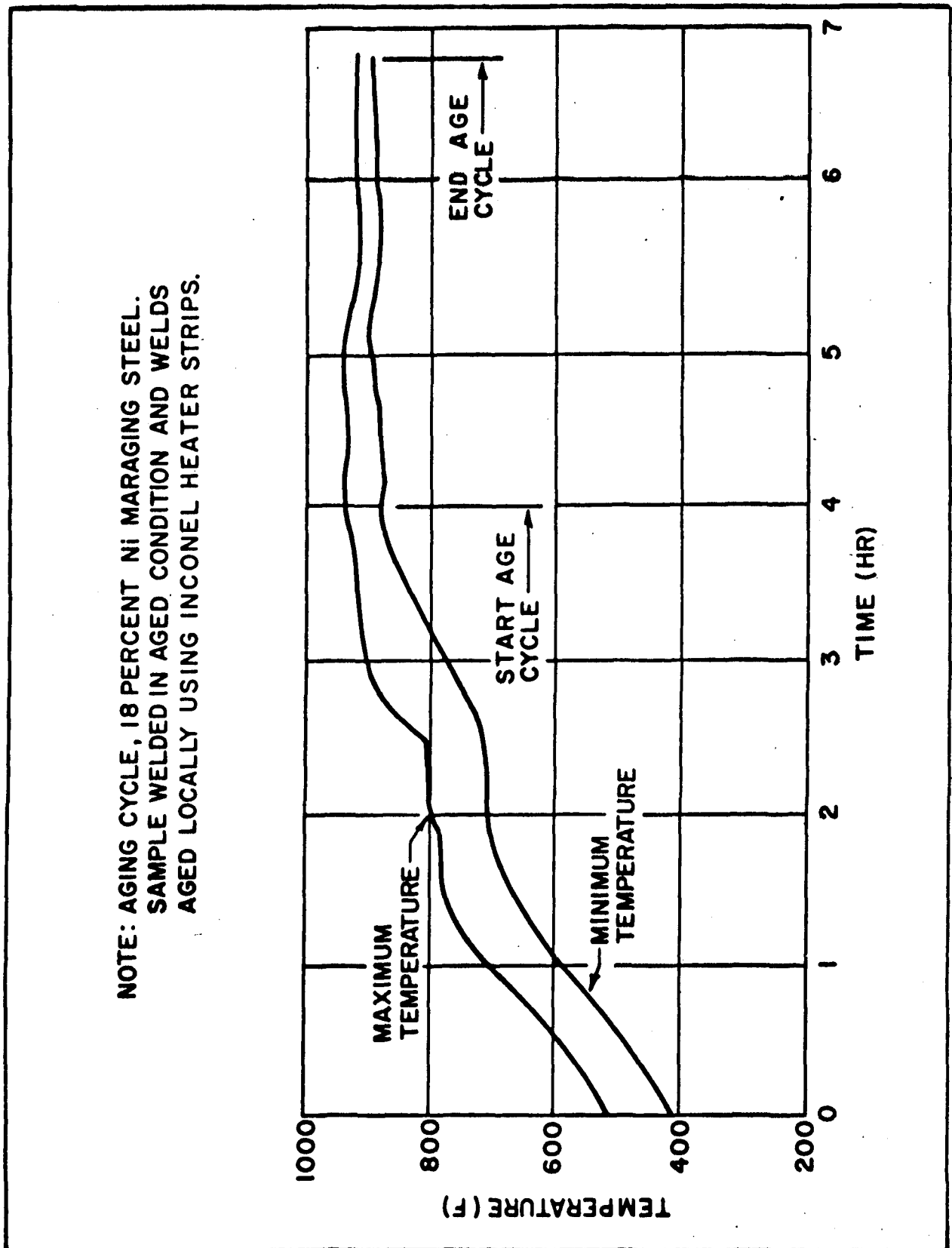
Figure 4ᵌ - Minimum and Maximum Thermocouple Temperatures Using
Electric Resistance Heater at 900 F

TABLE LXXVIII

LOCAL AGING SCHEDULE OF ADAPTER

Temperature Range ($^{\circ}$F)	Aging Time (hr)
500 - 800	2-1/4
800 - 825	1/2
825 - 850	1/2
825/850 $\to$ < 600	1/2

panels that had thermal treatment which was parallel with that of the adapter. Test data are in Table LXXIX. The data indicate that the local aging cycle experienced by the adapter did not adversely affect mechanical or fracture toughness properties of parent material or welds.

TABLE LXXIX

PHASE II - TESTING OF ADAPTER WELD TEST PANELS

	Ultimate Tensile Strength (ksi)	Yield Strength (ksi)	Elongation 1-in. (%)	Elongation 2-in. (%)	Reduction of Area (%)	Fracture Location	Fracture Toughness W/A (in.lb/in.^{2})			
							Plate HAZ	TIG Weld	Sub Arc HAZ	Forging HAZ
2A-Submerged arc welded, aged and re-aged	236.0	221.5	11.0	7.0	53	PM☆	1440	772	698	--
	244.5	230.5	7.5	4.0	25	Weld☆	1439	815	448	--
	246.5	236.0	11.0	6.0	48	PM☆	--	729	838	--
Average	242.3	229.3	9.8	5.7	42		1440	772	661	--
4A. - TIG weld repaired and aged	200.0	190.5	11.0	6.0	47	Weld	693	772	661	--
	196.0	187.0	7.5	4.0	17	Weld	815	853	278	--
	206.0	194.5	10.0	6.0	39	Weld	770	845	239	--
Average	200.7	190.7	9.5	5.3	34		759	815	315	--
804 to cone TIG weld repaired and aged	198.5	187.5	9.0	5.0	31	Weld	980	837	326	475
	205.0	190.0	8.0	5.0	33	Weld	902	774	839	438
							845	626	833	487
Average	201.8	188.8	8.5	5.0	32		909	745	666	467

☆ Parent metal

170

FINAL REPORT DISTRIBUTION LIST

SOLID ROCKET TECHNOLOGY

NASA Lewis Research Center
21000 Brookpark Road
Cleveland, Ohio 44135
Attn: Contracting Officer
    Mail Stop 500-313 (1)
    Solid Rocket Technology Branch
    Mail Stop 500-205 (8)
    Technical Library
    Mail Stop 60-3 (2)
    Tech. Report Control Office
    Mail Stop 5-5 (1)
    W. E. Roberts
    Mail Stop 3-17 (1)

National Aeronautics and
 Space Administration
Washington, D. C. 20546
Attn: RPM/William Cohen (3)
    RPS/Robert W. Ziem (1)
    ATSS-AL/Technical Library (2)

NASA Western Support Office
150 Pico Boulevard
Santa Monica, California 90406
Attn: Eugene F. Wyszpolski (1)
    Harry Williams (1)

NASA Ames Research Center
Moffett Field, California 94035
Attn: Technical Library (1)

NASA Langley Research Center
Langley Station
Hampton, Virginia 23365
Attn: Robert L. Swain (1)
    Technical Library (1)

NASA Goddard Space Flight Center
Greenbelt, Maryland 20771
Attn: Technical Library (1)

NASA Manned Spacecraft Center
2101 Webster Seabrook Road
Houston, Texas 77058
Attn: Technical Library (1)

NASA George C. Marshall Space
 Flight Center
Redstone Arsenal
Huntsville, Alabama 35812
Attn: Technical Library (1)
    R-P&VE-PA/K. Chandler (1)

Jet Propulsion Laboratory
California Institute of Technology
4800 Oak Grove Drive
Pasadena, California 91103
Attn: Richard Bailey (1)
    Technical Library (1)

Scientific and Technical Information
 Facility
NASA Representative
Post Office Box 33
College Park, Maryland 20740
Attn: CRT (1)

GOVERNMENT INSTALLATIONS

AF Space Systems Division
Air Force Unit Post Office
Los Angeles, California 90045 (1)
Attn: Col. E. Fink

AF Research and Technology Division
Bolling AFB, D. C. 20332
Attn: Dr. Leon Green, Jr. (1)

AF Rocket Propulsion Laboratory
Edwards AFB, California 93523
Attn: Norman Hirsch (1)
    RPM/Col. R. Harned (2)

AF Materials Laboratory
Wright-Patterson AFB, Ohio 45433
Attn: MANC/D. Schmidt   (1)
       MAAE   (1)

AF Ballistic Missile Division
Post Office Box 262
San Bernardino, California
Attn: WDSOT   (1)

Structures Division
Wright Patterson AFB, Ohio 45433
Attn: FDT/R. F. Hoener   (1)

Army Missile Command
Redstone Scientific Information Ctr.
Redstone Arsenal, Alabama 35809
Attn: Chief, Document Section   (1)

Ballistic Research Laboratory
Aberdeen Proving Ground,
Maryland 21005
Attn: Technical Library   (1)

Picatinny Arsenal
Dover, New Jersey 07801
Attn: Technical Library   (1)

Navy Special Projects Office
Washington, D. C. 20360
Attn: H. Bernstein   (1)

Naval Air Systems Command
Washington, D. C. 20360
Attn: AIR-330/Dr. O. H. Johnson   (1)

Naval Propellant Plant
Indian Head, Maryland 20640
Attn: Technical Library   (1)

Naval Ordnance Laboratory
White Oak
Silver Spring, Maryland 20910
Attn: Technical Library   (1)

Naval Ordnance Test Station
China Lake, California 93557
Attn: Edward W. Price   (1)
       Technical Library   (1)
       C. J. Thelen   (1)

Naval Research Laboratory
Washington, D. C. 20390
Attn: Technical Library   (1)

Chemical Propulsion Information
  Agency
Applied Physics Laboratory
8621 Georgia Avenue
Silver Spring, Maryland 20910   (1)

Defense Documentation Center
Cameron Station
5010 Duke Street
Alexandria, Virginia 22314   (1)

Defense Materials Information
  Center
Battelle Memorial Institute
505 King Avenue
Columbus, Ohio 43201   (1)

Materials Advisory Board
National Academy of Science
2101 Constitution Avenue, N. W.
Washington, D. C. 20418
Attn: Capt. A. M. Blamphin   (1)

Institute for Defense Analyses
1666 Connecticut Avenue, N. W.
Washington, D. C.
Attn: Technical Library   (1)

Advanced Research Projects Agency
Pentagon, Room 3D154
Washington, D. C. 20301
Attn: Technical Information Office   (1)

INDUSTRY CONTRACTORS

Aerojet-General Corporation
Post Office Box 1168
Solid Rocket Plant
Sacramento, California 94086
Attn: Dr. B. Simmons   (1)
       Technical Information Ctr.   (1)

Aerojet-General Corporation
Post Office Box 296
Azusa, California 91702
Attn: Technical Library   (1)

Aerospace Corporation
2400 East El Segundo Boulevard
El Segundo, California 90245
Attn: Technical Library   (1)
       Solid Motor Dev. Office   (1)

Aerospace Corporation
Post Office Box 95085
Los Angeles, California 90045
Attn: Technical Library   (1)

Atlantic Research Corporation
Shirley Highway at Edsall Road
Alexandria, Virginia 22314
Attn: Technical Library   (1)

Battelle Memorial Library
505 King Avenue
Columbus, Ohio 43201
Attn: Edward Unger   (1)

Boeing Company
Post Office Box 3999
Seattle, Washington 98124
Attn: Technical Library   (1)

Chrysler Corporation
Space Division
Michoud Operations
New Orleans, Louisiana
Attn: Technical Library   (1)

Douglas Missiles and Space Systems
Huntington Beach, California
Attn: T. J. Gordon   (1)

Hercules Company
Allegany Ballistics Laboratory
Post Office Box 210
Cumberland, Maryland 21502
Attn: Technical Library   (1)

Hercules Company
Bacchus Works
Post Office Box 98
Magna, Utah 84044
Attn: Technical Library   (1)

Lockheed Missiles and Space Company
Post Office Box 504
Sunnyvale, California
Attn: Technical Library   (1)

Lockheed Propulsion Company
Post Office Box 111
Redlands, California 92373
Attn: Bud White   (1)

Martin Marietta Corporation
Baltimore Division
Baltimore, Maryland 21203
Attn: Technical Library   (1)

Mathematical Sciences Corporation
278 Renook Way
Arcadia, California 91107
Attn: M. Fourney   (1)

Philco Corporation
Aeronutronics Division
Ford Road
Newport Beach, California 92660
Attn: F. C. Price   (1)

Rocketdyne
Solid Propulsion Operations
Post Office Box 548
McGregor, Texas
Attn: Technical Library   (1)

Rocketdyne
6633 Canoga Avenue
Canoga Park, California 91304
Attn: Technical Library   (1)

Rohm and Haas
Redstone Arsenal Research Division
Huntsville, Alabama 35807
Attn: Technical Library   (1)

Rohr Corporation
Space Products Division
8200 Arlington Boulevard
Riverside, California
Attn: H. Clements   (1)

Space Technology Laboratories, Inc.
5730 Arbor Vitae Street
Los Angeles, California 90045
Attn: Technical Library   (1)

Thiokol Chemical Corporation
Wasatch Division
Brigham City, Utah 84302
Attn: B. L. Petty   (1)

Thiokol Chemical Corporation
Elkton Division
Elkton, Maryland 21921
Attn: Technical Library   (1)

Thiokol Chemical Corporation
Huntsville Division
Huntsville, Alabama 35807
Attn: Technical Library   (1)

Thompson, Ramo, Wooldridge, Inc.
Structures Division
23444 Euclid Avenue
Cleveland, Ohio 44117
Attn: L. Russell   (1)

United Technology Center
Post Office Box 358
Sunnyvale, California 94088
Attn: Technical Library   (1)